COEFFICIENT OF THERMAL EXPANSION OF CONCRETE MIXES IN HAWAI`I: DETERMINATION AND IMPLICATIONS FOR CONCRETE PAVEMENT DESIGN

A THESIS SUBMITTED TO THE GRADUATE DIVISION OF THE UNIVERSITY OF HAWAI`I AT MĀNOA IN PARTIAL FULFILLMENT OF THE REQUIREMENTS FOR THE DEGREE OF

MASTER OF SCIENCE

IN

CIVIL ENGINEERING

December 2011

By

Stephen Anthony Havel

Thesis Committee:

A. Ricardo Archilla, Chairperson
Lin Shen
Peter G. Nicholson

ACKNOWLEDGEMENTS

I would like to thank Dr. Archilla for the opportunity to work on this project and his guidance throughout my study at the University of Hawaii at Manoa.

I would also like to thank Dr. Nicholson and Dr. Shen for being on my thesis committee and for the valuable comments on my work.

A special thank you to Wayne Kawano for presenting the idea of studying the Coefficient of Thermal Expansion of Hawaiian concrete mixes and getting me in contact with the three local concrete companies.

I would like to acknowledge the Hawaii Department of Transportation for funding this research. I would like to give a special thanks to Island Ready Mix, Hawaiian Cement, and West Hawaii Concrete for graciously providing all of the material for this project.

I would like to thank Jayanth Kumar Rayapeddi Kumar and Amir Mohamidapour for all of your help in the laboratory and your friendship throughout this experience.

What can I say about my friends Rajinder Sodhi and Patrick Reilly? Thank you guys so much for keeping me sane throughout this project and always being there to provide a good laugh.

I would like to thank and dedicate my thesis to my beautiful fiancée Julie, my lovely mother Ginny, and my amazing brother Patrick. Julie, you have been extremely supportive and I am grateful for that. I am pumped to have been able to share this unbelievable experience with you and it has just begun! Mother, thank you for always supporting me and believing that I could do anything. Thank you to both of you for grading ALL of my papers. And to my broham Patrick, thank you for all of the great times we have spent together and for your unwavering support. I love all of you very much.

TABLE OF CONTENTS

LIST OF FIGURES

LIST OF TABLES

CHAPTER 1: INTRODUCTION

1.1 Background

The pavement industry, both public and private, is concerned with the quality of today's roadways. Hawaii has recently been ranked below average compared to other states when it comes to the quality of its roadway infrastructure ("The Pew," 2011). According to a study done by The Pew Center on the States ("The Pew," 2011), the national average grade for infrastructure is a 'B-'. Hawaii falls beneath the average earning a grade of 'C'. The same website mentions that capital planning and maintenance are Hawaii's weakest points when the state's infrastructure is concerned. There was another study presented in September 2008 on the Report Card for America's Infrastructure ("The Report," 2008) website sponsored by the American Society of Civil Engineers (ASCE) stating that 71% of Hawaii's interstate pavements were in poor or mediocre condition and that Hawaii has a $187 million backlog of deferred road maintenance. The study also reported that vehicle travel on Hawaii's highways has increased by 28% from 1990 to 2007.

Figure 1.1 shows a breakdown, according to the Report Card for America's Infrastructure ("The Report," 2008), of where the nation's money could potentially be invested in the next 5 years. The study showed that nearly half (43.8%) of the nation's investment needs to be allocated to roads and bridges. With a $549.5 billion projected shortfall, efforts need to be made to construct long lasting and cost efficient structures.

Estimated 5-Year Investment Needs in Billions of Dollars				
CATEGORY	5-YEAR NEED (BILLIONS)	ESTIMATED ACTUAL SPENDING*	AMERICAN RECOVER AND REINVESTMENT ACT (P.L. III-005)	FIVE-YEAR INVESTMENT SHORTFALL
Aviation	87	45	1.3	(40.7)
Dams	12.5	5	0.05	(7.45)
Drinking Water and Wastewater	255	140	6.4	(108.6)
Energy	75	34.5	11	(29.5)
Hazardous Waste and Solid Waste	77	32.5	1.1	(43.4)
Inland Waterways	50	25	4.475	(20.5)
Levees	50	1.13	0	(48.87)
Public Parks and Recreation	85	36	0.835	(48.17)
Rail	63	42	9.3	(11.7)
Roads and Bridges Discretionary grants for surface transportation	930	351.5	27.5 1.5	(549.5)
Schools	160	125	0**	(35)
Transit	265	66.5	8.4	(190.1)
	2.122 trillion***	903 billion	71.76 billion	(1.176 trillion)
Total Need**** $2.2 trillion				

* 5 year spending estimate based on the most recent available spending at all levels of government and not indexed for inflation
** The American Recovery and Reinvestment Act included $53.6 billion for a State Fiscal Stabilization Fund for education, as of press time, it was not known how much would be spent on school infrastructure.
*** Not adjusted for inflation
**** Assumes 3% annual inflation

Figure 1.1 Estimated 5-year investment needs for the nation.

Rigid concrete pavement, or Portland Cement Concrete (PCC), competes directly with flexible asphalt pavements for their own space on the nation's roadways. Although both types of pavements have positive and negative aspects, this study focused on the rigid pavements design. Because of its versatility Portland Cement concrete is one of the most used construction materials, consuming 105 million metric tons of cement in 2000 (Mindess, Young, and Darwin 2003). This large quantity of production is due to the fact that concrete can be used to construct buildings, dams, piping, and most importantly for this study, pavements. A study completed by the United States Geological Survey (USGS) showed that, out of the 42,500 interstate miles studied, sixty percent of them were made of concrete, totaling 25,500 miles ("Materials in Use," 2006). With this in mind, it is important to look at the positive and negative attributes of concrete. Concrete is used because of its versatility, compressive strength, and workability, but the down side is that it is weak in tensile strength and can be susceptible to environmental conditions, for example; rain, snow, heating/cooling cycles (freeze-thaw attack), and chemicals from the environment (sulfates, chloride, de-icing solutions, etc.). The heating/cooling cycle, or expansion/contraction cycle, can be studied in the laboratory by determining the Coefficient of Thermal Expansion (CTE). AASHTO T 336, Standard Method of Test for the Coefficient of Thermal Expansion of Hydraulic Cement Concrete, is the accepted standard for testing this concrete property, which is useful in evaluating Portland Cement Concrete (PCC) pavement performance.

For this study, the Coefficient of Thermal Expansion (CTE) will be explored with a focus on mix designs that use aggregates found in Hawaii. "The coefficient of thermal expansion (CTE_{PCC}) is defined as the unit change in length per unit change in temperature and it has significant (practical) influence on the design of joints and temperature-related deformations (expansion/contraction and curling) in jointed concrete pavements (JCPs)" (Jahangirnejad et al. 2009). To date, there are no published studies on the value of the CTE of Hawaiian mixes. The CTE is an important input variable for the design of PCC pavements in the Mechanistic-Empirical Pavement Design Guide (MEPDG), which was developed to "provide the highway community with a state-of-the-practice tool for the design of new and rehabilitated pavement structures, based on mechanistic-empirical principles" (NCHRP 1-37A, 2004). In order to obtain the most accurate results for a specific location, it is important to know the value of CTE for the particular mixes used in that location. The MEPDG has three different levels of input when it comes to pavement design including the input of the CTE (Level 1, Level 2, and Level 3). Level 1 of the program allows for the all of the project inputs to be site specific. This is typically more beneficial for high profile jobs, i.e. Interstate and main freeways, due to the economical impact and extra time need for field studies to determine soil classifications, traffic volumes and characteristics, etc. Level 2 is an intermediate step that involves some of the design inputs to be site specific and some to be industry accepted values. Finally, Level 3 uses solely industry accepted values provided by the program. Level 3 is the least reliable but would be advantageous in the design of low profile jobs, e.g. an access road. Therefore, the increase in levels results in a decrease in site specific input requirements. There was a study performed by the Federal Highway Administration (FHWA) that gives typical values for a variety of geologically different types of aggregates. These values can be utilized in Level 2 and Level 3 of the MEPDG. The meaning and the significance of the three levels in MEPDG and the study completed by the FHWA will be described in greater detail in later chapters.

The CTE can vary greatly from one aggregate to the next and it can have a drastic effect on the life of a concrete pavement. According to Mindess, Young and Darwin (2003), typical values can range from 4 x 10^{-6}/°C for marble to 13 x 10^{-6}/°C for quartzite. A smaller value of CTE results in less expansion and contraction, giving the concrete pavement a higher likelihood of better performance. In this study, the MEPDG was used to estimate the effect that CTE can have on the performance of a concrete pavement through the amount of faulting, percent slabs cracked, and the international roughness index (IRI). These five performance criteria will be described in Chapter 2: Literature Research. The study completed by Jahangirnejad (Jahangirnejad 2009) has developed a table, based on the literature written by Mallela et al. (Mallela et al. 2005), showing the significant influence that the CTE has on the pavement performance criteria, breaking each distress down individually. Below, Table 1.1 illustrates the role that CTE has on the various pavement distresses. For this research, the main area of study will be on Jointed Plain Concrete Pavements (JPCP) rather than Continuously Reinforced Concrete Pavements (CRCP). Therefore, punchouts, a distress type that occur only on CRCP pavements, will not fall within the scope of this research, but this distress is presented in Table 1.1 just as a reference.

Table 1.1. Influence of CTE on Pavement Performance Criteria

Pavement Distress	Role of CTE
Early-age or premature random cracking due to excessive longitudinal slab movement	High CTE causes excessive longitudinal movement that, if restrained by forces, leads to cracking.
Mid-panel fatigue cracking	Higher curling (temperature-induced) stresses lead to higher mid-panel cracking.
Faulting	Higher corner deflections due to negative curling, which is a function of temperature gradients and CTE.
Joint spalling	Excessive joint opening and closing causes joint sealant failure and joint spalling.
Punchouts in Continuously Reinforced Concrete Pavements (CRCP)	Crack load transfer efficiency is affected by spacing and width of cracks which are impacted by CTE.

This study is important because, as stated previously, there is a large need for quality long lasting pavements that do not require a large amount of maintenance. By determining the CTE values of our local aggregates, companies can make more informed decisions on potentially changing the source of the coarse aggregate to use in their mix designs. More importantly, another benefit of knowing the CTE for the concrete companies is that they can account for it in the design phase. Alterations can be made to the design with the known CTE, including slab length and slab thickness, to meet the pavement design life requirements. This could potentially increase the life and quality of the concrete pavements in Hawaii, while slightly decreasing the amount of maintenance needed and hopefully reducing the percentage of poor to mediocre roadways. An example of the need for a high quality concrete pavement surface is the Interstate H-3, John A. Burns freeway, on the island of Oahu as seen in Figure 1.2. The freeway is one of the most expensive freeways ever built on a cost per mile scale, coming in at approximately $80 million per mile (“Interstate H-3,” 2011). With a price tag this large, the quality and durability of the concrete pavement surface is critical.

Figure 1.2 Example of a job utilizing concrete pavement surface on Oahu.

1.2 Problem Statement

The current edition of the MEPDG allows for the input of the CTE on various levels of site-specific accuracy. The CTE of concrete pavement can be a very important parameter in the design by affecting the overall performance and life of the pavement. Both CRCP and JPCP are affected by this parameter, but for this study JPCPs and their typical distresses will be the main focus (faulting, percent slabs cracked and the International Roughness Index (IRI)). If utilized correctly, the site specific CTE can minimize the variability and uncertainty that sometimes goes into a pavement design.

Currently the Hawaii Department of Transportation (HDOT) does not require the determination of the CTE in their concrete pavement design procedure. The goal of this study was to determine the value of the CTE for Hawaiian mixes and show the effects that the CTE has on the pavement distresses and design life through sensitivity testing. It is important to consider the site specific details, including the CTE, in every concrete pavement design to maximize the quality and life of Hawaii's pavement infrastructure. This study will provide details on the CTE testing done and report the result and findings of this study. Also included will be a review of what others have similarly done in this field of pavement engineering.

1.3 Research Objectives and Scope

1.3.1 Research Objectives

The objectives of the research project were as follows:

- Quantify the value of the CTE of various mixes prepared with different aggregates found throughout the state of Hawaii from various quarries.
- Study the effect that various aggregates from the different quarries and their curing times have on the value of the CTE of the mix.
- Compare the different mixes and aggregate types with the aid of MEPDG to predict the amount of degradation of the pavements over time.
- Determine at what curing age the CTE should be used as an input into the MEPDG program.

1.3.2 Research Scope

The scope of this research project is as follows:

- Acquire concrete cylinders from 3 local Hawaiian concrete plants (2 on Oahu and 1 on the Big Island) for determination of CTE.

- Perform field testing on the freshly-mixed concrete to ensure that the quality and accuracy of the sample meets the specifications of the mix design.
- Cure the concrete cylinders from each concrete quarry in a 100% humidity room for a set amount of days.
- Remove the cylinders from the curing room and saw to size.
- Place the cylinders in the water bath to determine the CTE and proceed to run the test.
- Acquire results to determine the CTE of each of the concrete specimens.
- Average the CTE for each of the set curing times.
- Use the calculated CTE in the MEPDG program to determine the effect that CTE has on the pavements performance over its life expectancy.
- Determine an appropriate curing time to use when imputing a CTE value into the MEPDG program.
- Give recommendations from the given results.

Figure 1.3 shows a hierarchical chart of the step-by-step process involved in this study. Not all steps are provided in the chart, but the process will be described in greater detail in later chapters. The chart shows the three different steps involved in this study, which include the field testing, the laboratory testing, and the office work.

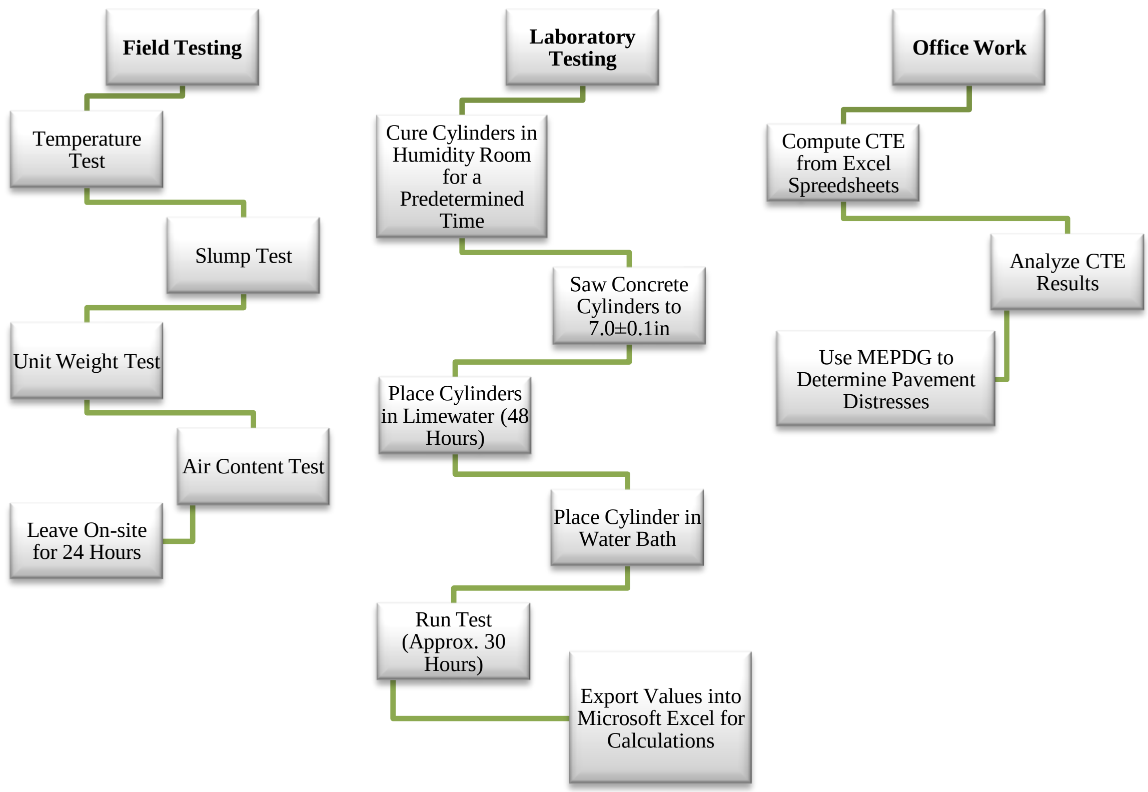

Figure 1.3 Hierarchical chart of the research process for this project.

1.4 Thesis Organization

The procedure followed by this research and the rest of this thesis, besides Chapter 2 Literature Review, is organized in the same order as illustrated in Figure 1.3. The field testing was performed first, followed by the laboratory testing and office work. Chapter 2 Literature Review gives an introduction on studies that have been done on the determination of the coefficient of thermal expansion of rigid concrete pavements. Chapter 2 provides a discussion of the software used to acquire the outputs needed to determine the CTE (LabVIEW SignalExpress Version 3.0) and to design a pavement section (Mechanistic-Empirical Pavement Design Guide (MEPDG)). Chapter 3 introduces the type and sources of the three different coarse aggregates used in each of the three mix designs studied in this research. Also, Chapter 3 defines the field testing involved in sampling concrete onsite as well as their AASHTO standards. In addition, Chapter 3 gives the equations necessary to compute a correction factor needed for the determination of the CTE, as well as the calculations for the CTE of the concrete specimens. Chapter 4 presents the results of the field testing, CTE testing, and sensitivity testing of the MEPDG program that were found from this study. Sample calculation and inputs are provided for clarity. Finally, Chapter 5 discusses the study results, recommendations for their use, as well as potential future research possibilities.

CHAPTER 2: LITERATURE RESEARCH

This chapter concentrates on the effect of concrete's Coefficient of Thermal Expansion (CTE) on the design of rigid pavements. Discussions will also be provided on the various inputs involved in the construction of the concrete specimens, the testing parameters, the testing equipment, and the validity of various test methods. The Mechanistic Empirical Pavement Design Guide (MEPDG) (NCHRP 1-37A 2004) program will be utilized to illustrate the effect that CTE has on faulting, percent slabs cracked and the International Roughness Index (IRI) of Jointed Plain Concrete Pavement (JPCP). Section 2.1 provides a definition of the CTE and describes the measuring equipment available to perform the testing. Section 2.2 describes the process used to measure the CTE of rigid pavements according to the literature and the American Association of State Highway Transportation Officials (AASHTO) standards. This section also provides a description of how the concrete specimens were prepared for the CTE laboratory testing and the type of equipment that was used, including; the thermocouples, a Linear Variable Differential Transformer (LVDT), and a custom water bath. Section 2.3 gives an introduction into the various ways of casting the concrete cylinders and the method chosen for this research. The next section, Section 2.4, discusses the types of factors that could potentially affect the CTE and the specific ones covered in this research. Section 2.5 explores the validity of the test method and equipment used in this study. This section talks about the various methods and water baths available and the validity of each one. Then in Section 2.6, the water bath used at the University of Hawaii at Manoa is described in greater detail. Section 2.7 gives a brief explanation of the software utilized to perform the CTE measurements. Finally, Section 2.8

explains the MEPDG and how it was employed in the study to determine various characteristics of each pavement type.

2.1 Definition of CTE

"The coefficient of thermal expansion (CTE_{PCC}) is defined as the unit change in length per unit change in temperature and it has significant (practical) influence on the design of joints and temperature- related deformations (expansion/contraction and curling) in jointed concrete pavements (JCPs)" (Jahangirnejad et al. 2009). For years CTE was ignored when it came to an input in the concrete pavement thickness design process, but that has recently changed. After years of research and proven results that CTE is indeed a critical piece of the puzzle, the 2004 version of MEPDG has implemented it into its design (Jahangirnejad 2009). Now that the effects of the CTE are better understood and that the CTE is more accurately and consistently tested, there are certain aspects that need to be accounted for. These include: the geology of the aggregate, the moisture conditioning of the specimen, and the curing time of the specimen. Studies have shown that the amount and type of aggregate significantly affects the value of CTE (Tran et al. 2008). For this study, all three of the factors mentioned were considered and documented to evaluate the significance of each of them. Many other similar studies have been completed on various inputs that could affect the value of the CTE and will be referenced later in this chapter. Geology, moisture conditioning, and the curing time of the specimens are thought to have the most significant effect on the CTE and therefore will be the focus of this research.

2.2 Measuring CTE

There is a specific way to calculate the CTE of concrete according to the *AASHTO T 336-09 Coefficient of Thermal Expansion of Hydraulic Cement Concrete,* known by its test protocol *AASHTO TP 60-00 Standard Test Method for the Coefficient of Thermal Expansion of Hydraulic Cement Concrete.* Most of the literature found in the research process refers to the test protocol AASHTO TP 60-00, which will be quoted as such in this thesis. The standard specifies that a concrete specimen, whether cast in the field, cast in the laboratory or extracted in the form of a core, must be 180 ± 2 mm (7.0 ± 0.1 in). In most cases, the concrete cylinders must be sawed down to meet the requirements. A concrete saw, such as the one in Figure 2.1, must be used. The saw must be capable of sawing the ends of a cylindrical specimen perpendicular to the axis while also being parallel to each other. In this particular study, concrete cylinders were cast on-site, following the standard AASHTO T23, and brought to the university pavement laboratory. Once in the laboratory, they were cured for a predetermined amount of days (for this research, 3, 7, 14, 28, and 56 days were considered) in a 100 percent humidity room.

Figure 2.1 UH Manoa concrete saw.

Once the specimens were sized, they were then placed in limewater for a minimum of 48 hours and a change in weight of less than 0.5 percent over a 24 hour period. The research literature revealed that the maximum CTE is found when the specimen is 70-80% saturated (Jahangirnejad 2009). However, for ease and consistency of testing, the standard calls for the specimens to be completely saturated before testing. Prior to placing the concrete specimen into the testing apparatus, a steel specimen with a known CTE is tested to determine the expansion and contraction of the steel frame. The specimen should be composed of a material which is essentially linearly-elastic, non-corroding, non-oxidizing, and non-magnetic, and it should have a thermal coefficient as close as possible to that of concrete (304 stainless steel, which has a CTE of 17.3 x 10^{-6}/°C, is a suitable material) (AASHTO T 336-09). At the University of Hawaii at Manoa (UH Manoa), a 410 stainless steel specimen with a CTE of 10.4 x 10^{-6}/°C was used to determine the amount of expansion and contraction of the measuring frame. The CTE value of 10.4 x 10^{-6}/°C falls within the range of values determined by a study completed by the Tanesi, Crawford, Nicolaescu, Meininger, and Gudimettla (2010) as part of an FHWA study. The FHWA test returned values for a 410 SS calibration specimen to be between 10.1 x 10^{-6}/°C and 10.4 x 10^{-6}/°C (Tanesi et al. 2010). Figure 2.2 shows a picture of the 410 stainless steel specimen on the left and on the right is one of the test specimens that was used at UH Manoa.

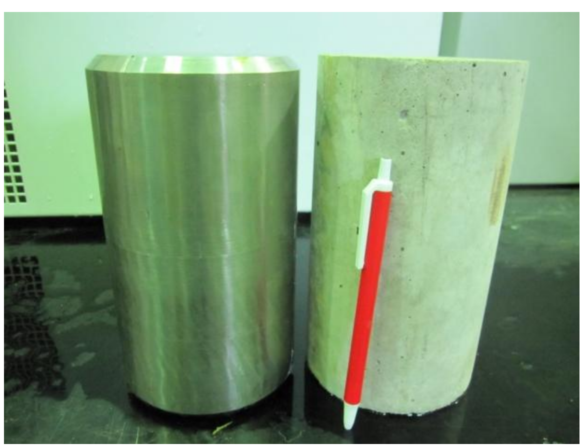

Figure 2.2 410 SS calibration specimen (left) along side sample concrete specimen (right).

Once the concrete specimen is completely saturated, it is placed inside a steel frame, whose expansion is determined using the steel calibration specimen. The frame must be placed in the water bath, completely submerging the test specimen as shown in Figure 2.3, and contain a Linear Variable Differential Transformer (LVDT) with a minimum resolution of 0.00025 mm (0.00001 in). The purpose of the LVDT is to capture the axial length change of the specimen due to the set temperature changes.

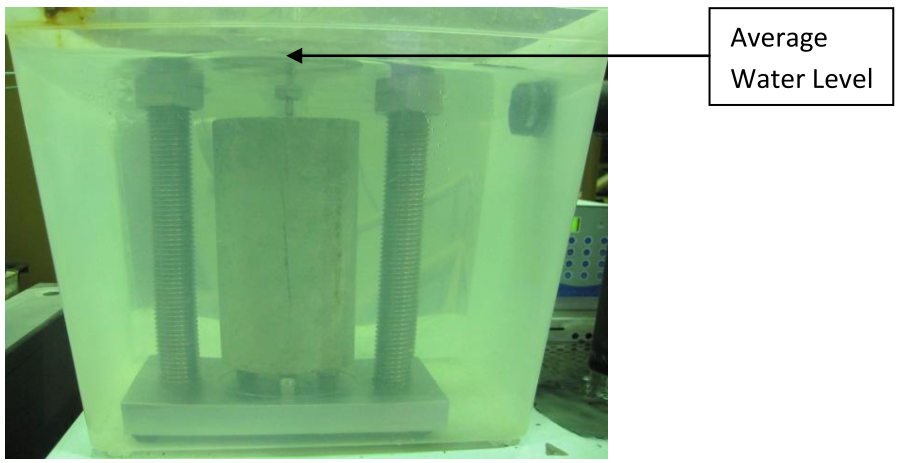

Figure 2.3 Concrete specimen completely submerged in the custom water bath.

Once the specimen is centered on the frame, it experiences two temperature cycles. It starts at 10 ± 1 °C (50 ± 2 °F), then it is heated up to 50 ± 1 °C (122 ± 2 °F), then it is cooled back down to 10 ± 1 °C (50 ± 2 °F), then it is heated again up to 50 ± 1 °C (122 ± 2 °F), and then finally it is cooled back to 10 ± 1 °C (50 ± 2 °F). In the AASHTO T 336 standard, there is no protocol regarding the rate at which the temperature change must occur. There has been a study by Crawford, Gudimettla, and Tanesi (2009) to determine if this can significantly affect the overall CTE, which will be discussed later in the chapter.

There were a total of five temperature plateaus per each of the concrete specimens. At each of the plateaus, the temperature is kept constant until thermal equilibrium of the specimen has been reached, as indicated by consistent readings of the LVDT, which is measured to the nearest 0.00025 mm (0.00001 in). The readings are taken every ten minutes over a one-half hour time period. There are a total of 4 thermocouples that are capable of recording the temperature in the water bath with a resolution of 0.1 °C (0.2 °F). The thermocouples are accurate to 0.2 °C (0.4 °F). The thermocouples are placed at various depths in the water bath to ensure that the concrete specimens are being uniformly heated to yield accurate and consistent results. The following figure, Figure 2.4, is the custom water bath used at the University of Hawaii at Manoa. The CTE test procedure will be described in greater detail in Chapter 3 Test Procedures.

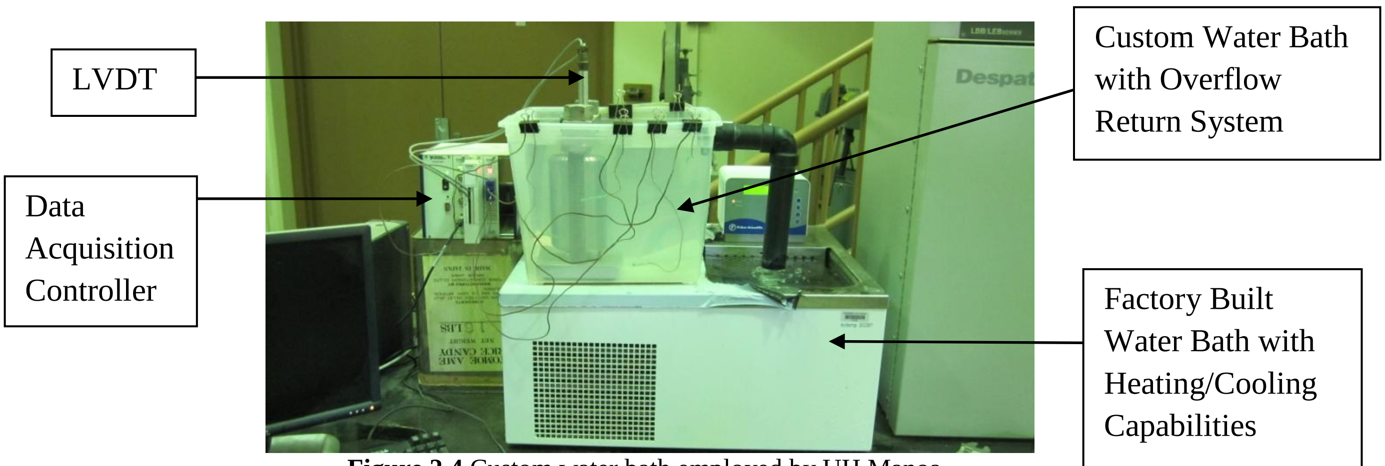

Figure 2.4 Custom water bath employed by UH Manoa.

2.3 Casting the Concrete Specimen

According to AASHTO T 336, there are three accepted methods for preparation of the concrete cylinders required for the CTE test. One of the methods available follows the standard AASHTO R 39, *Making and Curing Concrete Test Specimen in the Laboratory*. This method is very similar to the method used for this study, AASHTO T 23 (which will be described in greater detail later), in which the concrete cylinders are made in the field. Some of the differences include; assuring that the aggregates are sound and not segregated, determining characteristics of the materials before batching (absorption, moisture content, etc.), the use of the equipment (mixing drum, scales, measuring apparatuses), and, of course, the steps of the mixing process. The next method follows the standard AASHTO T 24, *Obtaining and Testing Drilled Cores and*

Sawed Beams of Concrete. This method is extremely representative of what is actually being used in the field; however, much care needs to be taken when sampling the cores. When drilling the cores some conditions need to be met, including that the concrete be strong enough to be drilled and ensuring that drilling occurs perpendicular to the horizontal axis in the center of the slab (or as close as possible). These two methods are widely used and have their benefits, which include; being able to control and adjust factors of the overall mix design by doing everything by hand and testing from an actual roadway. For this particular study, the method followed was according to the standard AASHTO T 23, *Making and Curing Concrete Test Specimen in the Field*. This particular method goes over the procedure for making and curing cylinders from representative samples of fresh concrete for a construction project. The AASHTO T 23 standard also calls for other various tests to be run on-site with a representative sample of concrete. These tests include a slump test, an air content test, and taking the temperature according to AASHTO T 119, AASHTO T 152, and AASHTO T 309M/T 309, respectively. These tests must be done in a timely manner so as to minimize the amount of water evaporation and initial setting of the concrete. Later in the report, the various tests will be described in greater detail along with tables of the measured values.

2.4 Factors affecting CTE

There are many variations of mixes available for use in the professional world of construction, but for this research the concentration will be placed on three particular variables. The CTE is influenced by (Jahangirnejad 2009):

1.) The volume and geology of coarse aggregate present in the mixture,

2.) Moisture conditioning of the sample at the time of testing, and

3.) The number of heating-and-cooling cycles applied to the test specimen.

These three variables mentioned by Jahangirnejad are not the only factors that influence the CTE, but they are the ones that were the focus for this research. “The thermal coefficient of expansion for PCC depends on many factors such as the water: cementitious material ratio, concrete age, richness of mix, relative humidity, and the type of aggregate in the mix. However, the type of coarse aggregate has the most influence” (Huang, 1993). Since the AASHTO T 336-09 standard calls for the specimen to be 100% saturated, the relative humidity will not be studied for this research. Huang et (1993) introduces a few more influence factors, but once again, this research focused on coarse aggregate type, specimen age (curing time), and number of heating-and-cooling cycles.

The idea that the coarse aggregate of a PCC mix controls the amount of expansion and contraction has been studied in-depth. At the Turner-Fairbanks Highway Research Center (TFHRC), the ‘Federal Highway Administration’ (FHWA) has tested more than 1,800 cores from concrete pavements throughout the country following the AASHTO TP 60 procedure (AASHTO TP 336) (Tanesi et al. 2007). These samples consisted of both drilled cores from the Long Term Pavement Performance (LTPP) testing by the TFHRC and laboratory cast specimens. The materials used in the LTPP’s CTE testing came from various sources throughout the country. This extensive CTE testing of various materials found throughout the United States provides a broad compilation that can be used in the MEPDG level three input. There are three different levels of input available in MEPDG. The three levels become less and less site specific as they increase (i.e. level 1 is very site specific, level 2 is a combination of site specific calculations and correlations, and level 3 uses default values). The levels are defined in the MEPDG manual (Chapter 4 part 3) (NCHRP 1-37A 2004) as follows:

a.) Level 1 – the use of site and/or material specific inputs for the project obtained through direct testing or measurements. Examples of Level 1 data include material properties obtained through laboratory testing and measured traffic volumes and weights near or at the project site.

b.) Level 2 – the use of correlations to establish or determine the required inputs. Examples of Level 2 data include the resilient modulus of the subgrade or unbound base materials estimated from California Bearing Ratios (CBR) or R-values using empirical correlations.

c.) Level 3 – the use of national default values or local experience to define the inputs. Examples of Level 3 input include the use of AASHTO soil classifications to determine a typical resilient modulus value or the use of roadway type and truck type classifications to determine normalized axle weight and truck classification distributions.

The following table, from FHWA research ("Pavements," 2011), provides typical displacement ranges of common aggregates found in Portland Cement Concrete that can be used in Level 3 of the MEPDG.

Table 2.1. Typical α Ranges for Common PCC Components

	Coefficient of Thermal Expansion	
	10^{-6}/°C	**10^{-6}/°F**
Aggregate		
Granite	7-9	4-5
Basalt	6-8	3.3-4.4
Limestone	6	3.3
Dolomite	7-10	4-5.5
Sandstone	11-12	6.1-6.7
Quartzite	11-13	6.1-7.2
Marble	4-7	2.2-4
Cement Paste (saturated)		
w/c = 0.4	18-20	10-11
w/c = 0.5	18-20	10-11
w/c = 0.6	18-20	10-11
Concrete	7.4-13	4.1-7.3
Steel	11-12	6.1-6.7

Another factor that affects the overall CTE of a mix is the length of curing time of the concrete cylinders. Theoretically, testing concrete cylinders with the same mix design should produce similar results. If the CTE is changing overtime due to curing, something must be happening to the cylinder itself or the chemical composition of the cylinder. According to the Portland Cement Association (PCA) cement tends to swell or shrink depending on the type of curing it underwent (Kosmatka et al. 1992). If the specimens are wet-cured in a humidity room or submerged in water they would tend to swell. On the contrary, if the concrete cylinders are dry-cured they tend to shrink, as seen in Figure 2.5. Therefore, if the specimens are wet-cured for the entirety of the curing time, swelling will occur, as well as a potential change in the chemical composition of the cement. How this effects the value of the CTE overtime is uncertain and further research would be needed.

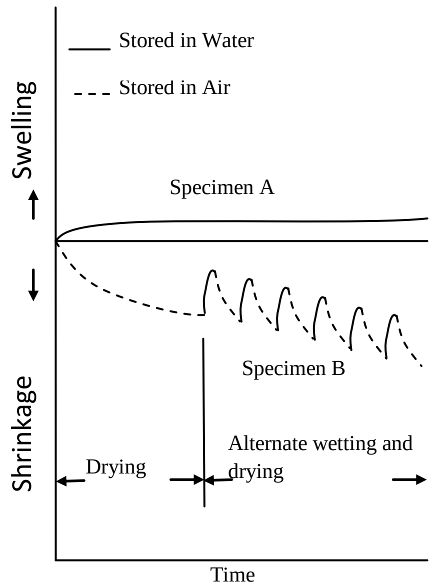

Figure 2.5 Effect of swelling on the cement paste in concrete cylinders (Figure redrawn after Kosmatka et al. 1992).

Another aspect that Tran et al. (2008) studied was the effect that different cement pastes would have on the CTE overtime. Tran, Hall, and James (2008) compared three potential cementitious materials, including; cement only, cement and 20% fly ash, and cement and 25% slag. The results showed that "For PCC with the same type of aggregates, using different cementitious materials did not significantly affect the CTE. This implies that the use of fly ash or ground granulated blast furnace slag as a cementitious material in the PCC mixture did not influence the mixture thermal expansion characteristics" (Tran et al., 2008).

As for the moisture condition, the literature indicates that the maximum value for the CTE of a concrete specimen is found at a relative moisture content of 60% to 70% (Tran et al. 2008) (70-80% saturated according to Jahangirnejad 2009), but this condition is not practical for a large scale project due to the difficulty of accurately obtaining the same degree of saturation for hundreds of samples. In order to achieve a certain percentage of saturation for every specimen, the dry weight of each individual specimen would need to be known which could potentially take a significant amount of time. Furthermore, concrete in the field typically has a relative humidity of 80% or more, except for the top portion of the slab which is dryer due to the environment (Mallela et al. 2005); therefore, using a relative moisture content of 60% to 70% (or 70% to 80%) is not representative. Tran, Hall, and James (2008) reported that "the CTEs of PCC mixtures and cement paste specimens at the fully saturated condition determined at 7 and 28 days were not significantly different. However, these CTE values would be significantly different if the samples were not fully saturated". As a result, according to AASHTO T 336, the concrete sample should be completely saturated in limewater until approximately100% relative moisture content is met (approximately 48+ hours).

2.5 Validity of test method and equipment

There are two test methods, AASHTO TP 60-00 and the modified AASHTO TP60 test method, for determining the CTE of concrete test specimens. A research project was performed to evaluate the validity and accuracy of the two methods (Crawford et al. 2009). The research consisted of measuring a total of 36 specimens, four of which were made using the Texas method (also known as the modified AASHTO TP60 test method) and 32 were made using the AASHTO TP 60 method. The literature, cited earlier in this report (Crawford et al. 2009), utilized the specifications from the AASHTO TP 60 provisional test, emphasizing that this method does not specify the rate of change of temperature from 10 to 50 °C (or 50 to 10 °C). Therefore, the specimen may or may not have the same temperature as the water bath during the expansion and contraction cycles. The question that then resulted was; does the rate of heating and cooling of the concrete specimen significantly change the results? The Texas method then took readings from the LVDT and the thermocouples every minute from 15°C to 45°C and used a regression analysis to compute the CTE. Once the specimens were tested and the measurements collected, it was determined that there was no significant difference between the Texas Method and the AASHTO TP 60 method. Therefore, either method is acceptable for making the specimens and determining the CTE. The test method AASHTO TP 60 (AASHTO T 336) will be applied for this particular research project and has been used for the research of the following literature sources: Crawford et al. (2009), Jahangirnejad et al. (2009), Tran et al. (2008), Won (2005), Mallela et al. (2005), Hall et al. (2005), and Tanesi et al. (2007).

As part of Crawford's 2009 experiment, the researchers wanted to determine the variability between factory-built water baths versus custom-built water baths around the nation. Several State Highway Agencies' (SHA) materials laboratories and university research centers have custom-built manually operated or automated CTE measuring devices based on recommendations from AASHTO TP 60 (Crawford et al. 2009). There were a total of 18 laboratories involved with this study throughout the nation from California to Florida. Out of the 18 laboratories, 11 used custom-built CTE devices and 7 used commercial CTE devices. Each of the 18 laboratories tested a calibration specimen (410 stainless steel (SS)) and two different types of concrete, one with a low CTE made predominately of limestone aggregates and the other with a high CTE made predominately with gravel aggregates. The accuracy of the CTE measurements from the inter-laboratory study was determined from the CTE value of a 410 SS specimen measured according to ASTM E 228 Standard Test Method for *Linear Thermal Expansion of Solid Material with a Push-Rod Dilatometer* test procedure (Crawford et al. 2009). The results from the inter-laboratory research showed that, according to a 5% significance level, the steel specimen and the concrete specimen with predominately limestone aggregates did not show a significant difference between laboratories. The results from the concrete specimen made predominately from gravel aggregate were inconclusive. According to Crawford et al. 2009, the results from the factory-built water baths were more accurate than that of the custom-built water baths. However, in that study the factory-built water baths were all built by the same company. To have a truly representative evaluation of the accuracy, the research should have included some water baths from different companies to match the variability of the individually custom built water baths. Overall, this study concluded that though the laboratory CTE results from the various machines were different; they were not significant enough to raise concerns.

2.6 Test equipment

The literature research presented in section 2.5 is important because the water bath available at the University of Hawaii at Manoa is custom-built and therefore the results found, according to findings of the previous section, can be considered acceptable. This is important when it comes to assuring that the mixes prepared in Hawaii are not over or under-designed due to a discrepancy in the testing techniques, methods and equipment.

The water bath at the University of Hawaii at Manoa is a combination of a factory-built water bath and a custom made water bath. The factory-built part consists of a water bath that was designed and built by Fisher Scientific, model Isotemp 3028P. This particular model is capable of controlling the water temperature to an accuracy of 0.01 °C (from -25 °C to 100 °C), which meets and exceeds the AASHTO T 336 standard of an accuracy of 0.1 °C ("Isotemp® Bath Circulators," 2005). The Fisher Scientific water bath is equipped with a powerful pump, 15 L/min, capable of circulating the water from the factory-built to the custom-built water bath. The custom portion consists of a plastic container capable of submerging the testing frame containing the specimen in question. An overflow tube is connected to the custom-built water bath so that the water is able to return to the factory-built bath, where it is either heated or cooled. Since there are a total of two baths involved in this study, the result is that more water needs to be heated and cooled. Consequently, the process of testing one specimen takes more time (approximately 30 hours). As stated earlier in the Crawford et al. (2009) study, there is no time requirement in the AASHTO T 336 standard.

2.7 Data Acquisition

The program LabVIEW SignalExpress Version 3.0 was used to acquire and display the temperature change recorded from the thermocouples and the length change measured by the LVDT. The information retrieved from the LVDT and thermocouples were a constant stream of data, but the values were actually recorded at 30 second intervals. This was done in order to obtain enough points to determine that the specimen was at thermal equilibrium at 10°C and 50°C. According to AASHTO T 336, thermal equilibrium is defined as when the LVDT values show consistent readings to the nearest 0.00025mm (0.00001 in) every 10 minutes over a one-half hour period. This study records many more points (one every 30 seconds) making it clearer as to when thermal equilibrium is met. The figure below, Figure 2.6, shows a screenshot of the output from LabVIEW SignalExpress Version 3.0, including the four thermocouples and LVDT readings.

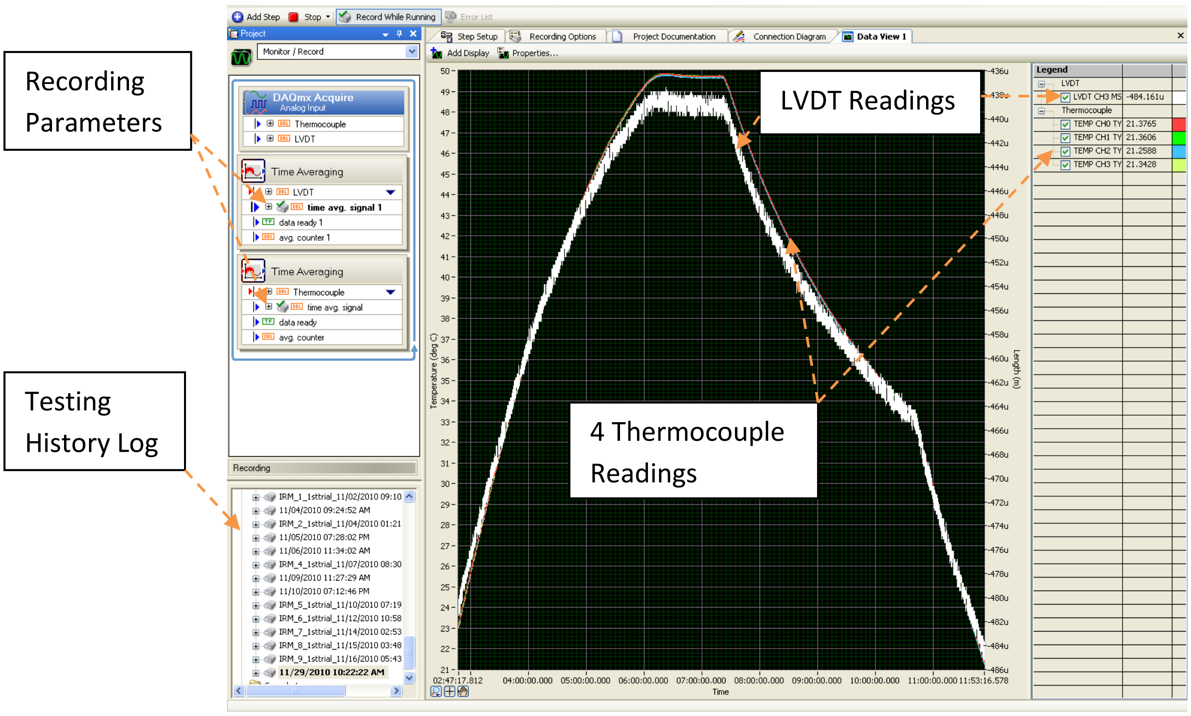

Figure 2.6 Typical outputs from LabVIEW SignalExpress Version 3.0.

2.8 MEPDG Evaluation

For the study of the sensitivity of CTE of the overall rigid pavement design, the Mechanistic-Empirical Pavement Design Guide (MEPDG) was utilized. The MEPDG provides many powerful and useful results to analyze the pavement performance, such as: faulting, load transfer efficiency (LTE), percent slabs cracked and the international roughness index (IRI). For this particular project, the focus was on faulting, percent slabs cracked and the international roughness index (IRI). These five distresses were the main focus of this study because a majority of the concrete pavements found on Hawaii's interstate system consist of jointed plain concrete pavements (JPCP).

Faulting is defined as a difference in elevation from one slab to another in a JPCP (NCHRP 1-37A 2004). Faulting can be caused by a combination of factors, including; repeated applications of moving heavy axle loads, poor load transfer across the joint, free moisture beneath the PCC slab, erosion of the supporting base/subbase, subgrade, or shoulder base material, and upward curling of the slab (NCHRP 1-37A 2004). Figure 2.7 illustrates the critical location of a heavy load on a PCC slab to inflict the most faulting distress. Erosion under the joints of a JPCP is created by the presence of water in the sub-layers causing pumping of the fines due to heavy loading. Overtime, the pumping of the fines will create a void under the joint, weakening the section. Because of temperature gradients, the CTE in particular can impact that amount of faulting due to the stress that is placed upon the joints because of expansion and contraction. As the joint spacing is increased the potential for pumping amplifies due to slab shrinking. It would be preferable to use a concrete pavement with a lower CTE value, if possible, to minimize the amount of movement and distress to the joints.

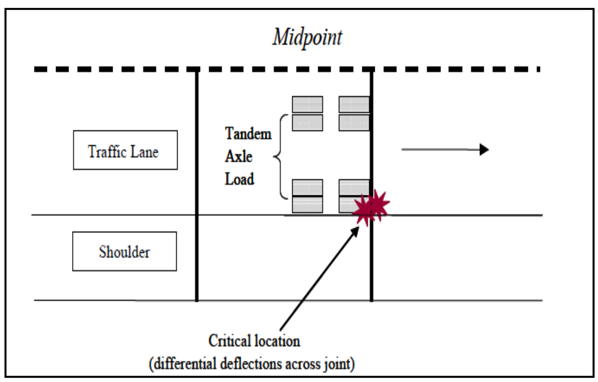

Figure 2.7 Critical load and structural response location for JPCP joint faulting analysis.

The MEPDG uses the following equations to compute faulting of JPCP:

$$Fault_m = \sum_{i=1}^{m} \Delta Fault_i$$

$$\Delta Fault_i = C_{34} * (FAULTMAX_{i-1} - Fault_{i-1})^2 * DE_i$$

$$FAULTMAX_i = FAULTMAX_0 + C_7 * \sum_{j-1}^{m} DE_j * Log(1 + C_5 * 5.0^{EROD})^{C_6}$$

$$FAULTMAX_0 = C_{12} * \delta_{curling} * [Log(1 + C_5 * 5.0^{EROD}) * Log\left(\frac{P_{200} * WetDays}{P_s}\right)]^{C_6}$$

where,

$Fault_m$	=	mean joint faulting at the end of the month, in.
$\Delta Fault_i$	=	incremental change (monthly) in mean transverse joint faulting during month i, in.
$FAULTMAX_i$	=	maximum mean transverse joint faulting for month i, in.
$FAULTMAX_0$	=	initial maximum mean transverse joint faulting, in.
EROD	=	base/subbase erodibility factor.
DE_i	=	differential deformation energy accumulated during month i.
EROD	=	base/subbase erodibility factor.
$\delta_{curling}$	=	maximum mean monthly slab corner upward deflection PCC due to temperature curling and moisture warping.
P_s	=	overburden on Subgrade, lb.
P_{200}	=	percent subgrade material passing #200 sieve.
WetDays	=	average annual number of wet days (greater than 0.1 in rainfall).

C_1 through C_8 and C_{12}, C_{34} are national calibration constrants:

$$C_{12} = C_1 + C_2 * FR^{0.25}$$
$$C_{34} = C_3 + C_4 * FR^{0.25}$$

where,

$C_1 = 1.29$	$C_5 = 250$
$C_2 = 1.10$	$C_6 = 0.4$
$C_3 = 0.001725$	$C_7 = 1.2$
$C_4 = 0.0008$	

FR = base freezing index defined as percentage of time the top base temperature is below freezing (32 °F) temperature.

There are potential steps that can be taken in order to minimize the effect of faulting of the JPCP, such as:

1. Increase the PCC thickness.
2. Increase the PCC modulus of elasticity.
3. Decrease the PCC coefficient of thermal expansion.
4. Improve LTE with shoulder, etc.

As mentioned above, one of the factors that affect the amount of faulting in a PCC slab is the amount of upward curling. Upward curling is a result of a temperature difference between the top and the bottom of a slab, i.e. the temperature is cooler at the top of the slab compared to the bottom. Therefore, it is important to minimize the value of the CTE if possible, which would also lessen the effect of the temperature gradient.

Both top-down and bottom-up cracking are computed in the same manner except that the location of the truck axle for each distress is different. Top-down cracking occurs when the truck axles are located at opposite edges of the slab (Figure 2.8). Top-down cracking can be amplified by a negative temperature gradient of the pavement, meaning that the top of the pavement section is cooler than the bottom. This results in fatigue cracking, where the crack initiates from the surface of the pavement and moves downwards. The CTE can magnify the effect of the cracking on the pavement depending on its value. The larger the CTE, the larger is the amount of expansion and contraction. This means that there would be a significant amount of contraction at the top of the slab and expansion at the bottom of the slab, increasing the amount of curling. A larger temperature gradient due to a higher CTE value would amplify the significance of the loads being applied to the joints of the slab, as in the example of Figure 2.8. With the presence of a larger negative temperature gradient due to a pavement with a higher CTE, a greater amount of fatigue damage would be induced as compared to a pavement with a lower CTE.

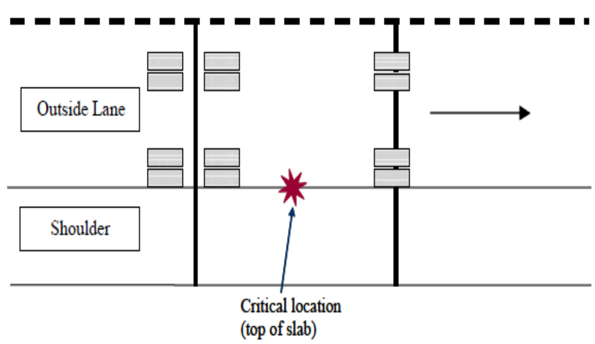

Figure 2.8 Critical load and structural response location for JPCP top-down transverse cracking.

Conversely, bottom-up cracking occurs when the single axle of the truck is located in the center of the slab (Figure 2.9) along with a high positive temperature gradient. This also results in fatigue cracking, but initiates from the bottom of the slab and propagates up. Similar to top down-cracking, bottom-up cracking can be amplified by a positive temperature gradient of the pavement meaning that the top of the pavement section is warmer than the bottom. This means that there would be a significant amount of expansion at the top of the section and contraction at the bottom of the section. The CTE can magnify the effect of the cracking on the pavement depending on its value. This temperature gradient due to a pavement with a high CTE value would amplify the significance of the loads being applied to the center of the slab, as in the example of Figure 2.9. With the presence of a higher positive temperature gradient, a greater amount of fatigue damage would be created as compared to a pavement with a lower CTE value.

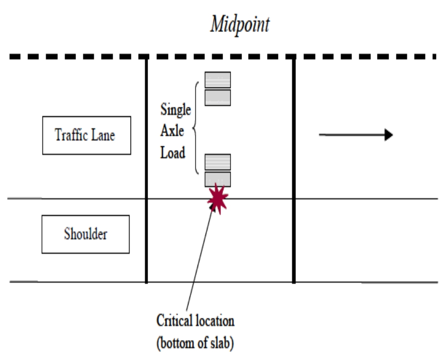

Figure 2.9 Critical load and structural response location for JPCP bottom-up transverse cracking.

The MEPDG uses the following equations to compute top-down and bottom-up cracking of JPCP:

$$CRK = \frac{1}{1 + FD^{-1.68}}$$

where,

CRK = predicted amount of bottom-up or top-down cracking (fraction).
FD = fatigue damage calculated using the following equation.

$$FD = \sum \frac{n_{i,j,k,l,m,n}}{N_{i,j,k,l,m,n}}$$

where,

FD	=	total fatigue damage (top-down or bottom-up).
$n_{i,j,k...}$	=	applied number of load applications at condition i, j, k, l, m, n.
$N_{i,j,k...}$	=	allowable number of load applications at condition i, j, k, l, m, n.
i	=	age (accounts for change in PCC modulus of rupture, layer bond condition, deterioration of shoulder LTE).
j	=	month (accounts for change in base and effective dynamic modulus of subgrade reaction).
k	=	axle type (single, tandem, and tridem for bottom-up cracking; short, medium, and long wheelbase for top-down cracking).
l	=	load level (incremental load for each axle type).
m	=	temperature difference.
n	=	traffic path.

The potential steps that can be taken in order to minimize the effect of top down and bottom-up cracking of the JPCP include:

1. Increase PCC thickness.
2. Increase slab length.
3. Use a widened slab.
4. Use a PCC with lower CTE.

The value of the CTE can be related to the bottom-up and top-down cracking equation through the fatigue damage variable. As the amount of fatigue damage increases, the amount of total cracking also increases. As mentioned above, the CTE can affect the amount of curling, positive or negative, due to the temperature gradient, which in-turn affects the amount of fatigue damage.

The percent slabs cracked is the summation of the top down and bottom-up cracking caused by a truck axle for an entire rigid pavement section. The equation itself is relatively simple and can be computed by;

$$TCRACK = \left(CRK_{Bottom-up} + CRK_{Top-down} - CRK_{Bottom-up} * CRK_{Top-down}\right) * 100\%$$

where,

TCRACK	=	total cracking (percent).
$CRK_{Bottom\text{-}up}$	=	predicted amount of bottom-up cracking (fraction).
$CRK_{Top\text{-}down}$	=	predicted amount of top-down cracking (fraction).

The International Roughness Index (IRI) is related to the smoothness, which is the result of a combination of the initial as-constructed profile of the pavement, any change in the longitudinal profile over time, and traffic (NCHRP 1-37A 2004). A larger CTE value would result in a larger IRI (Jahangirnejad et al. 2009). A higher CTE value could potentially create early life expansion cracks that could impact the overall IRI. The IRI in the MEPDG is computed with the following equations:

$$\mathrm{IRI} = \mathrm{IRI_I} + \mathrm{C1} * \mathrm{CRK} + \mathrm{C2} * \mathrm{SPALL} + \mathrm{C3} * \mathrm{TFAULT} + \mathrm{C4} * \mathrm{SF}$$

where,

IRI	=	predicted IRI, in/mi.
IRI_I	=	initial smoothness measured as IRI, in/mi.
CRK	=	percent slabs with transverse cracks (all severities).
SPALL	=	percent of joints with spalling (medium and high severities).
TFAULT	=	total joint faulting cumulated per mi, in.
C1	=	0.8203
C2	=	0.4417
C3	=	1.4929
C4	=	25.24
SF	=	site factor
	=	AGE $(1+0.5556*FI)*(1+P_{200})*10^{-6}$

Where,

AGE	=	pavement age, yr.
FI	=	freezing index, °F-days.
P_{200}	=	percent Subgrade material passing No. 200 sieve.

$$SPALL = \left[\frac{AGE}{AGE + 0.01}\right]\left[\frac{100}{1 + 1.005^{(-12*AGE+SCF)}}\right]$$

where,

SPALL	=	percentage joints spalled (medium- and high-severities).
AGE	=	pavement age since construction, years.
SCF	=	scaling factor based on site-, design-, and climate-related variables:

$$SCF = -1400 + 350 * AIR\% * (0.5 + PREFORM) + 3.4f'_c * 0.4$$
$$-0.2 * (FTCYC * AGE) + 43h_{PCC} - 536WC\_Ratio$$

where,

SCF	=	spalling prediction scaling factor.
AIR%	=	PCC air content, percent.
AGE	=	time since construction, years.
PREFORM	=	1 if preformed sealant is present; 0 if not.
f'_c	=	PCC compressive strength, psi.
FTCYC	=	average annual number of freeze- thaw cycles.
h_{PCC}	=	PCC slab thickness, in.
WC_Ratio	=	PCC water/cement ratio.

From the information that is computed with the aid of MEPDG, contractors will be provided another tool to determine the quality of the product that they are providing. The engineer will be able to focus on concerns including the potential life of the different concrete pavements if one particular aggregate is chosen over another. The figure below, Figure 2.10, shows a fictitious example of the difference various CTEs of 4.5, 5.5 and 6.5 x 10^{-6}/°C have on the concrete pavements performance including faulting, percent slabs cracked and International Roughness Index (IRI). Everything including traffic, slab length, location and weather conditions were held constant with a varying CTE. Care must be taken when reading the charts due to the different scales in the y-axis.

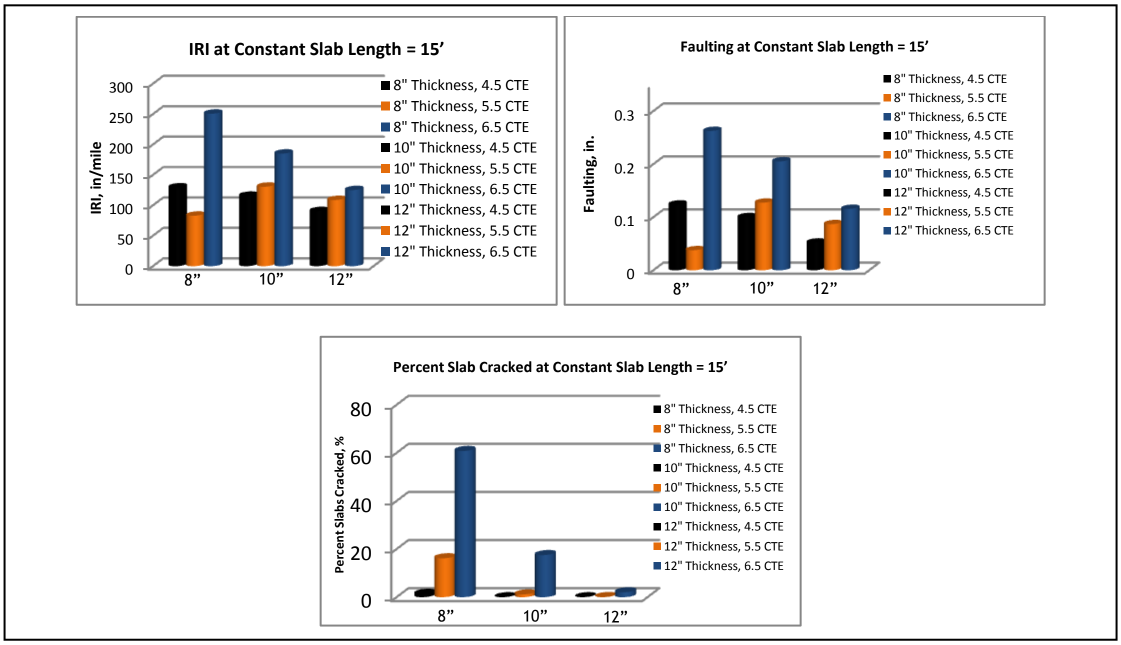

Figure 2.10 Fictitious example of the effect CTE has on concrete performance.

The information provided by MEPDG could then be used to determine the most cost effective option. As it can be seen in Figure 2.10, the concrete pavement that could be determined as the one with the highest quality in-terms of smoothness and lack of cracking, has a slab thickness of 12” and a CTE of 4.5 x 10^{-6} /°F. The problem with this particular pavement is the potential cost, due to the thicker pavement section and potentially higher quality coarse aggregate, of the entire projects. Although the CTE is not an input that can be controlled, the use of certain mineralogy of the coarse aggregate over others can potentially lower the value of the CTE (refer to Table 2.1) making it a more desirable product. Unfortunately, especially in Hawaii, there are not always multiple options of the type of large aggregate to use in a mix and therefore design is dictated by what is readily available. If there is a variation available in the aggregates, a life cycle cost analysis should be done to determine the best alternative, with the aid of programs such as RealCost, which is specifically developed to perform Life Cycle Cost

Analyses (LCCA) of pavement structures (“Asset Management,” 2011). This is outside of the scope of study for this paper and therefore will not be explored.

CHAPTER 3: AGGREGATES AND TEST PROCEDURES

This chapter concentrates on the coarse aggregates used in the mix designs, the various required tests, and the methods for casting, transporting, and testing the concrete specimens for the determination of the CTE to meet AASHTO's standards. Discussions will be provided on the type and location of the three quarries that supplied aggregates for this research. Section 3.1 discusses the locations of the quarries and the mineralogy of the corresponding aggregates. This section will introduce the companies that provided the mix designs and materials for this research. There is also a brief discussion on the aggregate mineralogy used by all three companies. Section 3.2 will look at the field testing that was performed and will discuss how the concrete cylinder samples were made and the standards that were followed. Sections 3.2.1, 3.2.2, 3.2.3, and 3.2.4 will provide the process for determining the slump, the air content and density, the temperature of the fresh concrete, and the procedure for casting the cylinders, respectively. The next section, Section 3.3, discusses the equipment that is required to run the test for the determination of the CTE. Sub-sections within Section 3.3 (Sections 3.3.1, 3.3.2, and 3.3.3) will describe the testing equipment involved in the determination of the CTE including the Linear Variable Differential Transformer (LVDT) and frame, the thermocouples, and the water bath, respectively. Finally, Section 3.4 will go in-depth on how the CTE is calculated. Equations are introduced on how to calculate the correction factor and the CTE of the concrete specimens.

3.1 Aggregate Sources and Mineralogy's

One of the goals of this study was to determine the variation of the CTE of PCC mixes prepared with different aggregate sources found throughout the Hawaiian Islands. Due to limitations, not all of the islands were included in this research; however, there is potential for further work in this area. The three aggregate sources include Island Ready Mix and Hawaiian Cement from the Island of Oahu and West Hawaii Concrete from the Island of Hawaii (also known as the Big Island, which is how it will be referred to in the rest of this thesis). Figure 3.1 shows a Google Maps (2011) image of the Hawaiian Island chain (A.) and two enlarged pictures, one of the Big Island (B.) and the other of Oahu (C.).

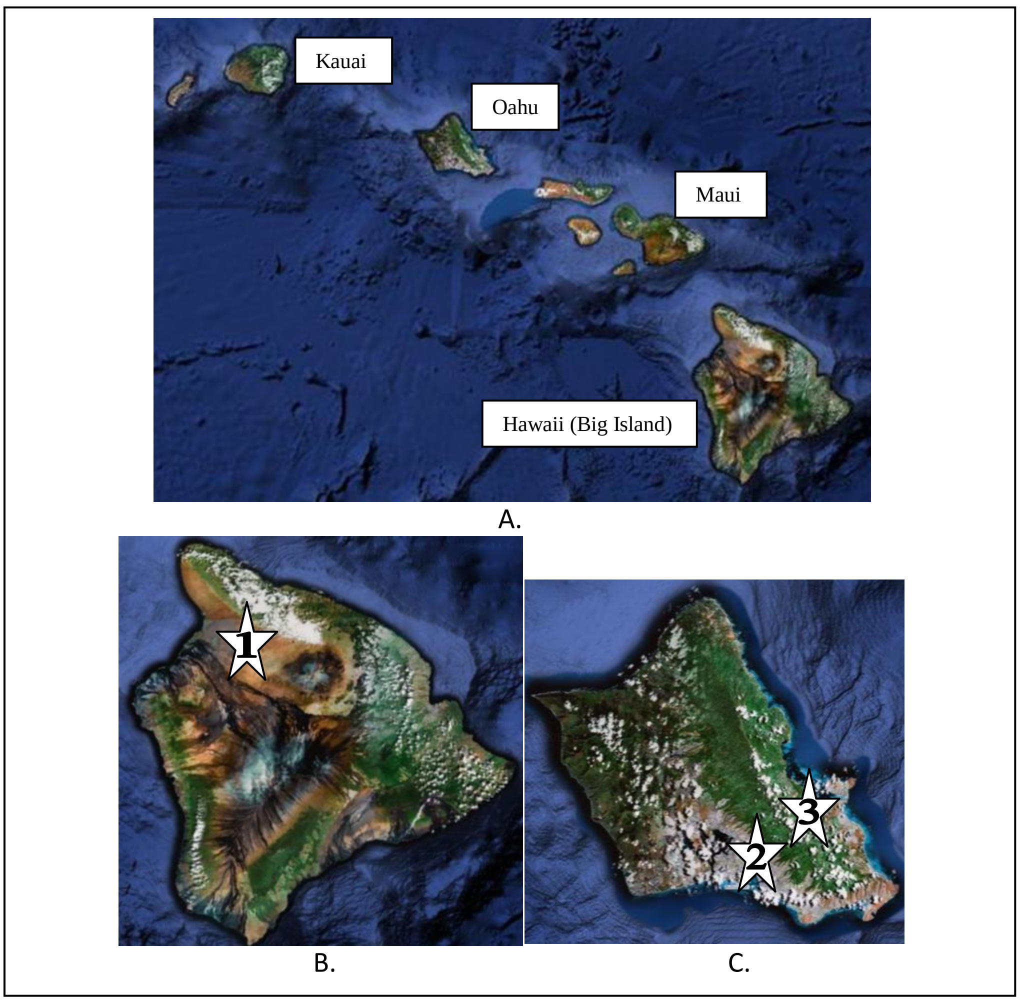

Figure 3.1 Aggregate source locations.

The star in Figure 3.1.B with the number '1' inside of it represents the location of the Waimea Quarry. This was the aggregate source utilized by the West Hawaii Concrete company. This was the only source used in this research not on the island of Oahu that was available for testing. Field tests and the concrete specimens were sampled onsite of the West Hawaii Concrete Mixing Plant. The star in Figure 3.1.C with the number '2' inside of it represents the location of the Halawa Quarry. Hawaiian Cement uses the aggregate from this part of the island for their mixes. Hawaiian Cement used a structural fiber in their mix that will be discussed in further detail in Chapter 4 Analyses and Results. The final star in Figure 3.1.C with the number '3' inside of it represents the location of the Kapaa Quarry. This quarry was used by a company on the west side of Oahu named Island Ready Mix. All of the specimens for this research were field tested and the cylinders were cast onsite of each of the company's mixing yards. The cylinders and the field testing of each of the three individual companies/quarries were produced from the same batch, respectively. This was to assure that the results were representative and to avoid any discrepancies due to varying batches and conditions.

The main focus of this thesis was to determine how the value of the CTE was affected by varying the coarse aggregate in the mix. The coarse aggregate that was used by all three companies consisted of basaltic rock. From Geology.com ("Basalt," 2005-2011) basaltic rock can be defined as "a dark-colored, fine-grained, igneous rock composed mainly of plagioclase and pyroxene minerals. It most commonly forms as an extrusive rock, such as a lava flow, but can also form in small intrusive bodies, such as an igneous dike or a thin sill". The photo below, Figure 3.2, is what typical basaltic rock initially looks like from the Hawaiian Islands. The aggregates are crushed to obtain a maximum nominal size of ¾ inch before they are introduced into the mix. This process of crushing the aggregates takes place onsite at the individual quarry.

Figure 3.2 Hawaiian basaltic rocks from the Big Island.

3.2 Acquiring the Concrete Cylinders

As stated above, the goal of this project was to determine the variation of the CTE of local aggregates in the state of Hawaii. For consistency, all of the concrete test specimens were cast onsite of their respective companies using the same testing procedures throughout. Air travel to the Big Island and automotive travel to local quarries on Oahu was necessary to guarantee the consistency and uniformity of each test method. The next few sections will discuss the field tests that were performed (temperature test, slump test and air content test) as well as the casting of the concrete cylinders.

The field testing and the casting of the concrete cylinders were performed in such a manner that complied with the AASHTO standards. The concrete was poured directly from the concrete trucks into a wheelbarrow and taken directly to the testing area. Here it was immediately stirred to minimize any segregation and any effects of premature drying. Once it was stirred the testing process went as follows: first the temperature test, then the air content test, then the slump test, and finally the casting of the cylinders. These tests were all performed on a solid level surface as stated in the standards. AASHTO specifies a time limit in which all of the field testing should take place. The AASHTO standard for taking the temperature of the freshly mixed concrete is within 5 minutes of obtaining the sample. For the rest of the testing the standard is "that the sample be at least 1 cu ft, used within 15 minutes of the time it was taken, and [be] protected from sunlight, wind, and other sources of rapid evaporation during this period" (Kosmatka et al. 1992). It is important to note that all of the tools used in the testing were dampened prior to use in an attempt to minimize the amount of moisture lost from the mix.

3.2.1 Temperature Test (AASHTO T 309-06)

This test is performed to ensure the conformance of any specific design requirements. Only a temperature measuring device, such as the thermometer in Figure 3.3, is needed for this test. Once a representative sample of concrete is attained and properly mixed to assure uniformity of the mix, the thermometer can be inserted. The temperature measuring device must be placed in the freshly mixed hydraulic concrete in such a way that there is a minimum radius of 3 inches of concrete coverage. The measuring device must be left in the concrete for at least 2 minutes or until the temperature reading stabilizes. This test must be completed in five minutes from the time of attaining the concrete to retrieving the temperature. The ambient temperature should also be recorded as a reference and a guide to assure that the design temperature can be maintained throughout the placement of the concrete.

Figure 3.3 Example of a temperature measuring device, Thermometer.

3.2.2 Air Content of Freshly Mixed Concrete (AASHTO T 152)

There are two different types of meters available to measure the amount of air content of freshly mixed hydraulic concrete. A pressure pot similar to the one shown in Figure 3.4 was used in this research. Once again, a representative sample of the freshly mixed hydraulic concrete must be obtained for this test. All of the field tests that need to be completed (temperature test, air content test, slump test, and casting of the cylinders) must come from the same sample batch.

This test must be performed on a flat, level and hard surface to prevent any bias of the results. The pressure pot and all of the tools needed to perform the test must be dampened, but not saturated, to minimize the amount of moisture loss. The concrete can then be placed in the pot in three layers, rodding each level 25 times while penetrating the lower level by about 1 inch. Between each level the pot should be smartly stricken 12-15 times to eliminate any trapped air. Once the pot is completely filled, the rim should flow over by about 1/8 inch, which is optimal, and the excess should be screened off. The rim is then cleared of any concrete and the top is placed on the bottom pot. This is done to assure an air tight seal to prevent any pressure loss due to air leakage. Water is then placed in the measuring device through the petcocks until all of the excess air is expelled. This can be seen when the opposite petcock is overflowing with water that lacks air bubbles. The air bleeder valve and petcocks are then closed so that pressurized air can be pumped in. Once the initial design air pressure is met for the pressure pot (unique value for each pot), the air can be released. This change in pressure readings is used to determine the air content of the concrete.

Note: This test can be combined in order to determine the density of the concrete. The bottom pot is weighed to determine the weight of the pot empty. Once the pot is filled level to the rim with concrete, it is weighed again. Then the two values are subtracted in order to get the weight of the concrete. That value is then divided by the volume of the pot, which for this study was 0.25 ft^3, to get the density.

Figure 3.4 Type B pressure pot used in research.

3.2.3 Slump test of Hydraulic Cement Concrete (AASHTO T 119M/T 119)

The slump test is performed to determine the amount of slump of plastic hydraulic cement concrete. From laboratory testing a pattern was found that generally the slump will increase proportionally with the amount of water added, giving it an inversely related relationship to the strength of the concrete (AASHTO T 119). This relationship is unclear when it comes to testing the slump in the field. Care was given to acquire the slump from the field for this project, but since strength of the concrete is not of concern, no relationship was researched. In order, to perform the slump test the following materials where needed:

- A metal mold in the form of the frustum of a cone
- A flat rigid steel base
- A tamping rod of diameter of 5/8 inch and length of 24 inches with a hemispherical tip
- A measuring device capable of measuring slump to an accuracy of ¼ inch

To perform the slump test, the mold, base and all of the tools needed for the test should be dampened to minimize moisture loss. The mold must be secured to the base by either clamps or by standing on the foot pieces on a solid rigid surface. The concrete is placed in the mold in three equal levels, rodding each level 25 times while assuring to penetrate the previous level. Unlike the air content test, one should not strike the mold between the levels. Strike off the excess concrete from the top of the mold so it is level with the rim. Continue to hold down the mold and remove the excess concrete from the base of the cone. Slowly and consistently pull the mold vertically off of the base without twisting. Turn the mold upside-down and place it next to the concrete on the base being careful not to disturb the sample. Place the tamping rod horizontally across the mold so that it is centered over the pile of concrete. With a measuring device, measure the amount of slump from the bottom of the tamping rod to the top of the concrete sample. Record the slump to the nearest ¼ inch. Figure 3.5 shows a picture of the equipment used for the slump test and a crude depiction of how the slump is determined.

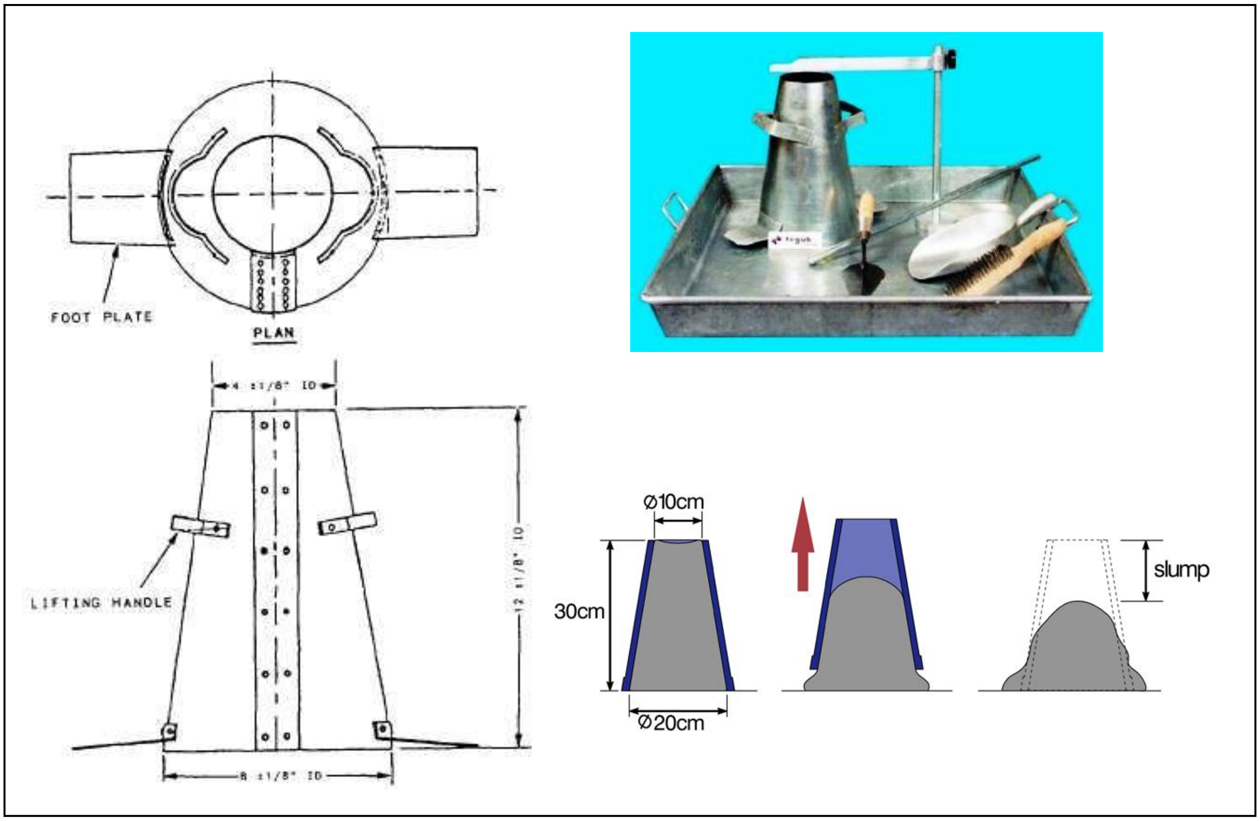

Figure 3.5 Slump test and procedure.

3.2.4 Casting and Curing of the Concrete Cylinders (AASHTO T 23-08)

The casting of the cylinders was the final step of the onsite testing. A total of 15 cylinders where obtained from each of the three companies. This was done so that at each of the five predetermined curing times (3 days, 7 days, 14 days, 28 days and 56 days) a total of three test specimens would allow for an average value to be computed. Results of this experiment are presented in the following chapter, Chapter 4 Analyses and Results.

The concrete cylinders were made according to the AASHTO T 23-08 (ASTM C 31-06) standard. The plastic molds were placed on a flat solid surface near the place where they were to be stored for initial curing. The plastic molds did not need to be moistened, but all other tools for casting the cylinders needed to be moistened. The concrete was mixed once again to minimize the effect of segregation and premature drying. Once the concrete was mixed, a scoop was used to transfer the material from the wheelbarrow to the molds. Care was taken with pouring the concrete into the mold around the perimeter in a circular motion to ensure uniformity of the mix. In this study a 4” x 8” mold was used. The AASHTO T 23-08 standard states that for this size mold it should be filled in two layers, rodding each layer 25 times. The second and final layer should be overflowing the rim no more than approximately ¼” and then the excess should be removed. If during the rodding of the second layer the concrete level falls beneath the rim of the mold, stop rodding immediately and refill the concrete then continue rodding, counting to count from the last number before refilling. After the first and second layer the mold should be ‘smartly’ tapped 10–15 times to release any air bubbles. Once the mold is filled and the top is leveled off, a lid should be placed on top and left to sit, undisturbed, for the initial curing. Figure 3.6 below shows the casting of the 15 concrete cylinders onsite of the Island Ready Mix plant.

Figure 3.6 Casting of concrete cylinders onsite of Island Ready Mix.

The concrete cylinders were also cured according to the AASHTO T 23-08 (ASTM C 31-06) standard. The initial curing was achieved onsite near the location of the casting. The cylinders were placed on a level rigid surface during this curing time. After the 24 hours of initial curing, the cylinders were carefully transferred to the lab. The cylinders were individually transported in bubble wrap to avoid any damage during transit. Once in the lab, the plastic lids and molds were removed from the concrete cylinders, taking care not to damage them. Each cylinder was then uniquely labeled and placed into the 100% humidity curing room.

3.3 Equipment Used in the Determination of the CTE

Determining the CTE of the test specimens requires some specific laboratory equipment and preparation. As per the AASTHO T 336 standard, the average temperature of the water bath, either factory or custom-built, must be recorded and averaged by a series of thermocouples. Then the linear expansion/contraction should be determined and recorded with the aid of an LVDT. A short discussion of the frame used in this experiment is included with the discussion of the LVDT. Finally, there is a description of the water baths used in this study and why they were chosen. A description of the LVDT, frame, thermocouples and water baths are presented in following sub-sections.

3.3.1 Linear Variable Differential Transformer (LVDT) and Frame

A vital element in determining the amount of linear movement of the test specimen was the Linear Variable Differential Transformer (LVDT). The LVDT was able to record the change in length to an accuracy of 0.000001 meters. An LVDT similar to the graphic in Figure 3.7 was used in this research. The LVDT was attached through the top of the frame that held the test specimens. The spring loaded contact tip was centered on the top of each of the individual specimens. The height of the frame needed to be adjusted in such a manner that when the specimen was placed in the frame, the contact tip/rod has a sufficient amount of room to expand and contract. Therefore, according to the depiction of Figure 3.7, the contact tip/rod should be approximately half of the difference between length 'A' and length 'B' when the concrete specimen is in place.

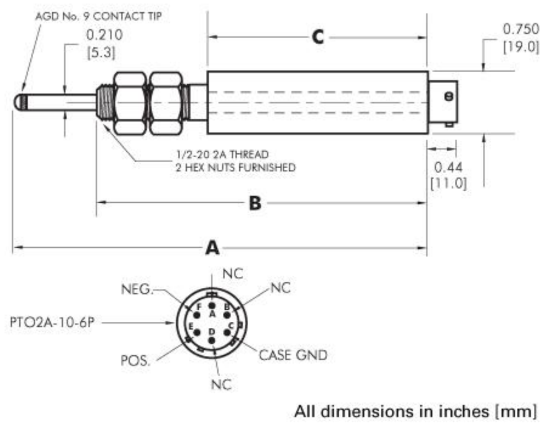

Figure 3.7 Graphic of a typical LVDT.

The frame used in this experiment is made of stainless steel and it is designed to be essentially linearly-elastic, non-corroding, non-oxidizing, and non-magnetic. This is because once the frame starts to corrode or oxidize; the amount of expansion/contraction will change. This could affect the determination of the specimen's CTE, which would introduce a bias to the results. The frame is also adjustable to accommodate for specimens of different lengths and to ensure that the system is level.

3.3.2 Thermocouples

For this study, a total of 4 thermocouples where used to determine the average temperature of the water bath. The 4 thermocouples where located at a depth of 1/4, 1/2, 3/4, and nearly at the bottom of the custom-built water bath. The temperature measuring apparatuses used by this research were type T thermocouples built by the Omega Engineering, Inc company (“Thermocouples,” 2011). The average temperature of the 4 readings was used in the determination of the CTE of each individual concrete specimen. The figure below, Figure 3.8, shows typical thermocouples.

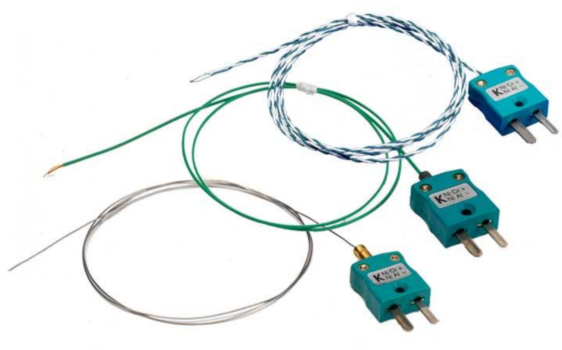

Figure 3.8 Examples of a thermocouple.

There were no thermocouples placed in the factory-built water bath for two reasons: first of all, everything for the experiment, including the frame and concrete cylinders, were located in the custom-built bath and secondly, the factory-built water bath had a built in thermometer.

3.3.3 Water Bath (Custom and Factory-Built)

The water bath that was used in this study was a combination of a custom and factory-built system. As stated in Chapter 2 Literature Review, the study done by Jahangirnejad, Buch, and Kravchenko (2009) shows that there is no significant difference in the results between the factory and custom built water baths. Figure 3.9, which is similar to the photo in Chapter 2 Literature Review, shows the actual water bath system that was used at the University of Hawaii at Manoa.

Figure 3.9 Water bath system used by UH Manoa.

As it can be seen in the photo, there are 4 thermocouples, a frame with a LVDT connected to the top, and an overflow pipe. The system worked by heating or cooling the water in the factory built water bath and then pumping it into the larger custom bath. It was necessary to design a custom water bath because the factory-built bath was not large enough to completely submerge the test specimens. Therefore, the main purpose of the factory-built bath was to heat or cool the water while the custom bath was used to submerge the cylinders. The overflow pipe was positioned above the cylinder so that the water could continue to circulate between baths, while ensuring that the test specimen remained submerged.

3.4 Process of Determining the CTE of Rigid Concrete Pavement

Once the field testing was done, the concrete cylinders were cast, and the specimens cured in the 100% humidity room for the predetermined number of days, it was time to determine the CTE. The specimens were removed from the curing room and immediately sawed down to size. The dimensions of the molds that the concrete was casted in was 4” x 8”. The AASTHO T 336 standard requires that the specimens be 4” x 7 ± 0.1” (180 ± 2 mm). Therefore, the saw in Figure 2.1, in Chapter 2 Literature Review, was used in this experiment to saw the cylinders down to size. A caliper was then used to determine the average length of the test specimen. A total of five measurements were taken per specimen to average its actual length.

After the lengths were recorded, the cylinders were weighed and place into a limewater bath for a minimum of 48 hours. Each specimen was reweighed at a 24 hour interval in its saturated surface dried (SSD) condition and the weight was recorded. This was done to ensure that the condition of 100% saturation was met, to an accuracy of 0.5 percent difference. A discussion was presented in Chapter 2 Literature Review about the reason that 100% saturation is required. The length measurements, as well as the specimen identification, date cast, date removed from humidity room, and saturation measurements, can be found in Figure 3.1 through 3.3. Figure 3.1, 3.2, and 3.3 are for the companies of interest including Island Ready Mix, Hawaiian Cement, and West Hawaii Concrete, respectively.

Table 3.1. Test Specimen Information, Including; IDs, Curing Times, Saturation Measurements, and Length Measurements for Island Ready Mix

Specimen ID	IRM 1	IRM 2	IRM 3	IRM 4	IRM 5	IRM 6	IRM 7	IRM 8	IRM 9	IRM 10	IRM 11	IRM 12	IRM 13	IRM 14	IRM 15
Date Cast	10/28/10	10/28/10	10/28/10	10/28/10	10/28/10	10/28/10	10/28/10	10/28/10	10/28/10	10/28/10	10/28/10	10/28/10	10/28/10	10/28/10	10/28/10
Date Removed from Wet Curing	10/31/10	10/31/10	10/31/10	11/4/10	11/4/10	11/4/10	11/11/10	11/11/10	11/11/10	11/25/10	11/25/10	11/25/10	12/23/10	12/23/10	12/23/10
Age (days)	3	3	3	7	7	7	14	14	14	28	28	28	56	56	56
Test Started	11/2/10	11/4/10	11/5/10	11/7/10	11/10/10	11/12/10	11/14/10	11/15/10	11/16/10	11/29/10	12/1/10	12/2/10	12/27/10	12/28/10	12/29/10
Initial Weight (g)	3435.5	3391.4	3410.0	3430.0	3437.2	3441.8	3476.5	3483.6	3474.0	3471.6	3484.0	3483.3	3504.3	3500.4	3474.7
First Weighing (g)	3451.8	3426.5	3449.5	3444.3	3457.6	3472.5	3491.1	3508.1	3496.7	3494.8	3496.9	3497.3	3516.6	3510.4	3483.8
Difference (g)	16.3	35.1	39.5	14.3	20.4	30.7	14.6	24.5	22.7	23.2	12.9	14.0	12.3	10.0	9.1
Difference (%)	0.47	1.03	1.16	0.42	0.59	0.89	0.42	0.70	0.65	0.67	0.37	0.40	0.35	0.29	0.26
Second Weighing (g)	3454.8	3428.8	3455.6	3447.8	3458.9	3480.1	3493.9	3510.3	3499.4	3498.1	3500.4	3500.4	3518.6	3512.9	3485.0
Difference (g)	3.0	2.3	6.1	3.5	1.3	7.6	2.8	2.2	2.7	3.3	3.5	3.1	2.0	2.5	1.2
Difference (%) (< 0.5 %)	0.09	0.07	0.18	0.10	0.04	0.22	0.08	0.06	0.08	0.09	0.10	0.09	0.06	0.07	0.03
Length Measurements(mm)	178.33	179.32	180.57	179.13	178.96	180.11	180.88	180.26	180.31	180.34	180.24	180.28	180.67	180.60	180.29
	178.11	179.31	180.90	179.53	178.74	180.06	180.87	180.57	180.34	180.44	180.07	180.47	180.47	180.60	180.33
	178.45	178.12	178.12	178.99	178.19	179.75	180.65	180.66	180.03	180.55	180.50	180.38	180.64	180.51	180.24
	178.62	178.82	178.11	178.81	178.33	179.97	180.79	180.47	180.34	180.46	180.20	180.21	180.63	180.42	180.23
	178.41	178.55	178.33	179.07	178.48	179.80	180.86	180.39	180.49	180.42	180.54	180.33	180.83	180.50	180.58
Average (mm)	178.38	178.82	179.21	179.11	178.54	179.94	180.81	180.47	180.30	180.44	180.31	180.33	180.65	180.53	180.33

Table 3.2. Test Specimen Information, Including; IDs, Curing Times, Saturation Measurements, and Length Measurements for Hawaiian Cement

Specimen ID	HC 1	HC 2	HC 3	HC 4	HC 5	HC 6	HC 7	HC 8	HC 9	HC 10	HC 11	HC 12	HC 13	HC 14	HC 15
Date Cast	1/14/11	1/14/11	1/14/11	1/14/11	1/14/11	1/14/11	1/14/11	1/14/11	1/14/11	1/14/11	1/14/11	1/14/11	1/14/11	1/14/11	1/14/11
Date Removed from Wet Curing	1/17/11	1/17/11	1/17/11	1/21/11	1/21/11	1/21/11	1/28/11	1/28/11	1/28/11	2/11/11	2/11/11	2/11/11	3/11/11	3/11/11	3/11/11
Age (days)	3	3	3	7	7	7	14	14	14	28	28	28	56	56	56
Test Started	1/19/11	1/20/11	1/21/11	1/23/11	1/24/11	1/25/11	2/2/11	2/3/11	2/4/11	2/13/11	2/14/11	2/15/11	3/14/11	3/16/11	3/17/11
Initial Weight (g)	3487.5	3477.2	3470.3	3490.2	3492.5	3497.2	3486.2	3478.8	3460.2	3522.6	3493.2	3495.2	3515.8	3513.1	3484.8
First Weighing (g)	3504.6	3486.0	3480.5	3493.0	3494.9	3501.9	3494.8	3488.3	3473.4	3523.0	3493.8	3501.5	3517.9	3515.0	3490.5
Difference (g)	17.1	8.8	10.2	2.8	2.4	4.7	8.6	9.5	13.2	0.4	0.6	6.3	2.1	1.9	5.7
Difference (%)	0.49	0.25	0.29	0.08	0.07	0.13	0.25	0.27	0.38	0.01	0.02	0.18	0.06	0.05	0.16
Second Weighing (g)	3506.4	3489.0	3483.3	3494.3	3496.5	3503.3	3495.7	3489.1	3475.5	3523.1	3494.0	3502.8	3518.9	3515.3	3493.3
Difference (g)	1.8	3.0	2.8	1.3	1.6	1.4	0.9	0.8	2.1	0.1	0.2	1.3	1.0	0.3	2.8
Difference (%) (< 0.5 %)	0.05	0.09	0.08	0.04	0.05	0.04	0.03	0.02	0.06	0.00	0.01	0.04	0.03	0.01	0.08
Length Measurements(mm)	181.09	180.04	180.65	180.43	180.22	180.37	180.77	180.83	180.92	180.84	180.01	180.64	180.69	180.39	181.15
	180.75	180.44	180.21	180.26	180.44	180.62	180.77	180.70	180.45	180.94	180.14	180.51	180.82	180.39	180.65
	180.72	180.59	179.89	180.16	180.76	180.27	180.30	180.29	180.53	180.66	180.81	180.54	180.18	180.92	180.26
	180.87	180.71	180.38	180.52	180.48	180.03	180.57	180.38	180.69	180.67	180.89	180.76	180.69	180.99	180.35
	180.87	180.97	180.52	180.43	180.07	180.21	180.90	180.71	180.75	180.96	180.22	180.73	180.22	180.77	180.61
Average (mm)	180.86	180.55	180.33	180.36	180.39	180.30	180.66	180.58	180.67	180.81	180.41	180.64	180.52	180.69	180.60

Table 3.3. Test Specimen Information, Including; IDs, Curing Times, Saturation Measurements, and Length Measurements for West Hawaii Concrete

Specimen ID	WHC 1	WHC 2	WHC 3	WHC 4	WHC 5	WHC 6	WHC 7	WHC 8	WHC 9	WHC 10	WHC 11	WHC 12	WHC 13	WHC 14	WHC 15
Date Cast	1/20/11	1/20/11	1/20/11	1/20/11	1/20/11	1/20/11	1/20/11	1/20/11	1/20/11	1/20/11	1/20/11	1/20/11	1/20/11	1/20/11	1/20/11
Date Removed from Wet Curing	1/23/11	1/23/11	1/23/11	1/27/11	1/27/11	1/27/11	2/3/11	2/3/11	2/3/11	2/17/11	2/17/11	2/17/11	3/17/11	3/17/11	3/17/11
Age (days)	3	3	3	7	7	7	14	14	14	28	28	28	56	56	56
Test Started	1/26/11	1/27/11	1/28/11	1/29/11	1/30/11	2/1/11	2/5/11	2/6/11	2/7/11	2/19/11	2/20/11	2/21/11	3/19/11	3/20/11	3/21/11
Initial Weight (g)	3565.6	3556.5	3548.0	3568.1	3540.3	3523.8	3564.5	3547.3	3539.9	3587.6	3576.4	3554.6	3595.5	3569.7	3581.1
First Weighing (g)	3579.9	3572.9	3568.0	3576.2	3569.1	3556.3	3570.9	3564.1	3562.6	3589.4	3585.7	3573.9	3599.4	3581.7	3597.5
Difference (g)	14.3	16.4	20.0	8.1	28.8	32.5	6.4	16.8	22.7	1.8	9.3	19.3	3.9	12.0	16.4
Difference (%)	0.40	0.46	0.56	0.23	0.81	0.92	0.18	0.47	0.64	0.05	0.26	0.54	0.11	0.34	0.46
Second Weighing (g)	3583.2	3576.4	3570.7	3579.8	3571.4	3561.9	3572.4	3567.2	3564.4	3590.7	3588.1	3576.0	3601.0	3585.0	3600.0
Difference (g)	3.3	3.5	2.7	3.6	2.3	5.6	1.5	3.1	1.8	1.3	2.4	2.1	1.6	3.3	2.5
Difference (%) (< 0.5 %)	0.09	0.10	0.08	0.10	0.06	0.16	0.04	0.09	0.05	0.04	0.07	0.06	0.04	0.09	0.07
Length Measurements(mm)	180.57	180.23	180.59	180.43	180.31	180.22	180.25	180.57	180.45	180.27	181.06	180.98	180.76	180.80	180.73
	180.49	180.78	180.93	180.43	180.32	180.51	180.34	180.51	180.59	180.25	180.93	180.77	180.57	180.84	180.85
	180.82	180.82	180.93	179.83	180.00	180.69	180.52	180.50	180.61	180.50	180.82	180.85	180.81	180.98	180.62
	180.61	180.65	180.21	179.81	179.85	180.70	180.35	180.54	180.69	180.84	180.72	180.63	180.88	180.76	180.56
	180.50	180.45	180.29	180.42	180.06	180.58	180.48	180.75	180.57	180.81	180.74	180.37	180.82	180.82	180.70
Average (mm)	180.60	180.59	180.59	180.18	180.11	180.54	180.39	180.57	180.58	180.53	180.85	180.72	180.77	180.84	180.69

Once a cylinder had soaked in the limewater for at least 48 hours, it was time to put it into the water bath. There was some pretest setup that was needed for the bath and equipment. The custom bath is positioned on top of the factory-built bath in such a manner that the overflow pipe that is connected to the custom bath is directly above the factory water bath. Both baths need to be filled with regular tap water to the designated level. The 4 thermocouples were then securely placed at staggered depths to achieve a representative average temperature of the custom water bath. Then, prior to placing the frame into the custom bath, the support knobs of the frame and the tip of the LVDT needed a thin layer of waterproof lubrication applied. This was to avoid any friction between the frame, LVDT, and the test specimens. The frame, with the LVDT connected to it, was then placed into the custom water bath. Checks and necessary adjustments were performed to make sure that the frame was leveled. Finally, the test specimen was centered in the frame and it was then ready to begin the CTE testing.

The first test was run with a 410 stainless steel (SS) calibration specimen. The steel calibration specimen was factory machined and designed to be essentially linearly-elastic, non-corroding, non-oxidizing, and non-magnetic, and having a thermal coefficient as close as possible to that of concrete (AASHTO T 336-09). The research done by Crawford et al. (2010) found that the 410 SS specimen was slightly magnetic, but did not show any effect on the value of the CTE. The range of values for the CTE of this particular specimen, $10.1 \times 10^{-6}/°C$ and $10.4 \times 10^{-6}/°C$, was determined by a study done by the FHWA (Crawford et al. 2010) and the value of $10.4 \times 10^{-6}/°C$ was used in all required calculations for this research. Three consecutive tests were done, as per the standard, on the stainless steel specimen to acquire an average value. The equations below, according to the AASHTO T 336 standard, show how the Correction Factor was computed for this study.

$$C_f = \frac{\Delta L_f}{\frac{L_{cs}}{\Delta T}}$$

where,

C_f = correction factor.
ΔL_f = length change of the measuring apparatus during temperature change, mm.
L_{cs} = measured length of the calibration specimen at room temperature, mm.
ΔT = measured temperature change, °C (increase = positive, decrease = negative).

$$\Delta L_f = \Delta L_a - \Delta L_m$$

where,

ΔL_a = actual length change of calibration specimen during temperature change, mm.
ΔL_m = measured length change of calibration specimen during temperature change, mm (increase = positive, decrease = negative).

$$\Delta L_a = L_{cs} * \alpha_c * \Delta T$$

In which α_c is equal to the CTE of calibration specimen, °C (known).

The reason for testing a specimen with a known CTE was to determine the amount of expansion and contraction of the frame, which was translated to the other equation through the correction factor. The following equations show how the CTE was computed. As mentioned earlier, an average CTE of three concrete cylinders was taken for each of the curing times.

$$CTE = \frac{\left({\Delta L_a}/{L_0} \right)}{\Delta T}$$

where,

ΔL_a = actual length change of specimen during temperature change, mm.
L_0 = measured length of specimen at room temperature, mm.
ΔT = measured temperature change (average of the four sensors), °C (increase = positive, negative = decrease).

$$\Delta L_a = \Delta L_m + \Delta L_f$$

in the above equation the variables are,

ΔL_m = measured length change of specimen during temperature change, mm (increase = positive, negative = decrease).
ΔL_f = length change of the measuring apparatus during temperature change, mm.

$$\Delta L_f = C_f * L_0 * \Delta T$$

where,

C_f = correction factor accounting for the change in length of the measurement apparatus with temperature, in.$^{-6}$/in./°C.

The CTE of each individual specimen was determined and then an average of the three test specimens per each curing time was calculated. These values are presented and discussed in the following chapter, Chapter 4 Analyses and Results.

CHAPTER 4: ANALYSES AND RESULTS

This chapter presents the results of the field testing, the CTE testing, and the sensitivity of the MEPDG program. The mix designs for each of the three companies studied are also presented. Section 4.1 covers the results of the field testing as well as their importance. Section 4.2 covers the mix design characteristics for the concrete used in this study. The process of calculating the CTEs and the results are presented in Section 4.3. Microsoft Excel graphs of the output from the water bath experiment are presented to demonstrate the process of calculating the CTE. Section 4.4 provides the inputs that were used for this particular study. A short discussion of what inputs where considered in the Level 1, Level 2, or Level 3 in the MEPDG program. Finally, the sensitivity study with varying CTE in the MEPDG is presented in Section 4.5. The characteristics of the distress limits, faulting, IRI, and percent slabs cracked are described and compared.

4.1 Freshly Mix Concrete Properties

Field testing is an important quality assurance step in the process of testing concrete because it ensures that the freshly mixed concrete is per design. The field testing done for this study, include; ambient and concrete temperature, slump, air content, and density of the concrete. The process for each of these field tests can be found in Chapter 3 Aggregates and Test Procedures. The following table, Table 4.1, shows the results of the field testing done to the freshly mixed concrete at each individual site. The values inside of the parentheses in Table 4.1 are the specifications provided by each of the individual mix designs. It is important to note that all tests passed the quality assurance specifications of the design and that they were done on-site to minimize the effect of any possible error or bias. If the field testing results did not meet the quality assurance specifications of the design, that batch of concrete should not be used. Another batch of freshly mixed concrete would need to be made to meet the design requirements. The standards, as described in Chapter 3 Aggregates and Test Procedures, were followed as closely as possible to maximize uniformity.

Table 4.1. On-Site Field Test Results of Freshly Mixed Concrete

	Island Ready Mix	Hawaiian Cement	West Hawaii Concrete
Ambient Temperature (°C)	29.2	24.6	27.8
Concrete Temperature (°C)	29	26.3	25.0
Slump (in)	2.5 (3.5±1)	4.0 (4.0 MAX)	3.5 (2.5±1)
Air Content (%)	4.0 (3.0±1)	1.6 (2.5±1)	3.5 (3.0±1)
Mold Weight (lbs)	7.80	7.70	8.05
Mold + Concrete Weight (lbs)	44.60	44.90	46.15
Weight of Concrete (lbs)	36.80	37.20	38.10
Volume of Mold (ft^3)	0.25	0.25	0.25
Density of Concrete (pcf)	147.2 (149.6)	148.8	152.4 (149.3)
Number of Specimens Cast	15	15	15

4.2 Mix Designs

The goal of this project was to determine the CTE of the most common mix designs of three separate Hawaiian concrete companies. As mentioned earlier, the three companies consist of two on Oahu (Island Ready Mix and Hawaiian Cement) and one on the Island of Hawaii (West Hawaii Concrete). The mix designs for each of the companies studied can be found in Table 4.2 through Table 4.4. The aggregates from the three quarries consist of basaltic rock that has been crushed into a gradation with a nominal maximum aggregate size of 3/4 inch used as the coarse aggregate. The water/cement (w/c) ratio did vary from one mix to another, but the type (Type I/II) and source of the cement used in all three mixes was from the same location. According to the study done by Tran, Hall, and James (2008), the type or mixture of cement (i.e. cement mixed with fly ash) does not significantly affect the CTE. This was not of concern for this study because, due to time constraints; further testing on the effect that the type or mixture of cement used in the w/c ratio and other variables present in the mixes (i.e. sand, fine aggregates, and admixtures) have on the CTE were not researched.

Table 4.2. Mix Design for Island Ready Mix

Island Ready Mix							
Materials	Cement	Sand	Crushed Fine	3F	3C	Water	Total
Source & Type	Hawaiian (Type I/II)	Maui	Kapaa	Kapaa	Kapaa	C&C	-
SSD Weight (Lbs.)	799	212	845	763	1146	275	4040
Specific Gravity	3.15	2.65	2.65	2.70	2.70	1.00	-
Absolute Volume (ft^3)	4.06	1.28	5.11	4.53	6.80	4.41	26.19
Admixture(s) & Dosage	Master Builders' Pozz 322N (Water-Reducer) @ 1 - 5 oz/cwt, Pozz 100XR (Set-Retarding) @ 0 - 5 oz/cwt, Micro Air (Air-Entraining) @ 0.1 - 1.0 oz/cwt						
Water/Cement Ratio	0.34						

Note: F = Fine, C = Coarse

Table 4.3. Mix Design for Hawaiian Cement

Hawaiian Cement*							
Materials	Cement	#3FW	3/8" Chips	Sand	No. 4	Water	Total
Source & Type	Hawaiian (Type I/II)	Halawa	Halawa	ORCA	Halawa	C&C	-
SSD Weight (Lbs.)	893	1360	338	851	210	275	3927
Specific Gravity	3.15	2.65	2.65	2.69	2.65	1.00	-
Admixture(s) & Dosage	Glenium 3030 (Water-Reducer) @ 54 oz/cy, DELVO (Hydration Control) @ 22 oz/cy, VMA (Viscosity-Modifying) 362 @ 17.9 oz/cy, FIBER (Strength Reinforcement) @ 3.5 Lbs/cy						
Water/Cement Ratio	0.35						

Note: FW = Fine Washed

Table 4.4. Mix Design for West Hawaii Concrete

West Hawaii Concrete						
Materials	Cement	Fine Aggregate	3C	Coarse 3/8" Chips	Water	Total
Source & Type	Hawaiian (Type I/II)	Kona	Waimea	Waimea	C&C	-
SSD Weight (Lbs.)	682	1383	1650	0	317	4032
Specific Gravity	3.15	2.90	2.65	2.65	1.00	-
Absolute Volume (ft^3)	3.47	7.64	9.98	0.00	5.07	26.16
Admixture(s) & Dosage	Micro Air (Air-Entraining) @ 1.36%, Pozz 220N (Water-Reducing) @ 25.23 oz					
Water/Cement Ratio	0.46					

Note: C = Coarse

The (*) next to Hawaiian Cement in Table 4.3 is to note that FORTA-FERRO® Fibers were used in their mix. FORTA-FERRO® Fibers are a plastic fibrous material “made of 100% virgin copolymer/ polypropylene consisting of a twisted bundle non-fibrillating monofilament and a fibrillating network fiber, yielding a high-performance concrete reinforcement system. FORTA-FERRO® is used to reduce plastic and hardened concrete shrinkage, improve impact strength, and increase fatigue resistance and concrete toughness” (“FORTA-Ferro,” 2011). This is noted because Hawaiian Cement is the only company that used the FORTA-FERRO® Fibers, which could affect the measurements of the CTE.

Other admixtures were used throughout the mix designs of each of the companies. The admixtures were used for increased strength, durability, and workability. These design aspects, along with the FORTA-FERRO® admixture, were not part of the scope of this study and therefore their effects were not studied.

4.3 CTE of Cured Specimens

The CTE testing was done at the University of Hawaii at Manoa’s Pavement Laboratory in accordance with AASHTO T 336-09. The concrete test specimens were cured in a 100%

humidity room for 3, 7, 14, 28, and 56 days, which are the typical curing times found in industry for curing concrete. These particular curing times were also chosen to be as representative to actual field conditions while still being able to test the effect that curing time has on the CTE. There was a study by Jahangirnejad et al. (2009), where the curing times of 3, 7, 14, 28, 90, 180, and 365 days were tested. The last few curing times are not very representative unless the concrete was designed for an underwater application.

The first step in calculating the CTE of each specimen is to determine the amount of expansion and contraction of the frame, as stated in Chapter 3 Aggregates and Test Procedures, through the correction factor. Figure 4.1 shows a typical output from the LabVIEW SignalExpress Version 3.0 program in Microsoft Excel format. The outputs from the LVDT reading and the average temperature readings of the water bath from the four thermocouples can be seen in Figure 4.1. The specimen was allowed time for the temperature and the length change (expansion or contraction) to stabilize. This can be seen in Figure 4.1 by the horizontal lines at the end of each heating or cooling cycle. These values were used as inputs in the calculations for the correction factor, which in turn is used later in the calculations of the CTE of the concrete specimens. For example, ΔT for the Expansion 1, in table 4.1, is equal to 49.70˚C - 10.06˚C or 39.64˚C and ΔL_m (the length change of the specimen during the temperature change) is equal to 0.002224m – 0.002168 or 0.000056m (0.056mm). This same procedure was used to determine the amount of expansion and contraction for the two cycles. Then, according the AASHTO T 336-09, the final value for the expansion and the final value for contraction were averaged to determine that particular specimen CTE value. It is important to note that Figure 4.1 is the output from one of the calibration specimen’s test and is unique to this specimen. The two other calibration specimens' tests and each of the concrete specimen's tests are unique and have their own figures similar to Figure 4.1. The outputs for the other tests can be found in Appendix A.

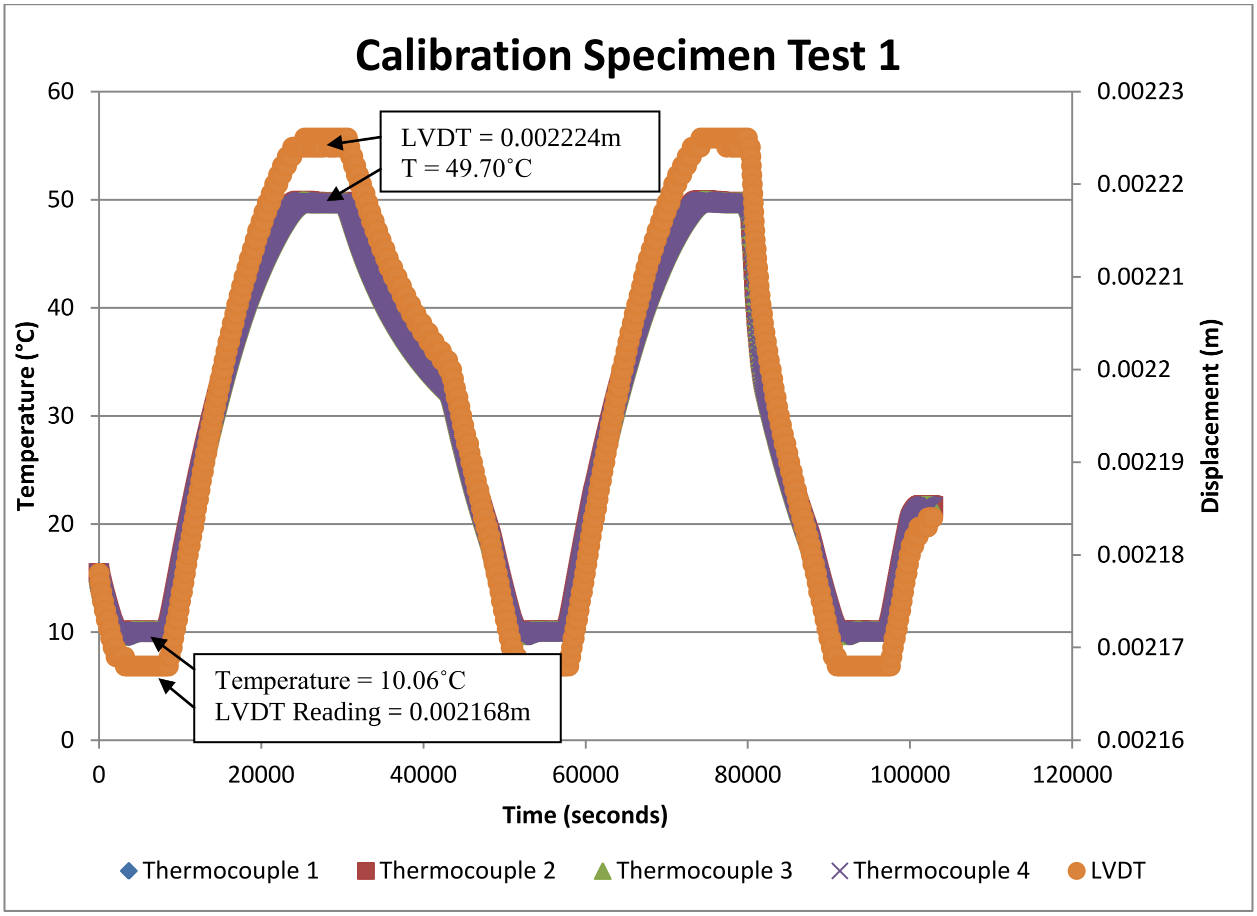

Figure 4.1 Output from a calibration specimen's CTE test in Microsoft Excel format.

The calculations of the correction factor, following the AASHTO T 336-09 standard, of the 410 stainless steel (SS) can be seen in Table 4.5. The calculations for the rest of the specimens can be found in Appendix A. As stated in Chapter 2 Literature Review and Chapter 3 Aggregates and Test Procedures, a range for the value of CTE (α_c) for the 410 SS test specimen to be from 10.1×10^{-6}/°C to 10.4×10^{-6}/°C. For this experiment, the input for the value of the CTE of the steel specimen was taken as α_c = 10.4×10^{-6}/°C, which falls within the range provided by the FHWA study (Crawford et al. 2010). Also, the length of the steel specimen (L_{cs}) was taken with the aid of a digital caliper at room temperature before the CTE test. For this study an L_{cs} = 177.82mm was used throughout the three iterations to calculate the correction factor. The correction factor calculated from the average of the three tests done with the calibration specimen was used for determining the CTE of the concrete cylinders.

Table 4.5. Computation of the CTE of the 410 Stainless Steel Specimens

	Calibration Test 1	Calibration Test 2	Calibration Test 3
Expansion 1			
ΔL_a (mm) $= L_{cs} * \alpha_c * \Delta T$	7.33E-02	7.33E-02	7.33E-02
ΔL_m (mm)	5.7E-02	5.7E-02	5.6E-02
ΔL_f (mm) $= \Delta L_a - \Delta L_m$	1.63E-02	1.63E-02	1.73E-02
$C_f = \Delta L_f / \Delta L_{cs} / \Delta T$	2.31E-06	2.31E-06	2.46E-06
Contraction 1			
ΔL_a (mm) $= L_{cs} * \alpha_c * \Delta T$	-7.33E-02	-7.32E-02	-7.34E-02
ΔL_m (mm)	-5.7E-02	-5.6E-02	-5.6E-02
ΔL_f (mm) $= \Delta L_a - \Delta L_m$	-1.63E-02	-1.72E-02	-1.74E-02
$C_f = \Delta L_f / \Delta L_{cs} / \Delta T$	2.31E-06	2.45E-06	2.46E-06
Expansion 2			
ΔL_a (mm) $= L_{cs} * \alpha_c * \Delta T$	7.33E-02	7.32E-02	7.33E-02
ΔL_m (mm)	5.7E-02	5.6E-02	5.6E-02
ΔL_f (mm) $= \Delta L_a - \Delta L_m$	1.63E-02	1.72E-02	1.73E-02
$C_f = \Delta L_f / \Delta L_{cs} / \Delta T$	2.31E-06	2.44E-06	2.46E-06
Contraction 2			
ΔL_a (mm) $= L_{cs} * \alpha_c * \Delta T$	-7.33E-02	-7.33E-02	-7.33E-02
ΔL_m (mm)	-5.7E-02	-5.6E-02	-5.6E-02
ΔL_f (mm) $= \Delta L_a - \Delta L_m$	-1.63E-02	-1.73E-02	-1.73E-02
$C_f = \Delta L_f / \Delta L_{cs} / \Delta T$	2.31E-06	2.45E-06	2.45E-06
Correction Factor	2.31E-06	2.41E-06	2.46E-06
Average C_f =	**2.39E-06**		

To calculate the CTE of the concretes from the three Hawaiian companies, a similar process to the determination of the correction factor was followed. The equations necessary to compute the CTE of the concrete specimens, according to AASHTO T 336-09, can be found in Chapter 3 Aggregates and Test Procedures. A sample calculation from West Hawaii Concrete for the three day and seven day curing times can be seen in Table 4.6. The ΔT and ΔL_m were measured exactly the same way as in the calibration specimen. The length of the concrete specimen at room temperature, L_0, was taken after curing and before the CTE test. The actual length change of the specimen, ΔL_a, was a function of the specimen length change and the frame's length change, ΔL_f, which was a function of the correction factor. Finally, the CTE could be computed for each of the predetermined curing times.

Table 4.6. Computation of the CTE of the West Hawaii Concrete Specimens at Three and Seven Days Curing

	WHC #1	WHC #2	WHC #3	WHC #4	WHC #5	WHC #6
		3 Day Curing			7 Day Curing	
Expansion 1						
L_0 (mm)	180.60	180.59	180.59	180.18	180.11	180.54
ΔT (°C)	39.9	39.9	39.8	39.9	39.7	39.8
ΔL_f (mm)	1.73E-02	1.73E-02	1.72E-02	1.72E-02	1.71E-02	1.72E-02
ΔL_m (mm)	7.3E-02	7.4E-02	7.3E-02	7.7E-02	7.3E-02	7.1E-02
ΔL_a (mm)	9.03E-02	9.13E-02	9.02E-02	9.42E-02	9.04E-02	8.82E-02
CTE (microstrains/°C)	12.5E-6	12.7E-6	12.5E-6	13.1E-6	12.6E-6	12.3E-6
Contraction 1						
L_0 (mm)	180.60	180.59	180.59	180.18	180.11	180.54
ΔT (°C)	-39.9	-39.9	-39.8	-39.9	-39.7	-39.8
ΔL_f (mm)	-1.72E-02	-1.72E-02	-1.72E-02	-1.72E-02	-1.71E-02	-1.72E-02
ΔL_m (mm)	-7.1E-02	-7.0E-02	-7.1E-02	-7.5E-02	-7.1E-02	-7.0E-02
ΔL_a (mm)	-8.82E-02	-8.72E-02	-8.82E-02	-9.22E-02	-8.84E-02	-8.72E-02
CTE (microstrains/°C)	12.3E-6	12.1E-6	12.3E-6	12.8E-6	12.4E-6	12.1E-6
Expansion 2						
L_0 (mm)	180.60	180.59	180.59	180.18	180.11	180.54
ΔT (°C)	39.9	39.9	39.8	40.0	39.8	39.8
ΔL_f (mm)	1.72E-02	1.72E-02	1.72E-02	1.72E-02	1.72E-02	1.72E-02
ΔL_m (mm)	7.2E-02	7.2E-02	7.2E-02	7.6E-02	7.2E-02	7.1E-02
ΔL_a (mm)	8.92E-02	8.92E-02	8.92E-02	9.32E-02	8.97E-02	8.82E-02
CTE (microstrains/°C)	12.4E-6	12.4E-6	12.4E-6	12.9E-6	12.5E-6	12.3E-6
Contraction 2						
L_0 (mm)	180.60	180.59	180.59	180.18	180.11	180.54
ΔT (°C)	-39.7	-39.8	-40.1	-39.9	-39.8	-39.7
ΔL_f (mm)	-1.72E-02	-1.72E-02	-1.73E-02	-1.72E-02	-1.72E-02	-1.72E-02
ΔL_m (mm)	-7.2E-02	-7.2E-02	-7.2E-02	-7.6E-02	-7.2E-02	-7.1E-02
ΔL_a (mm)	-8.92E-02	-8.92E-02	-8.93E-02	-9.32E-02	-8.97E-02	-8.82E-02
CTE (microstrains/°C)	12.4E-6	12.4E-6	12.3E-6	13.0E-6	12.5E-6	12.3E-6
Ave. CTE (microstrains/°C)	12.4E-6	12.4E-6	12.4E-6	13.0E-6	12.5E-6	12.3E-6
Ave. CTE (per Age) (microstrains/°C)		12.4E-6			12.6E-6	
Ave. CTE (per Age) (microstrains/°F)		**6.9E-6**			**7.0E-6**	

Table 4.7 presents the CTE of each of the 45 concrete specimens tested as well as the average CTE value of the three cylinders per curing time. The missing data point from Island Ready Mix at three days of curing was due to technical problems and therefore was left out. The

value of the CTE for the concretes with Hawaiian basaltic rock that was tested, with a CTE of the calibration specimen of $10.4\times10^{-6}/^{\circ}C$, ranges from $6.0\times10^{-6}/^{\circ}F$ to $7.0\times10^{-6}/^{\circ}F$. If a CTE of the calibration specimen of $10.1\times10^{-6}/^{\circ}C$ had been used for the calculation of this study's CTE, the range would have been lowered to $5.8\times10^{-6}/^{\circ}F$ to $6.8\times10^{-6}/^{\circ}F$. For all calculations in this study a CTE of the calibration specimen of $10.4\times10^{-6}/^{\circ}C$ was used. The CTE of the concrete specimens computed in this study differ significantly with the range of values in the literature for the CTE of basaltic rock as a constituent in the concrete mix from $3.3\times10^{-6}/^{\circ}F$ to $4.4\times10^{-6}/^{\circ}F$ (Mindess et al. 2003).

Table 4.7. CTE Values of the Concretes from Three Companies Along with their Averages

	Island Ready Mix			Hawaiian Cement			West Hawaii Concrete		
	CTE 1	CTE 2	CTE 3	CTE 1	CTE 2	CTE 3	CTE 1	CTE 2	CTE 3
Curing Time	(micro strains/˚F)			(micro strains/˚F)			(micro strains/˚F)		
3 Days	7.1E-06	6.9E-06	-	6.1E-06	6.4E-06	6.4E-06	6.9E-06	6.9E-06	6.9E-06
3 Day Average		7.0E-06			6.3E-06			6.9E-06	
7 Days	6.7E-06	6.9E-06	6.4E-06	6.3E-06	6.6E-06	6.4E-06	7.2E-06	6.9E-06	6.8E-06
7 Day Average		6.7E-06			6.4E-06			7.0E-06	
14 Days	6.1E-06	6.1E-06	6.2E-06	6.1E-06	5.9E-06	6.0E-06	6.9E-06	6.8E-06	6.8E-06
14 Day Average		6.1E-06			6.0E-06			6.8E-06	
28 Days	6.2E-06	6.2E-06	6.1E-06	6.1E-06	6.2E-06	6.0E-06	6.8E-06	6.5E-06	6.6E-06
28 Day Average		6.2E-06			6.1E-06			6.7E-06	
56 Days	6.1E-06	6.1E-06	5.9E-06	6.2E-06	6.3E-06	6.0E-06	6.6E-06	6.4E-06	6.5E-06
56 Day Average		6.0E-06			6.2E-06			6.5E-06	

Figure 4.2 shows the effect of the curing time on the value of the CTE of the three companies. It can be seen from the graph that there is no trend from one curing time to the next between the three companies. For example, the CTE value of Hawaiian Cement and West Hawaii Concrete specimens increase from 3 days to 7 days of curing, while the Island Ready Mix specimen's CTE value decreases. Then, after 7 days of curing, West Hawaii Concrete has a gradual decrease in CTE and the other two companies do not follow a trend. There is no clear explanation for these discrepancies of results between mixes. Nevertheless, in all cases the

values at 3 and 7 days are higher than those at 28 and 56 days. The percentage difference changes with the values selected (3 or 7 days and 28 or 56 days) but are roughly between 5 and 10%. It is clear, due to the large variation of CTEs in Figure 4.2, that curing time played a significant role in the CTE measured in this study. However, there is no recommendation in the MEPDG regarding the most appropriate curing time to determine the CTE of concrete specimens for pavement design. Overall, this study shows that the trend they all follow is that the CTE decreases from 3 days to 56 days, but it tends to stabilize at 28 days. The nonlinearity of each of the three company's results could be due to the amount of cement and coarse aggregates in the mix. For example, since the concrete cylinders were manmade (potential error), the cylinders tested from one curing time to another could potentially have more or less cement or coarse aggregate content even though they came from the same mix.

The trend found in this study contradicts the findings from the study done by Jahangirnejad et al. (2009). Jahangirnejad's et al. (2009) trend showed that the CTE value increased overtime while this study showed a decrease. With the idea of the cement swelling and a potential change in the chemical composition of the cement paste when moist-cured, it is logical that the CTE value decreases with time. However, more studies would be needed to justify the results of this research. Jahangirnejad (2009) also found that "the magnitudes of the measured CTE_{PCC} at the early ages (3, 7, 14, 28 days) were significantly (statistically) different than the magnitudes determined at the end of 90, 180, and 365 days". Due to time constraints, the effects of long term (90, 180, and 365 days) curing times were not analyzed in this study. Further study would be needed to compare long-term results.

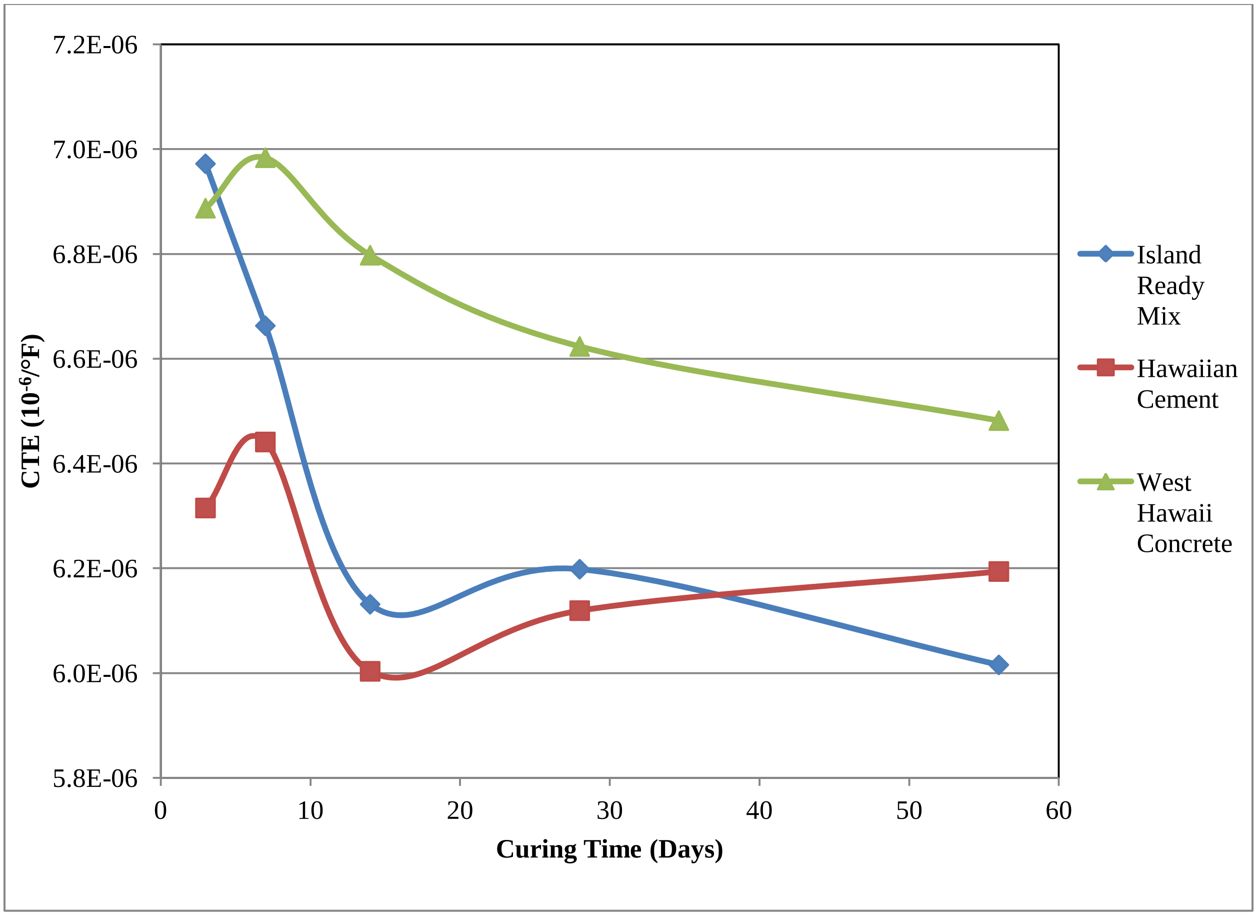

Figure 4.2 Variation of the CTE with respect to curing time of concrete specimens for Hawaiian companies.

4.4 Inputs for Design in MEPDG

Part of this project was to compare the effect that the CTE value found in Hawaii has on rigid Jointed Plain Concrete Pavement (JPCP) design with the aid of the MEPDG program. Currently the Hawaii Department of Transportation (HDOT) does not use the Mechanistic-Empirical Pavement Design Guide (MEPDG) (NCHRP 1-37A 2004) as their pavement design method, but it is considering its implementation. The MEPDG addresses many aspects that were missing or that were inadequately addressed in other pavement design procedures. The consideration of the CTE in the design procedure is perhaps one of the most important shortcomings addressed by the MEPDG. Its consideration gives the engineer a more site-specific design possibility. Several runs of the program were performed to determine the effect that CTE, slab thickness, and slab length have on the design. The figure below, Figure 4.3, is a visual representation of the parameters that went into a sensitivity analysis of PCC pavement designs using the MEPDG software. For every CTE measured in the lab, 3 slab lengths (12, 15, and 18 feet) and 3 slab thicknesses (8, 9, and 10 inches) were considered for inputs into the MEPDG. Therefore, a total of 9 runs were carried out for each of the 15 averaged CTEs (an average of three specimens per curing time) measured, totaling 135 runs.

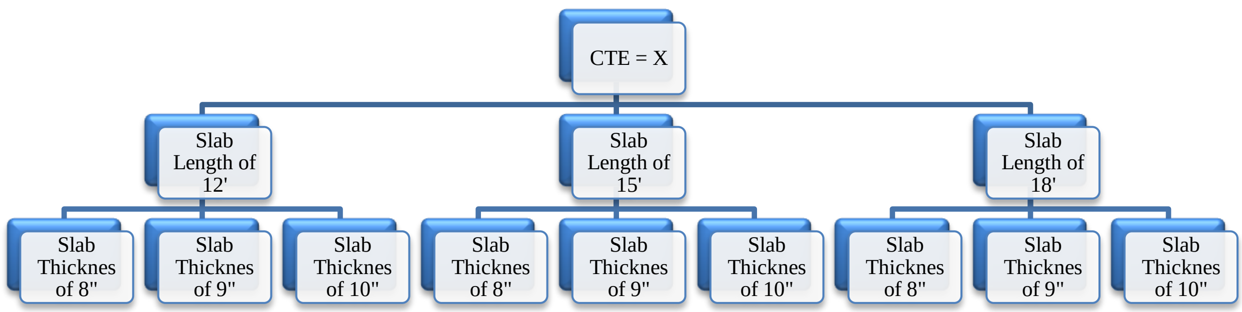

Figure 4.3 Hierarchical relationship of the sensitivity inputs into MEPDG.

Screen shots of the inputs into MEPDG can be seen in Figures 4.4, 4.5, and 4.7. Figure 4.4 has the inputs of the traffic and design life of the pavement section. A design life of 35 years was selected and an AADTT of 4500 was selected as a reasonable value from information provided by the Hawaii Department of Transportation (HDOT) collected in 2006. The project site, where the traffic information and freeway layout was taken, is located on the H1 Freeway (or Queen Liliuokalani Freeway) passing through Kapolei on the Island of Oahu. That section of the freeway is currently three lanes in each direction and was constructed with a PCC.

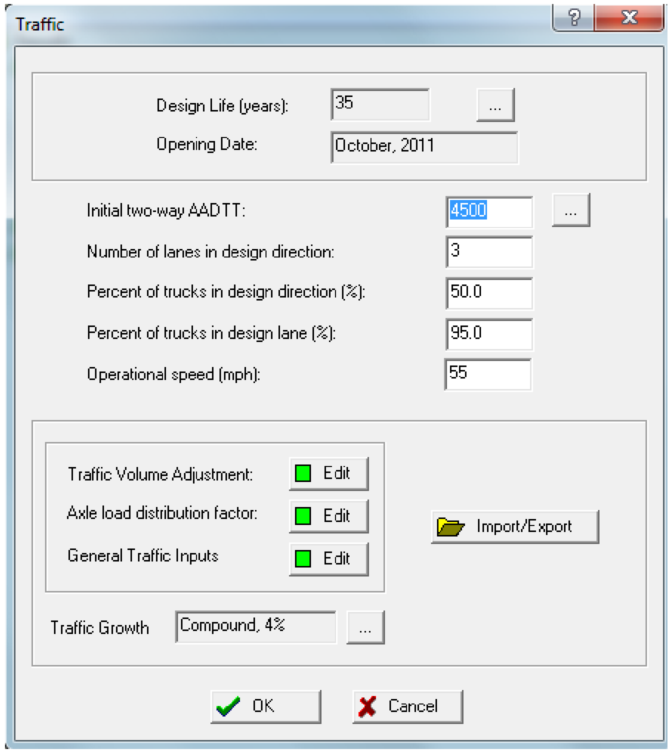

Figure 4.4 Screen shot of traffic inputs into the MEPDG program.

The parameters for the JPCP input are shown in the screen shots in Figure 4.5. This particular run of the MEPDG has a slab thickness of 9 inches and slab length of 15 feet. Also, 1-inch dowels were considered at a spacing of 12 inches to minimize the effect of faulting. This is an important input because this study found that faulting was the limiting distress for the concrete pavement design, which will be discussed later. By increasing the size of the dowels and/or minimizing the spacing of the dowels, as inputs show in Figure 4.4, the amount of faulting would decrease.

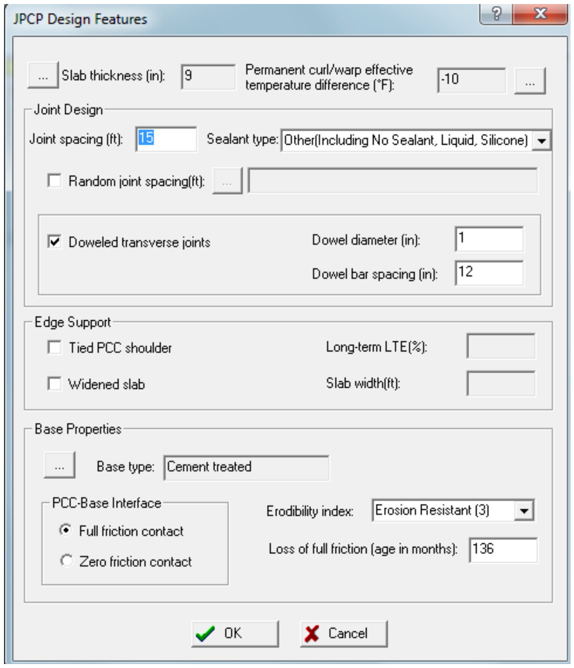

Figure 4.5 Screen shot of the JPCP design features into the MEPDG program.

Figure 4.6 shows the characteristics of a representative pavement cross-section in the area of this study. The thicknesses and type of materials were obtained from a computer program developed at UH (Archilla and Diaz, 2011) to analyze the data from a pavement data mining effort performed by HDOT. The section consisted of a rigid PCC material (8 to 10 inches thick), a 4-inch layer of a chemically stabilized material, a 6-inch layer of crushed gravel, followed by an "infinite" layer of low plasticity clay (CL) subgrade. The subgrade information was obtained from the United States Department of Agriculture's (USDA) soil classification charts ("Published Soil Surveys," 1972).

Figure 4.6 Pavement Structure of H1 by Kapolei used in this study.

Certain aspects of the layers were inputs that the MEPDG program recommended, such as Poisson's ratio and the coefficient of lateral pressure which is designated by a Level 3 input. Table 4.8 shows the inputs from the MEPDG program required for the climate, structure, and pavement layers.

Table 4.8 Climate, Structure and Pavement Layer Inputs into the MEPDG Program

Parameter	Input
Climate	
Location	Honolulu International Airport
Depth to water table	10 ft
Structure	
Joint spacing	15 ft
Slab thickness	9 in.
Dowels	yes
Layers (from top to bottom)	
Portland Cement Concrete (PCC)	
Layer thickness	9 in.
Coefficient of Thermal Expansion	6.1, 6.2, 6.6 x 10^{-6}
Joint spacing	15 ft
Unit Weight	150 pcf
Poisson's Ratio	0.2
Cement Stabilized	
Layer thickness	4 in.
Elastic/resilient modulus	2000000 psi
Unit Weight	150 pcf
Crushed gravel	
Layer thickness	6 in.
Modulus	25000 psi
Subgrade (CL)	
Layer thickness	∞
Modulus	16000 psi

4.5 Design Sensitivity with MEPDG

This section illustrates the effect of CTE on pavement performance by using the MEPDG. The effects of changes in CTE are shown for a Jointed Plain Concrete Pavement (JPCP) section with all other variables held constant. The purpose of the analysis was not to show absolute values of the different distresses as these may vary for different design parameters (slab thickness, use of dowels, joint spacing, traffic, and climate conditions). Instead the goal was to illustrate the differences that can be observed in the amount of time required to reach the individual distress thresholds with the different CTE values obtained in this study. The analysis also intends to illustrate the difference between using a level 3 analysis (with a default CTE value for PCC mixes with basaltic aggregates) and using a level 1 analysis with the CTE value corresponding to one of the local mixes analyzed in this study.

The outputs from the MEPDG program, the effect of changing the CTE, slab length, and slab thickness were studied. As expected, the pavement performed the best with a lower CTE, a shorter slab length, and a higher slab thickness. In Figures 4.7 through 4.10, the influence that a varying CTE has on faulting, IRI, and percent slabs cracked with a constant slab length and thickness is shown. A slab thickness of nine inches and length of 15 feet was used to compare the distress results because that is representative of the thickness and length used by the HDOT in the area studied (H1 passing through Kapolei). It must be pointed out however, that these sections were not originally built with dowels. The results from the other slab thicknesses (8 and 10 inches) and slab lengths (12 and 18 feet) are presented in Appendix B.

It can be seen in the following figures that a change in CTE does affect the amount of time for the pavement to reach the individual distress limit. It is important to note that the difference in the CTE is not only caused by curing time, but also the age of the concrete. When the concrete stops curing after 7 days, the concrete still hydrates and the CTE will continue to change. The faulting distress threshold of 0.12 inches with a reliability target of 90 percent was used for this study. From Figure 4.7, the difference from using the largest CTE value to the smallest is nearly three years. This time difference can be exaggerated with a change in the pavement section as well.

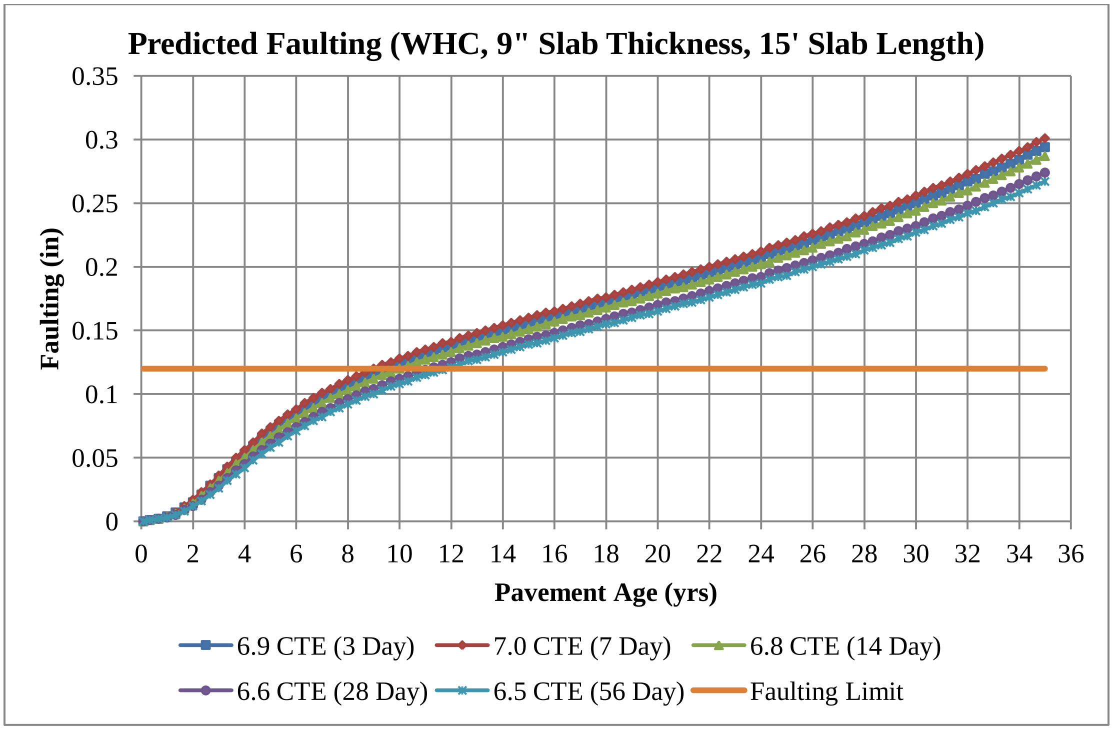

Figure 4.7 Predicted faulting in MEPDG with constant slab length and thickness with varying CTE from West Hawaii Concrete.

The IRI is a combination of the initial construction roughness with the roughness gained over time. Since a new pavement is never 100% smooth, an initial roughness of 63 in/mi was considered. An IRI distress target of 172 in/mi with a reliability target of 90 percent was chosen. Similar to the faulting distress, the IRI had a difference, when changing the value of the CTE from 7.0×10^{-6}/°F to 6.5×10^{-6}/°F, of nearly 5 years. This difference can be seen in Figure 4.8.

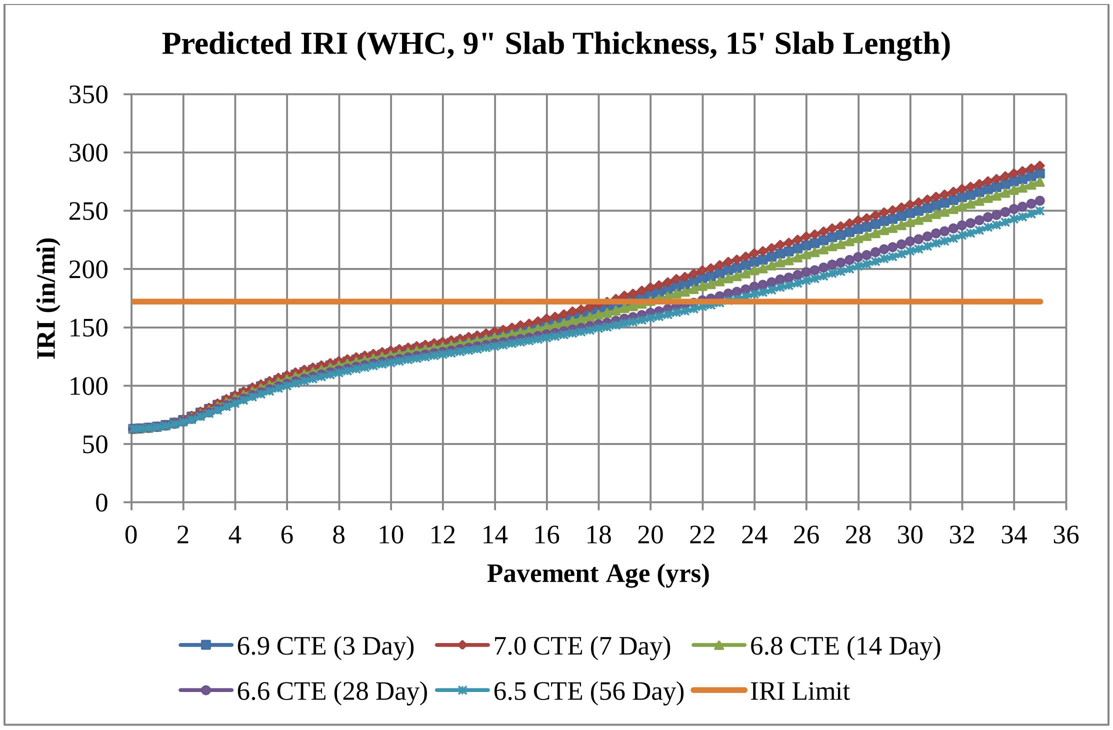

Figure 4.8 Predicted IRI in MEPDG with constant slab length and thickness with varying CTE from West Hawaii Concrete.

As stated in Chapter 2 Literature Review, the percent slabs cracked is a function of the top-down and bottom-up cracking. The MEPDG output for percent slabs cracked can be seen in Figure 4.9. The distress target of 15 percent with a 90 percent reliability target was used to judge the quality of each pavement section in terms of slabs cracked. The inputs into the MEPDG for Figure 4.9 consisted of a pavement section of a length of 15 feet and a thickness of 9 inches, with a varying CTE. All other inputs including traffic, climate, and structure were held constant.

As it can be seen from Figure 4.9, the pavement section reaches the fatigue target of 15 percent with a reliability target of 90 percent after nearly 18 years. This range from 17.7 to 22.3 years or nearly five years is unique to these set of circumstances and can vary greatly depending on the slab length and thickness. Other figures of percent slabs cracked for the two other companies can be found in Appendix B.

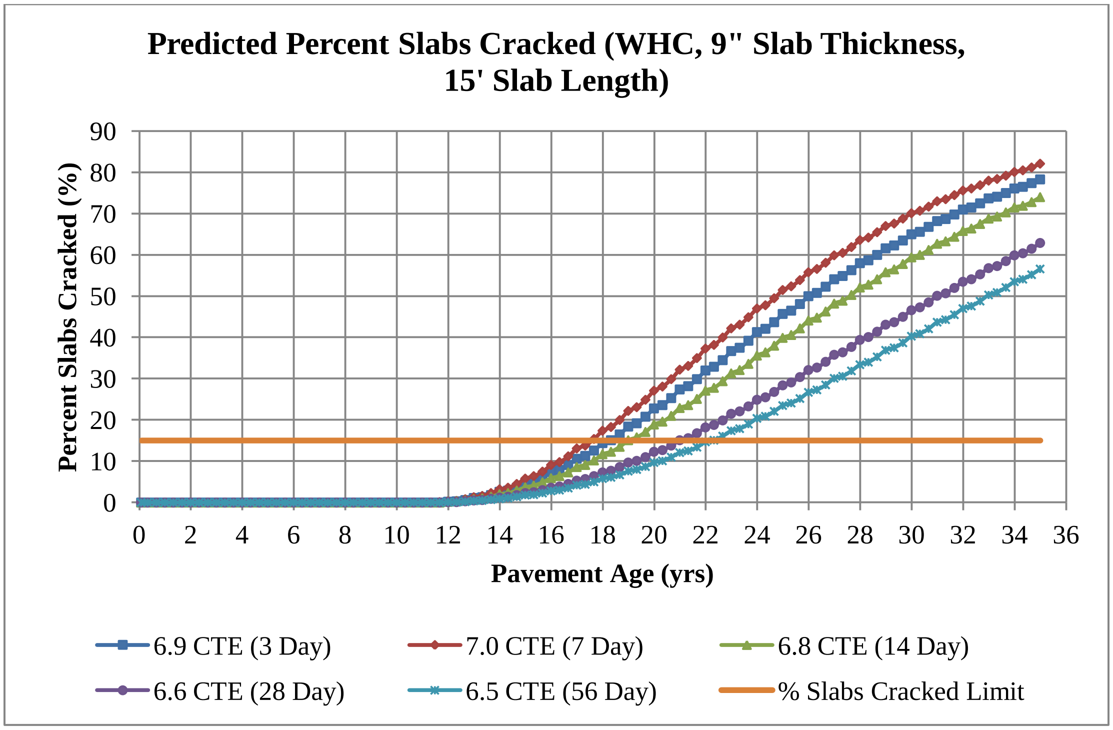

Figure 4.9 Predicted percent slabs cracked in MEPDG with constant slab length and thickness with varying CTE from West Hawaii Concrete.

An important aspect of the MEPDG program is the fact that it can give a designer a realistic idea of a pavement's service life. The controlling distress can vary from one design to the next depending on certain factors, including traffic characteristics, weather patterns, and especially the pavement section characteristics. For this particular design, faulting was determined to be the limiting distress for the pavement's service life, as seen in Figure 4.10. The design parameters were all held constant with a slab length of 15 feet and a slab thickness of 9 inches, and the only variable was the value of the CTE. The pavement section included dowels in the design (1" diameter at 12" spacing for this study). The CTE was taken from 28 days of curing for each of the Hawaiian companies. The only value that was not computed from this research is an accepted CTE value of 4.8×10^{-6}/°F (Kosmatka et al. 1992). From Figure 4.10, the importance of designing with the actual tested CTE for the mix is shown by the difference in service life. For example, if a value of 4.8×10^{-6}/°F were used in a design instead of the range found in this study of 6.1×10^{-6}/°F to 6.6×10^{-6}/°F, the design could be overestimated by nearly 20.5 years (with faulting being the limiting distress for the particular case studied).

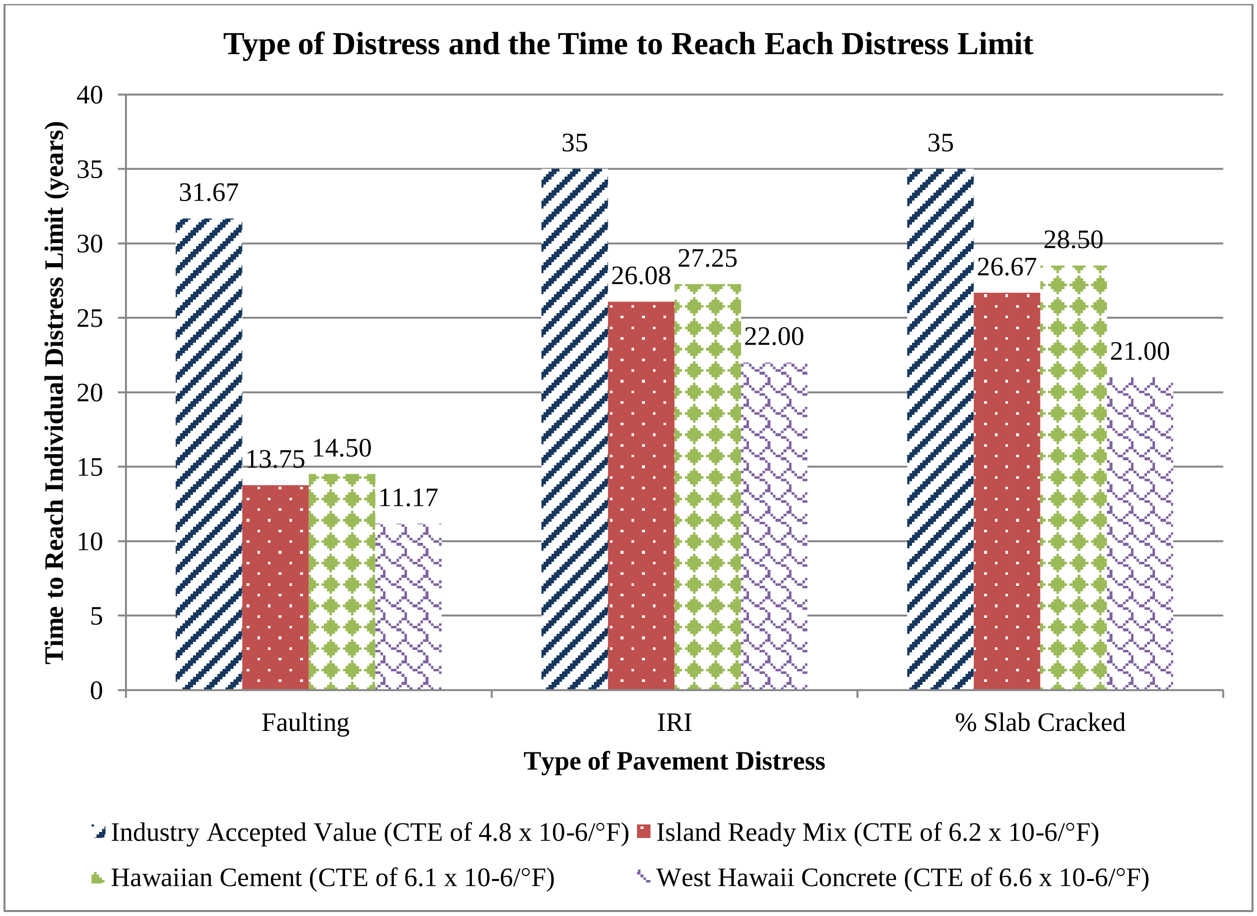

Figure 4.10 Effect of the Average 28 Day Curing Time CTE on the service life of a concrete pavement.

As expected and seen in Figure 4.10, the CTE affects the service life of the pavement. For instance, the higher the CTE the shorter the expected service life. An example of this is that for faulting there is nearly a 3.5 year difference in the service life from 6.1 to 6.6×10^{-6}/°F. The service life differences can be compared for the two other distresses in Figure 4.10. As mentioned above, the default value for the CTE of basaltic aggregates is 4.8×10^{-6}/°F, which is much lower than the values found in this study. If this default value is used in the MEPDG over the local values, the design will be overestimated (Figure 4.10).

CHAPTER 5: SUMMARY AND CONCLUSION

5.1 Summary of Work Performed

Three Hawaiian Companies were involved in the determination of the coefficient of thermal expansion of concrete mixes found in Hawaii. A total of 45 concrete cylinders were cast, 15 from each company (three per curing time), and all quality assurance field testing was completed at the batching plants. Codes and standards, provided in the text, were followed to minimize any bias or human error from the equation.

An introduction to other similar studies that have measured the coefficient of thermal expansion is presented in Chapter 2 Literature Review. This was important to understand and gave this study a direction in-order to proceed. This study found similar results to other studies but there were a few discrepancies found that have been described in Chapter 4 Analyses and Results.

The variables that were studied include the type/location of the aggregate and the curing time. Each set of 15 concrete cylinders per company were cured for a predetermined amount of time of 3, 7, 14, 28, and 56 days. The locations of the quarries where the aggregates were mined as well as the mix designs from each of the companies can be found in Chapter 3. The field tests performed, as well as the process of determining the CTE and the equipment needed, can also be found in Chapter 3.

The results from the field testing, CTE testing, and sensitivity testing of the Mechanistic-Empirical Pavement Design Guide (MEPDG) program can be found in Chapter 4 Analyses and Results. The field testing was completed and presented solely for quality assurance measures. It is important that the concrete being tested is actually what was designed by the engineer. Graphs and tables were designed to show the effect that curing time and type/source of the aggregate had on the CTE value. The sensitivity analysis was performed to give pavement designers or potentially political entities a practical resource to show the importance of CTE as a design input.

Finally, recommendations were made to improve the repeatability of the CTE test and give the Hawaii Department of Transportation (HDOT) a potential range of values for some of the aggregates found in Hawaii.

5.2 Factors Affecting the CTE and Pavement Performance

From the constituents of a mix design to the construction of the test specimens themselves, there are many factors that can affect the outcome of determining the value of the CTE. Once the CTE has been determined, the MEPDG allows for many inputs to customize a pavement design, and this also presents multiple variables. Due to time constraints, not all of the factors that could potentially affect the value of the CTE were studied. The factors that were studied in this research showed how the sensitivity of the change in the CTE may be affected by the change in just one variable.

5.2.1 Factors Effecting the Measurement of CTE

This research has returned some interesting results that could benefit the industry in a positive manner. The main conclusions of this study include:

- There is a large discrepancy between the industry accepted CTE for basaltic rock ($4.8 \times 10^{-6}/°F$) compared to the values found in Hawaii (6.1 to $6.6 \times 10^{-6}/°F$). This can lead to an inaccurate and overestimated design.

- There is an effect on the CTE of each mix design as a function of curing time (3, 7, 14, 28, 56 days). It was found that the longer the concrete specimen spent in the humidity room, the lower the CTE.
- The AASHTO T 336 method is appropriate for determining the CTE and it is easy to replicate with suitable equipment.

5.2.2 Sensitivity of the Pavement Performance

The sensitivity of the MEPDG program with concerns to a change in the CTE value, slab length, and slab thickness was considerable. The change in the CTE was the main focus for this project, but the effects of slab thickness and slab length was also explored. The results of changing the CTE were as expected, through the output from the MEPDG program in the form of pavement service life.

The CTE value found in the literature was equal to 4.8×10^{-6}/°F (Kosmatka et al. 1992), and it showed that a pavement section with a slab length of 15 feet and a slab thickness of 9 inches would last nearly 32 years before one of the distress target limits was met (faulting). On the contrary, that same section with a different CTE value computed from a mix in Hawaii only lasted approximately 11 years (refer to Figure 4.10). This is a considerable overestimate of a concrete pavement design. This substantial difference is the more important when considering that the MEPDG is not yet locally calibrated. Thus, when determining the local MEPDG calibration factors it is important that the locally determined CTE values be used.

5.3 Recommendations

This study discovered some interesting findings, but it also brought up more questions. Further study could potentially focus on:

- Including more companies from all five major islands (Oahu, Kauai, Maui, Molokai, and Hawaii) to increase the reliability of the study, since due to time and economical reasons, only three of the potential five quarries were studied. This could help solidify a range of values that could be used as a Level 2 input into MEPDG for Hawaiian mixes.
- Due to the large discrepancy between the values found in this study, 6.1 to 6.6$\times 10^{-6}$/°F, and that of the accepted value of 4.8 $\times 10^{-6}$/°F for basaltic rock, more testing would be warranted. Testing the accuracy of the system with another type of calibration specimen (i.e. 304 stainless steel) would be an economical route to verify this study's results.
- This study contradicts the findings found by Jahangirnejad et al. (2009). More testing on the effects of the curing time would be warranted to determine the discrepancy between the two papers.
- The MEPDG does not indicate in its manual which curing time to use for the determination of the CTE. As seen in Figure 4.2, the CTE is unstable until about the 28 days of curing time and then it tends to stabilize. This study shows that the value of the CTE for the design should be taken from the curing time of 28 days. This is due to the fact that after 28 days of curing, the rate of hydration of the cement tends to slow significantly.
- The CTE can have a significant effect on the outcome of a MEPDG pavement design. The effect of a small change in the value of the CTE can have a large effect on the years

of the pavement's service life. As expected, the higher the value of the CTE the shorter the service life. This study's findings reconfirm this fact.

5.4 Future Research Opportunities

The goal of this study was to determine the value of the coefficient of thermal expansion of aggregates found in the state of Hawaii and the effect that curing time has on the CTE. The results found were interesting, but also invoked some more questions.

Future research would be important to answer some of the questions and also solidify this study's results with a large scale project. Future research opportunities include:

- Perform chemical and performance tests on the aggregates used throughout Hawaii to determine if they are unique or not.
- Study the effect that moist curing, versus oven-dry curing, versus oven-dry and moist curing combined has on the CTE. This could help determine the effect that swelling of the cement paste has on the CTE and also determine how much each particular paste swells.
- For a more controlled study, the cylinders could be cast in the lab so that each individual constituent of the mix can be managed. For this study the coarse aggregate was of concern, but if one was able to control the mix, other properties could be researched, including the effect of: water/cement ratio, fine aggregates, sand, admixtures, and mix proportions as well.
- Calibrate and validate the MEPDG. Although the MEPDG is not currently being used as a design tool for HDOT, the design of the existing concrete pavements could be used as input into the program and the output compared to the distresses in the field if measurements of these are available.

REFERENCES

U.S Department of Transportation Federal Highway Administration. *Asset Management.* April 7, 2011. http://www.fhwa.dot.gov/infrastructure/asstmgmt/lccasoft.cfm (accessed September 27, 2011).

http://www.pewcenteronthestates.org/ (accessed April 13, 2011).

2008 AASHTO Provisional Standards. Washington, D.C.: American Association of State Highway and Transportation Officials, 2008.

American Society of Civil Engineers. *Report Card for Amaerica's Infrastructure.* 2010. http://www.infrastructurereportcard.org/state-page/hawaii (accessed September 17, 2010).

Archilla, A. R., and L. G. Diaz. "Development of an Inventory Processing Tool to Generate Historical Pavement Structure Information." *Proceedings of the 8th International Conference on Managing Pavement Assets, ICMPA 2011, November 15-19.* Santiago, Chile (forthcoming), 2011.

Basalt. What is Basalt,How Does it Form and How is it Used? 2005-2011. http://geology.com/rocks/basalt.shtml (accessed March 20, 2011).

Crawford, Gary L., Jagan M. Gudimettla, and Jussara Tanesi. "Inter-Laboratory Study on Measuring Coefficient of Thermal Expansion of Concrete." *Transportation Research Record: Journal of the Transportation Board, No.2164, Transportation Research Board of the National Academies, Washington, D.C.*, 2010: pp. 58-65.

Fisher Scientific. *Isotemp Bath Circulators.* 2005. http://mcdonald.ucdavis.edu/Manual/IsotempBathCirculators.pdf (accessed Decemember 13, 2010).

FORTA-Ferro . 2011. http://www.forta-ferro.com/products/macrofibers/forta-ferro/ (accessed August 9, 2011).

"Guide for Mechanistic-Emperical Design of New and Rehabilitated Pavement Structures." *Final Report for Project 1-37A, Part 1 and 3, Chapter 4. TRB, National Research Council, Washington D.C.* March 2004. www.trb.org/mepdg/ (accessed April 2010).

Hall, Kevin D., and Steven Beam. "Estimating the Sensitivity of Design Input Variables for Rigid Pavement Analysis with a Mechanistic-Empirical Design Guide." *Transportation Research Record: Journal of the Transportation Board, No.1919, Transportation Research Board of the National Academies, Washington, D.C.*, 2005: pp. 65-73.

Huang, Yang H. *Pavement Analysis and Design.* Upper Saddle River, New Jersey: Prentice Hall, 1993.

Interstate H-3. August 2, 2011. http://en.wikipedia.org/wiki/Interstate_H-3 (accessed February 13, 2011).

Jahangirnejad, Shervin. "Evaluation fo Portland Cement Concrete Coefficient of Thermal Expansion Test Protocol and the Impact of the CTE on Performance of Jointed Concrete Pavements." A Dissertation, Michigan State University, 2009.

Jahangirnejad, Shervin, Neeraj Buch, and Alexandra Kravchenko. "Evaluation of Coefficient of Thermal Expansion Test Protocol and Its Impact on Jointed Concrete Pavement Performance." *ACI Materials Journal, V. 106, No. 1*, 2009: 64-71.

Kosmatka, Steven H., and William C. Panarese. *Design and Control of Concrete Mixtures (Thirteenth Edition).* Skokie, Illinois: Portland Cement Association, 1992.

Mallela, Jagannath, Ala Abbas, Tom Harman, Chetana Rao, Rongfang Liu, and Michael I. Darter. "Measurement and Significance of the Coefficient of Thermal Expansion of Concrete in Rigid Pavement Design." *Transportation Research Record: Journal of the Transportation Board, No.1919, Transportation Research Board of the National Academies, Washington, D.C.*, 2005: pp. 38-46.

Mindess, Sidney, J. Francis Young, and David Darwin. *Concrete.* Upper Saddle River: Prentice Hall, 2003.

Omega. *Thermocouples an Introduction.* 2011. http://www.omega.com/prodinfo/thermocouples.html (accessed September 28, 2011).

Pavements. http://www.fhwa.dot.gov/pavement/pccp/thermal.cfm (accessed September 2010).

Standard Specifications for Transportation Materials and Methods of Sampling and Testing. Washington, D.C.: American Association of State Highway and Transportation Officials, 2010.

Tanesi, Jussara, Gary Crawford, Mihai Nicolaescu, Richard Meininger, and Jagan Gudimettla. "How will the new AASHTO T336-09 CTE Test Method Impact You?" *Transportation Research Record: Journal of the Transportation Board, No.2164, Transportation Research Board of the National Academies, Washington, D.C.*, 2010: 52-57.

Tanesi, Jussara, M. Emin Kutay, Ala Abbas, and Richard Meininger. "Effect of Coefficient of Thermal Expansion Test Variability on Concrete Pavement Performance as Predicted by Mechanistic-Emperical Pavement Design Guide." *Transportation Research Record: Journal of the Transportation Board, No.2020, Transportation Research Board of the National Academies, Washington, D.C.*, 2007: pp. 40-44.

Tran, Nam H., Kevin D. Hall, and Mainey James. "Coefficient of Thermal Expansion of Concrete Materials." *Transportation Research Record: Journal of the Transportation Board, No.2087, Transportation Research Board of the National Academies, Washington, D.C.*, 2008: pp. 51-56.

United States Department of Agriculture. *Published Soil Surveys for Hawaii.* 2011. http://soils.usda.gov/survey/printed_surveys/state.asp?state=Hawaii&abbr=HI (accessed November 1, 2010).

USGS. *Materials in Use in U.S. Interstate Highways.* October 2006. http://pubs.usgs.gov/fs/2006/3127/2006-3127.pdf (accessed July 22, 2011).

Won, Moon. "Improvements to Testing Procedures for Concrete Coefficient of Thermal Expansion." *Transportation Research Record: Journal of the Transportation Board, No.1919, Transportation Research Board of the National Academies, Washington, D.C.*, 2005: pp. 23-28.

APPENDIX A: CTE TEST RESULTS

Calibration Specimen

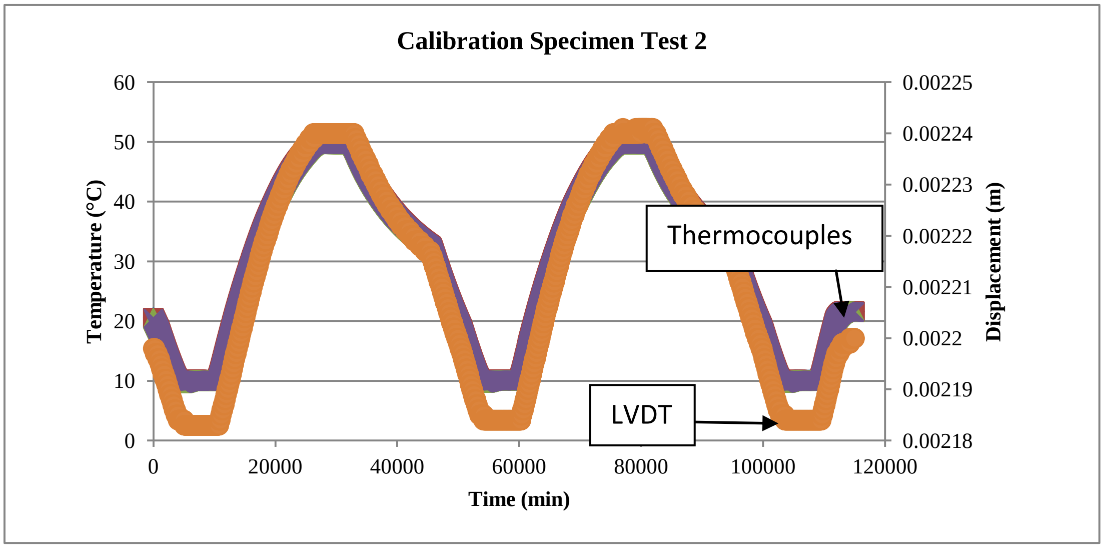

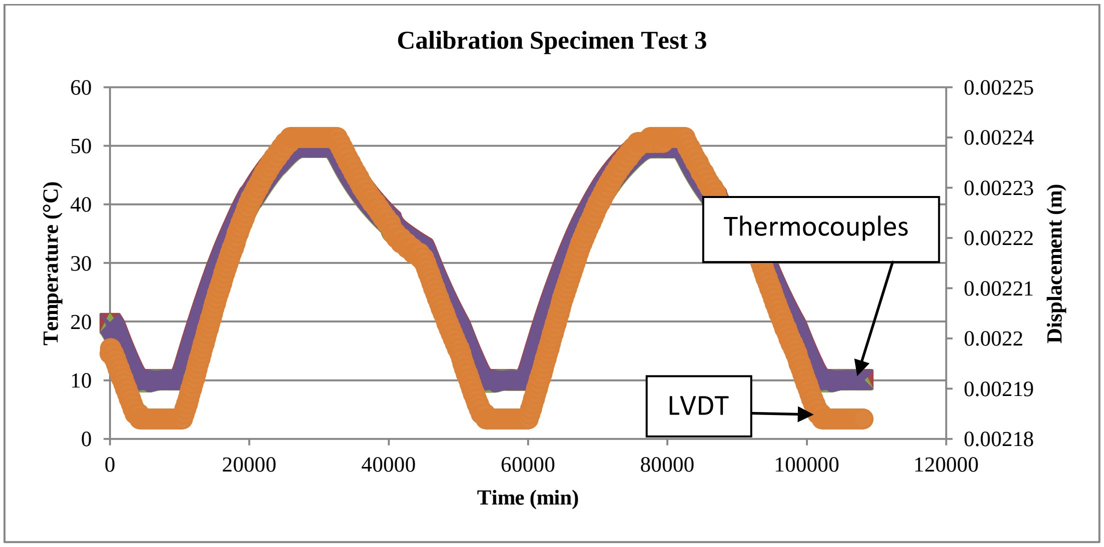

Island Ready Mix

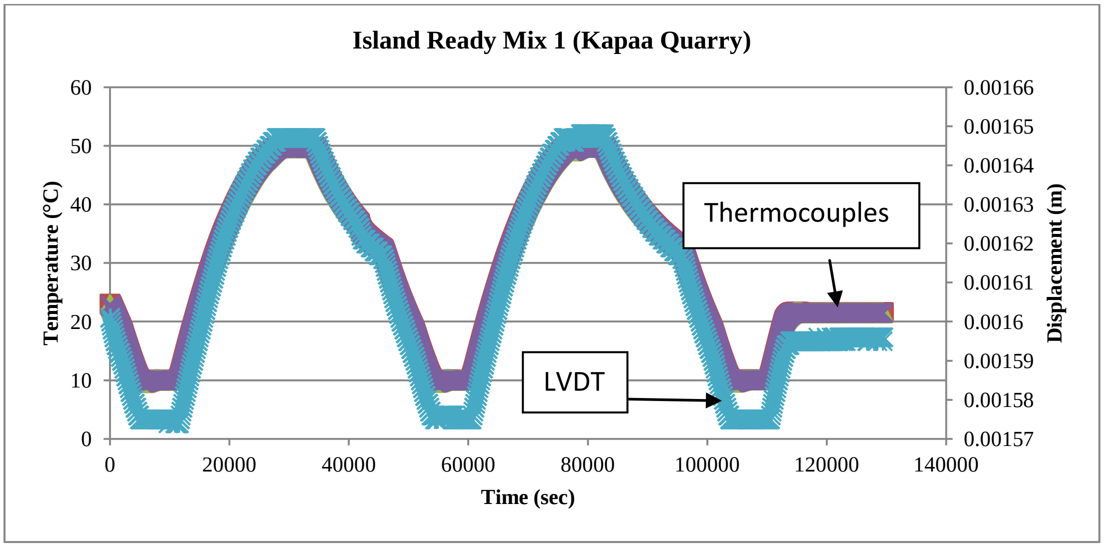

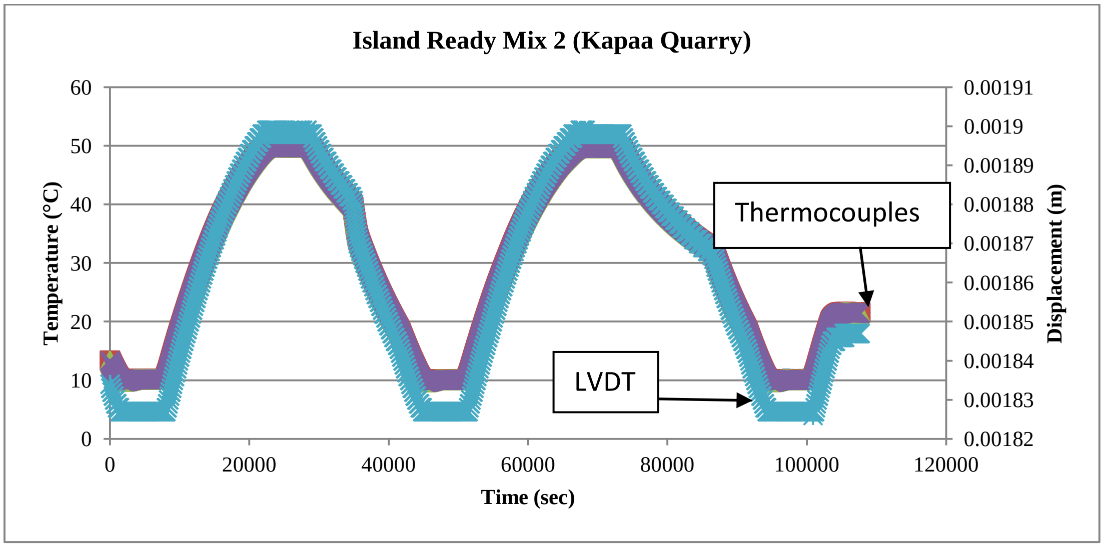

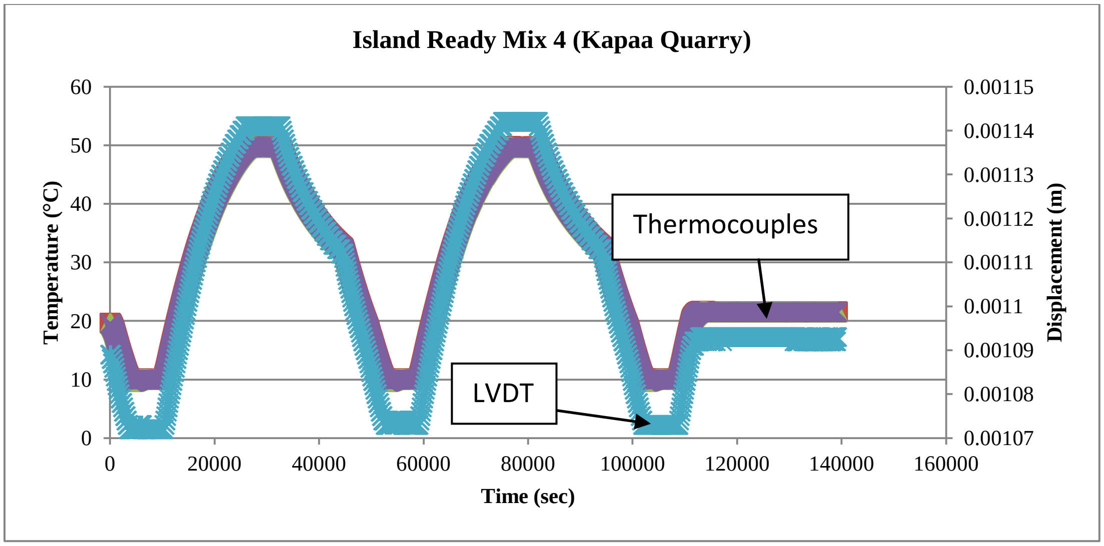
Island Ready Mix 4 (Kapaa Quarry)
Temperature (°C)
Displacement (m)
Time (sec)
Thermocouples
LVDT
0
10
20
30
40
50
60
0.00107
0.00108
0.00109
0.0011
0.00111
0.00112
0.00113
0.00114
0.00115
0
20000
40000
60000
80000
100000
120000
140000
160000

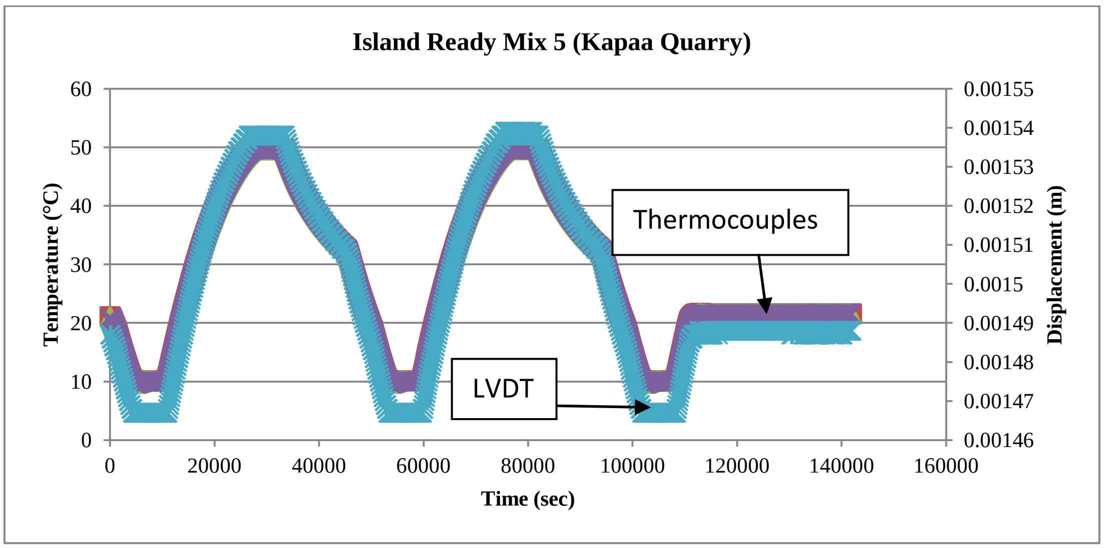
Island Ready Mix 5 (Kapaa Quarry)
Temperature (°C)
Displacement (m)
Time (sec)
Thermocouples
LVDT
0
10
20
30
40
50
60
0.00146
0.00147
0.00148
0.00149
0.0015
0.00151
0.00152
0.00153
0.00154
0.00155
0
20000
40000
60000
80000
100000
120000
140000
160000

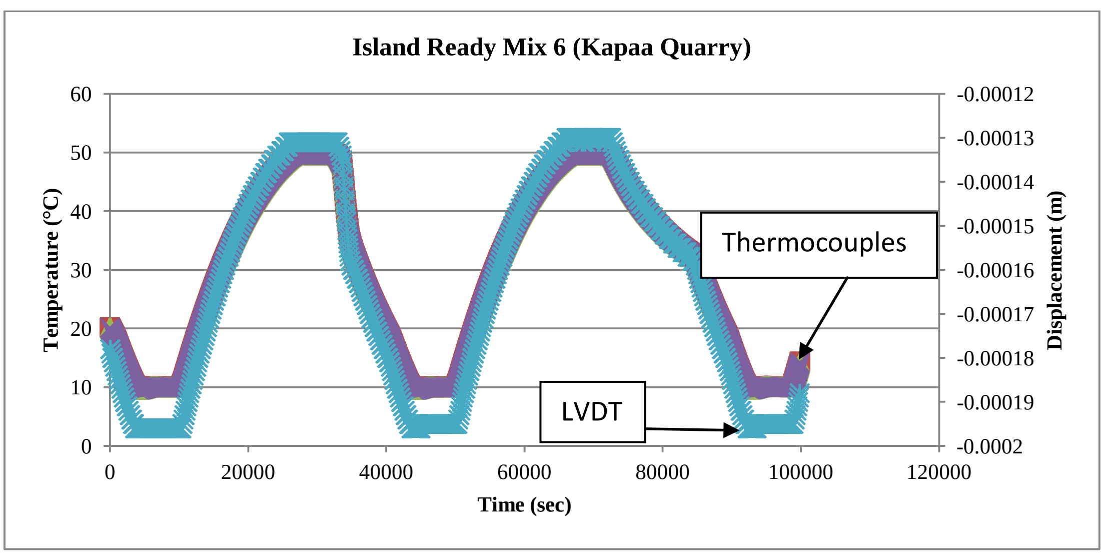
Island Ready Mix 6 (Kapaa Quarry)
Temperature (°C)
Displacement (m)
Time (sec)
Thermocouples
LVDT
0
10
20
30
40
50
60
-0.0002
-0.00019
-0.00018
-0.00017
-0.00016
-0.00015
-0.00014
-0.00013
-0.00012
0
20000
40000
60000
80000
100000
120000

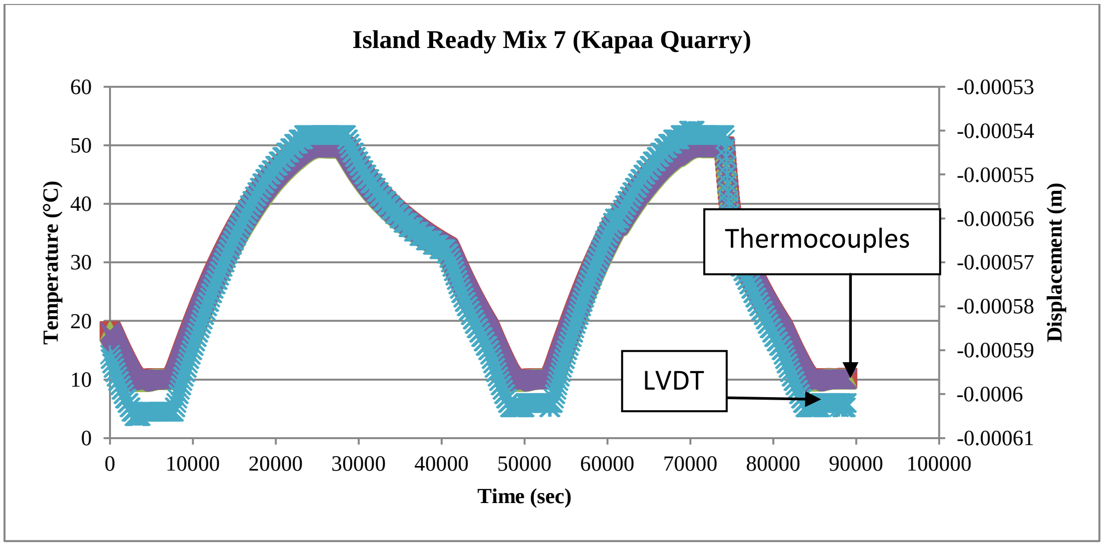
Island Ready Mix 7 (Kapaa Quarry)
Temperature (°C)
Displacement (m)
Time (sec)
Thermocouples
LVDT
0
10
20
30
40
50
60
-0.00053
-0.00054
-0.00055
-0.00056
-0.00057
-0.00058
-0.00059
-0.0006
-0.00061
0
10000
20000
30000
40000
50000
60000
70000
80000
90000
100000

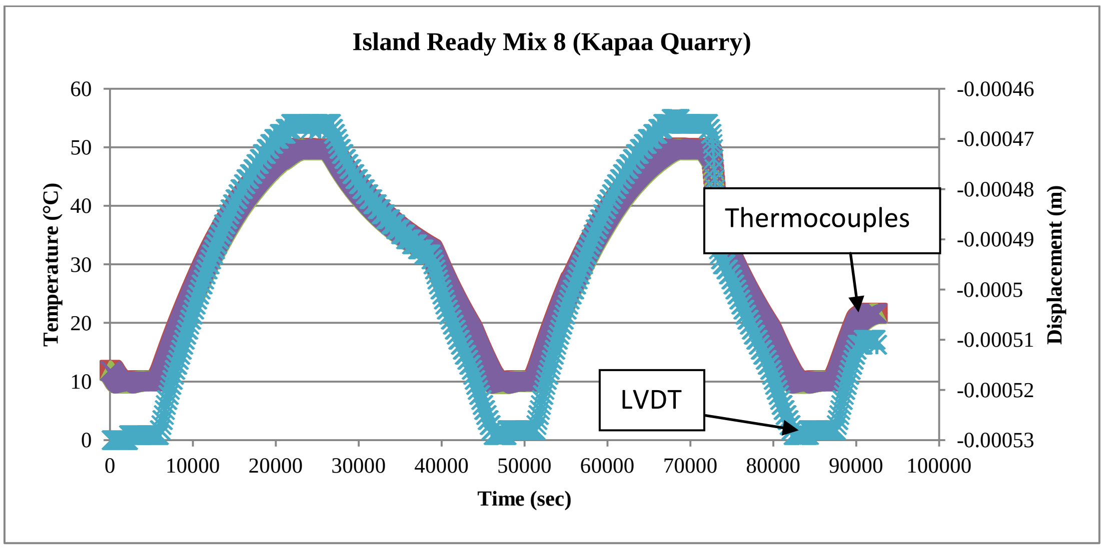
Island Ready Mix 8 (Kapaa Quarry)
Temperature (°C)
Displacement (m)
Time (sec)
Thermocouples
LVDT
0
10
20
30
40
50
60
-0.00046
-0.00047
-0.00048
-0.00049
-0.0005
-0.00051
-0.00052
-0.00053
0
10000
20000
30000
40000
50000
60000
70000
80000
90000
100000

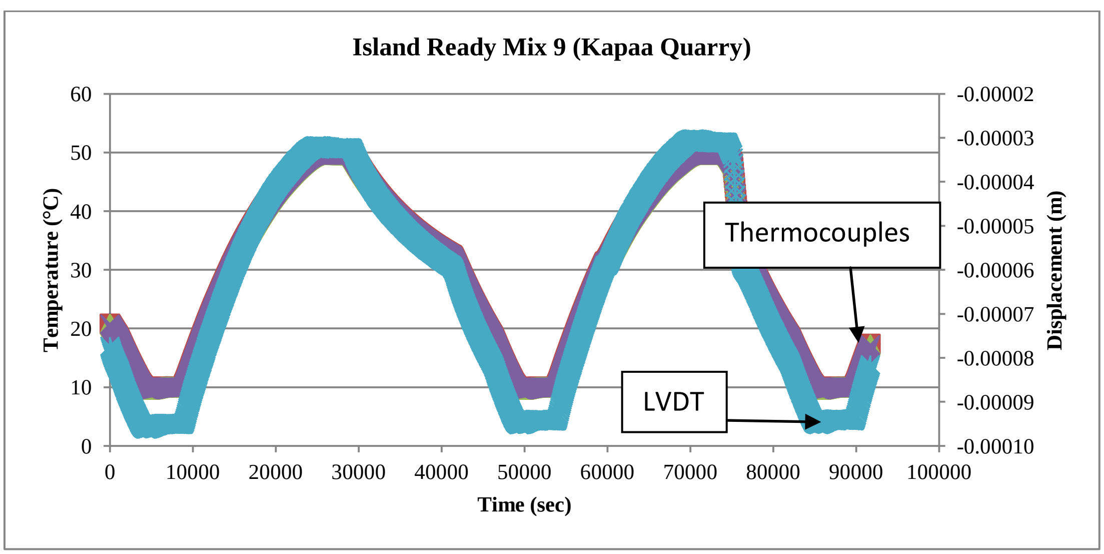
Island Ready Mix 9 (Kapaa Quarry)
Temperature (°C)
Displacement (m)
Time (sec)
Thermocouples
LVDT
0
10
20
30
40
50
60
-0.00002
-0.00003
-0.00004
-0.00005
-0.00006
-0.00007
-0.00008
-0.00009
-0.00010
0
10000
20000
30000
40000
50000
60000
70000
80000
90000
100000

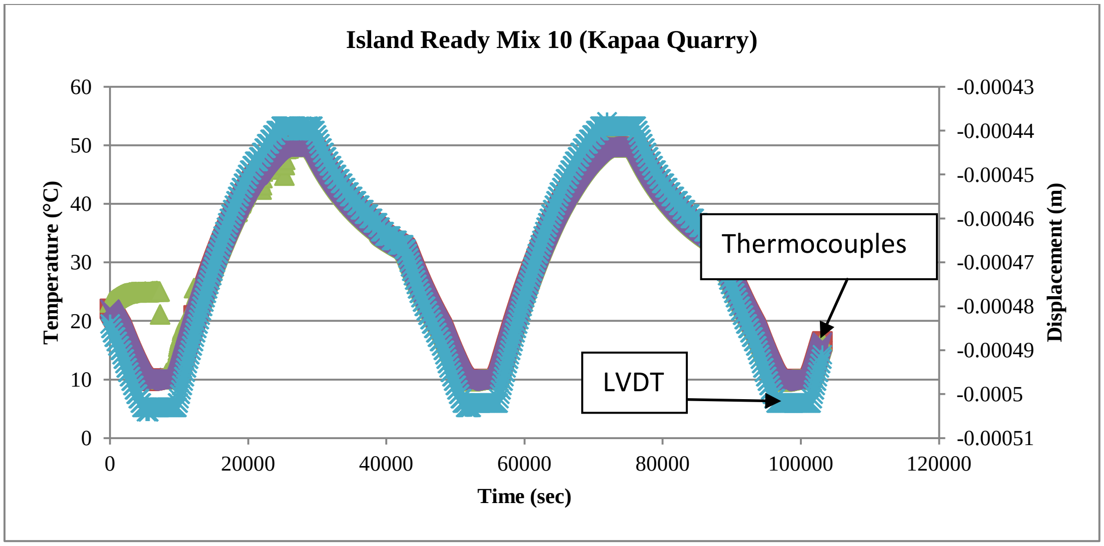
Island Ready Mix 10 (Kapaa Quarry)
Temperature (°C)
Displacement (m)
Time (sec)
Thermocouples
LVDT
60
50
40
30
20
10
0
-0.00043
-0.00044
-0.00045
-0.00046
-0.00047
-0.00048
-0.00049
-0.0005
-0.00051
0
20000
40000
60000
80000
100000
120000

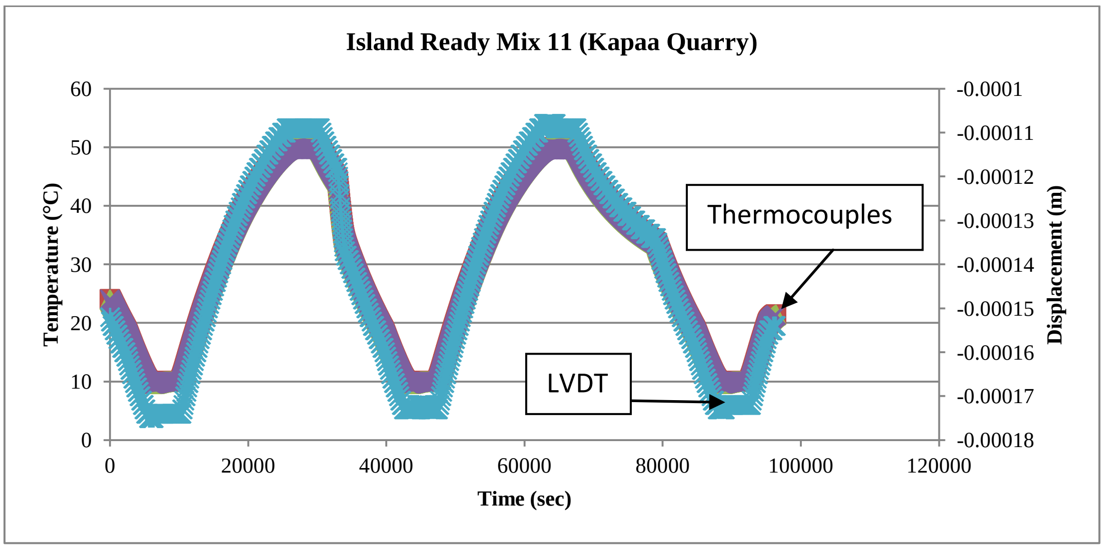
Island Ready Mix 11 (Kapaa Quarry)
Temperature (°C)
Displacement (m)
Time (sec)
Thermocouples
LVDT
60
50
40
30
20
10
0
-0.0001
-0.00011
-0.00012
-0.00013
-0.00014
-0.00015
-0.00016
-0.00017
-0.00018
0
20000
40000
60000
80000
100000
120000

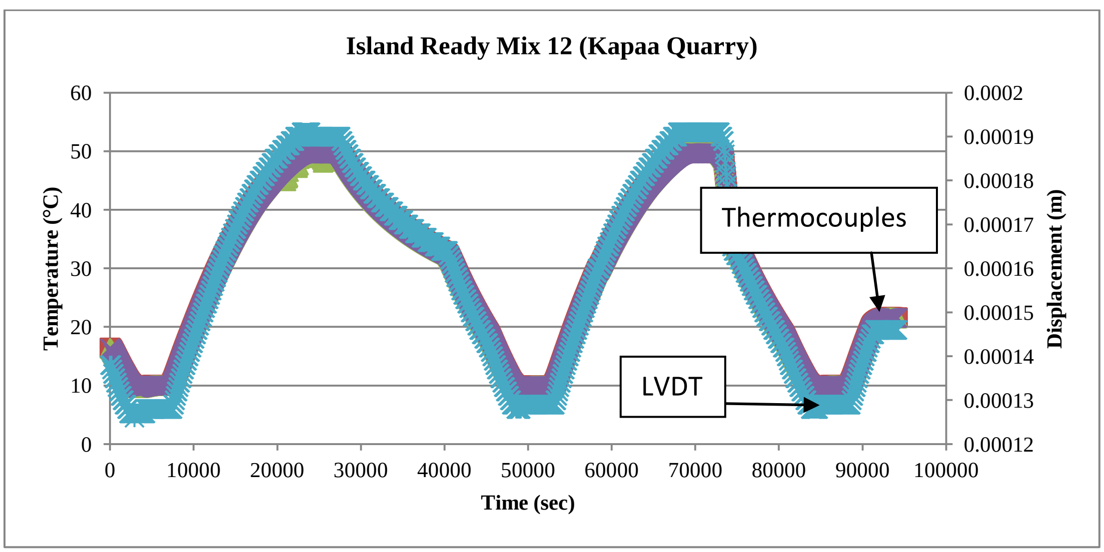
Island Ready Mix 12 (Kapaa Quarry)
Temperature (°C)
Displacement (m)
Time (sec)
Thermocouples
LVDT
60
50
40
30
20
10
0
0.0002
0.00019
0.00018
0.00017
0.00016
0.00015
0.00014
0.00013
0.00012
0
10000
20000
30000
40000
50000
60000
70000
80000
90000
100000

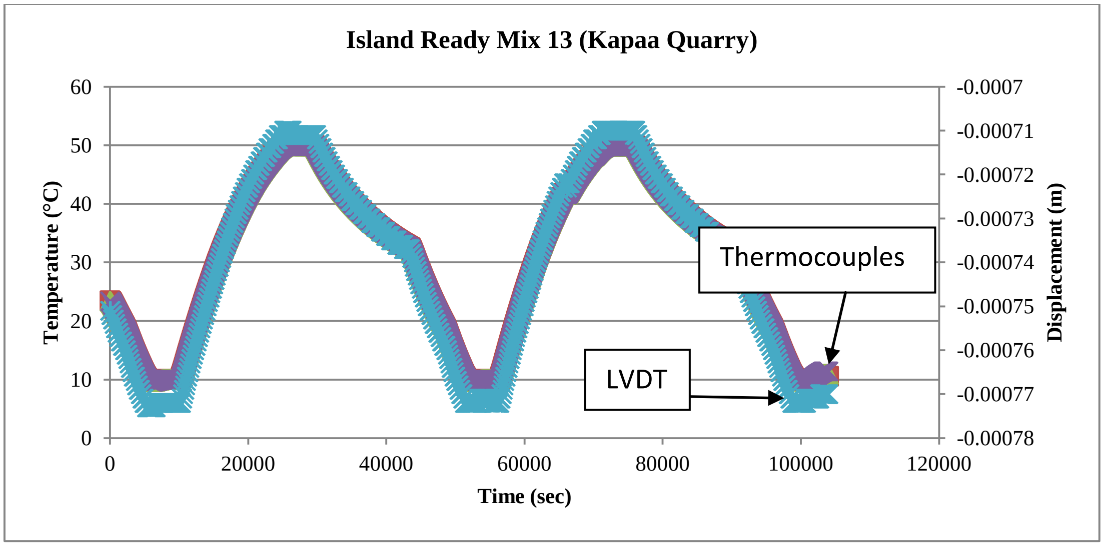
Island Ready Mix 13 (Kapaa Quarry)
Temperature (°C)
Displacement (m)
Time (sec)
Thermocouples
LVDT
0
10
20
30
40
50
60
-0.0007
-0.00071
-0.00072
-0.00073
-0.00074
-0.00075
-0.00076
-0.00077
-0.00078
0
20000
40000
60000
80000
100000
120000

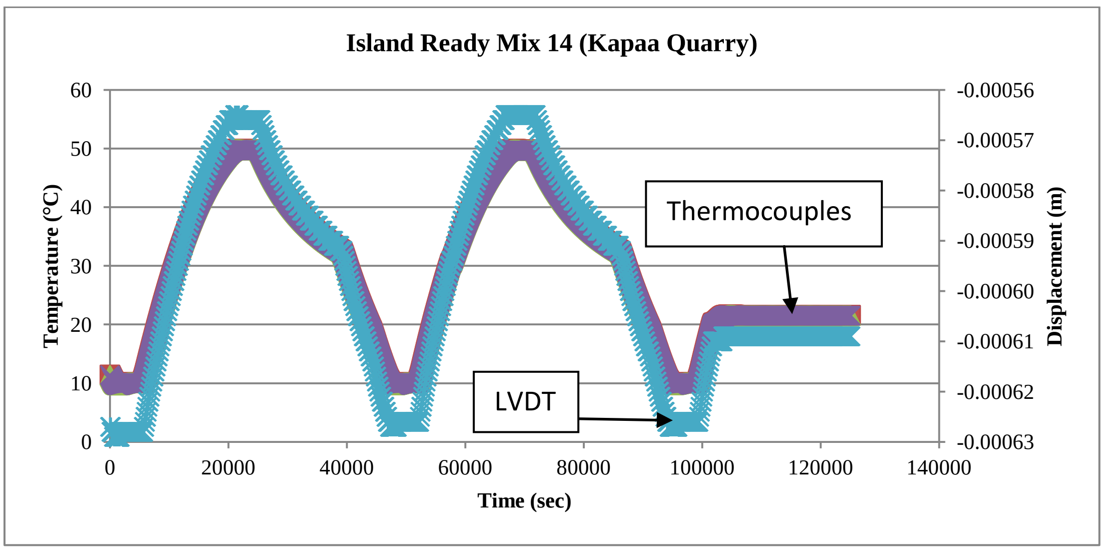
Island Ready Mix 14 (Kapaa Quarry)
Temperature (°C)
Displacement (m)
Time (sec)
Thermocouples
LVDT
0
10
20
30
40
50
60
-0.00056
-0.00057
-0.00058
-0.00059
-0.00060
-0.00061
-0.00062
-0.00063
0
20000
40000
60000
80000
100000
120000
140000

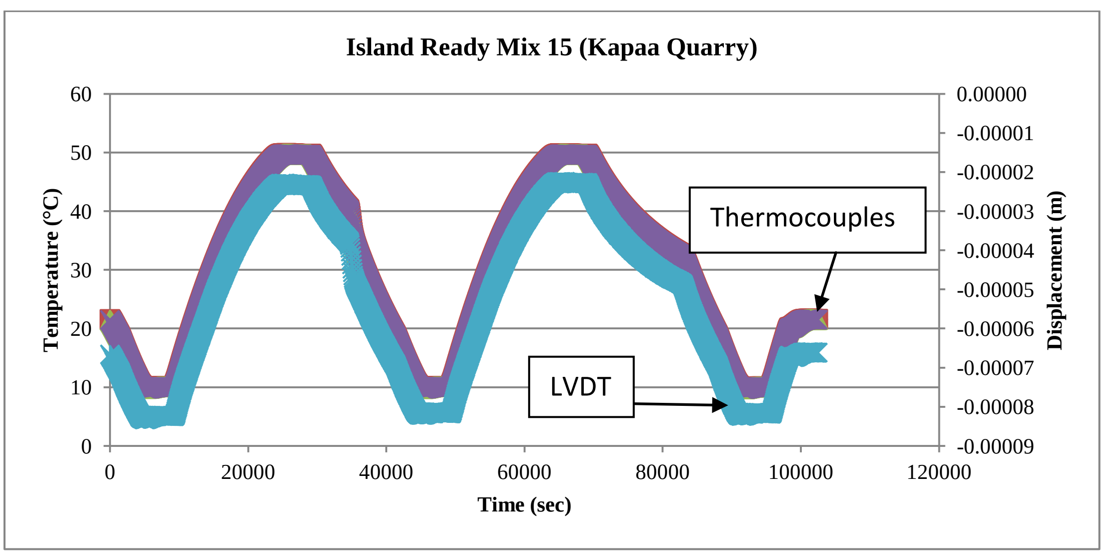
Island Ready Mix 15 (Kapaa Quarry)
Temperature (°C)
Displacement (m)
Time (sec)
Thermocouples
LVDT
0
10
20
30
40
50
60
0.00000
-0.00001
-0.00002
-0.00003
-0.00004
-0.00005
-0.00006
-0.00007
-0.00008
-0.00009
0
20000
40000
60000
80000
100000
120000

	IRM #1	IRM #2	IRM #3	IRM #4	IRM #5	IRM #6	IRM #7	IRM #8	IRM #9	IRM #10	IRM #11	IRM #12	IRM #13	IRM #14	IRM #15
		3 Day Curing			7 Day Curing			14 Day Curing			28 Day Curing			56 Day Curing	
Expansion 1															
L_0 (mm)	178.38	178.82	179.21	179.11	178.54	179.94	180.81	180.47	180.30	180.44	180.31	180.33	180.65	180.53	180.334
ΔT (°C)	39.5	39.4	#VALUE!	39.6	39.5	39.5	39.7	39.5	39.6	39.8	40.0	39.8	40.2	40.2	39.9
ΔL_f (mm)	1.69E-02	1.69E-02	#VALUE!	1.70E-02	1.69E-02	1.70E-02	1.72E-02	1.71E-02	1.71E-02	1.72E-02	1.72E-02	1.72E-02	1.74E-02	1.74E-02	1.72E-02
ΔL_m (mm)	7.2E-02	7.1E-02	#VALUE!	6.9E-02	7.1E-02	6.5E-02	6.3E-02	6.2E-02	6.3E-02	6.4E-02	6.5E-02	6.2E-02	6.3E-02	6.3E-02	5.9E-02
ΔL_a (mm)	8.89E-02	8.79E-02	#VALUE!	8.60E-02	8.79E-02	8.20E-02	8.02E-02	7.91E-02	7.97E-02	8.12E-02	8.22E-02	7.92E-02	8.04E-02	8.04E-02	7.67E-02
CTE (microstrains/°C)	12.6E-6	12.5E-6	#VALUE!	12.1E-6	12.5E-6	11.5E-6	11.2E-6	11.1E-6	11.2E-6	11.3E-6	11.4E-6	11.0E-6	11.1E-6	11.1E-6	10.7E-6
Contraction 1															
L_0 (mm)	178.38	178.82	179.21	179.11	178.54	179.94	180.81	180.47	180.30	180.44	180.31	180.33	180.65	180.53	180.334
ΔT (°C)	-39.5	-39.5	#VALUE!	-39.6	-39.5	-39.6	-39.6	-39.6	-39.7	-39.9	-39.9	-39.9	-40.2	-40.0	-40.0
ΔL_f (mm)	-1.69E-02	-1.69E-02	#VALUE!	-1.70E-02	-1.69E-02	-1.70E-02	-1.72E-02	-1.71E-02	-1.71E-02	-1.72E-02	-1.72E-02	-1.72E-02	-1.74E-02	-1.73E-02	-1.73E-02
ΔL_m (mm)	-7.2E-02	-7.1E-02	#VALUE!	-6.7E-02	-7.1E-02	-6.4E-02	-6.1E-02	-6.1E-02	-6.2E-02	-6.3E-02	-6.4E-02	-6.1E-02	-6.2E-02	-6.0E-02	-5.9E-02
ΔL_a (mm)	-8.89E-02	-8.79E-02	#VALUE!	-8.40E-02	-8.79E-02	-8.10E-02	-7.82E-02	-7.81E-02	-7.89E-02	-8.02E-02	-8.12E-02	-7.82E-02	-7.94E-02	-7.73E-02	-7.61E-02
CTE (microstrains/°C)	12.6E-6	12.4E-6	#VALUE!	11.8E-6	12.5E-6	11.4E-6	10.9E-6	10.9E-6	11.0E-6	11.1E-6	11.3E-6	10.9E-6	10.9E-6	10.7E-6	10.6E-6
Expansion 2															
L_0 (mm)	178.38	178.82	179.21	179.11	178.54	179.94	180.81	180.47	180.30	180.44	180.31	180.33	180.65	180.53	180.334
ΔT (°C)	39.7	39.6	#VALUE!	39.5	39.5	39.5	39.6	39.6	39.7	39.8	39.8	39.9	40.2	39.9	39.9
ΔL_f (mm)	1.69E-02	1.69E-02	#VALUE!	1.69E-02	1.69E-02	1.70E-02	1.72E-02	1.71E-02	1.71E-02	1.72E-02	1.72E-02	1.72E-02	1.74E-02	1.72E-02	1.72E-02
ΔL_m (mm)	7.3E-02	7.1E-02	#VALUE!	6.8E-02	7.1E-02	6.5E-02	6.1E-02	6.1E-02	6.3E-02	6.3E-02	6.4E-02	6.2E-02	6.2E-02	6.1E-02	5.9E-02
ΔL_a (mm)	8.99E-02	8.79E-02	#VALUE!	8.49E-02	8.79E-02	8.20E-02	7.82E-02	7.81E-02	8.03E-02	8.02E-02	8.12E-02	7.92E-02	7.94E-02	7.82E-02	7.64E-02
CTE (microstrains/°C)	12.7E-6	12.4E-6	#VALUE!	12.0E-6	12.4E-6	11.5E-6	10.9E-6	10.9E-6	11.2E-6	11.2E-6	11.3E-6	11.0E-6	10.9E-6	10.9E-6	10.6E-6
Contraction 2															
L_0 (mm)	178.38	178.82	179.21	179.11	178.54	179.94	180.81	180.47	180.30	180.44	180.31	180.33	180.65	180.53	180.334
ΔT (°C)	-39.7	-39.6	#VALUE!	-39.5	-39.5	-39.5	-39.6	-39.6	-39.6	-39.9	-39.9	-39.8	-39.6	-39.9	-39.8
ΔL_f (mm)	-1.69E-02	-1.69E-02	#VALUE!	-1.69E-02	-1.69E-02	-1.70E-02	-1.71E-02	-1.71E-02	-1.71E-02	-1.72E-02	-1.72E-02	-1.72E-02	-1.71E-02	-1.72E-02	-1.72E-02
ΔL_m (mm)	-7.3E-02	-7.1E-02	#VALUE!	-6.9E-02	-7.1E-02	-6.5E-02	-6.1E-02	-6.1E-02	-6.3E-02	-6.3E-02	-6.3E-02	-6.2E-02	-6.1E-02	-6.2E-02	-5.9E-02
ΔL_a (mm)	-8.99E-02	-8.79E-02	#VALUE!	-8.59E-02	-8.79E-02	-8.20E-02	-7.81E-02	-7.81E-02	-8.01E-02	-8.02E-02	-8.02E-02	-7.92E-02	-7.81E-02	-7.92E-02	-7.62E-02
CTE (microstrains/°C)	12.7E-6	12.4E-6	#VALUE!	12.1E-6	12.5E-6	11.5E-6	10.9E-6	10.9E-6	11.2E-6	11.2E-6	11.1E-6	11.0E-6	10.9E-6	11.0E-6	10.6E-6
Ave. CTE (microstrains/°C)	12.7E-6	12.4E-6	#VALUE!	12.1E-6	12.5E-6	11.5E-6	10.9E-6	10.9E-6	11.2E-6	11.2E-6	11.2E-6	11.0E-6	10.9E-6	10.9E-6	10.6E-6
Ave. CTE (per Age)(microstrains/°C)		12.6E-6			12.0E-6			11.0E-6			11.1E-6			10.8E-6	
Ave. CTE (per Age)(microstrains/°F)		7.0E-6			6.7E-6			6.1E-6			6.2E-6			6.0E-6	

Hawaiian Cement

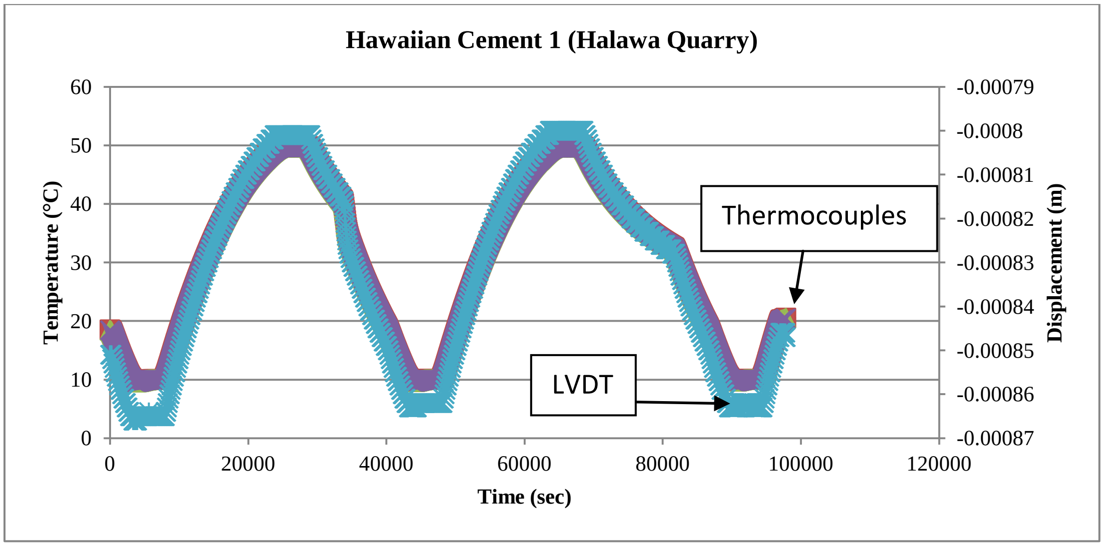

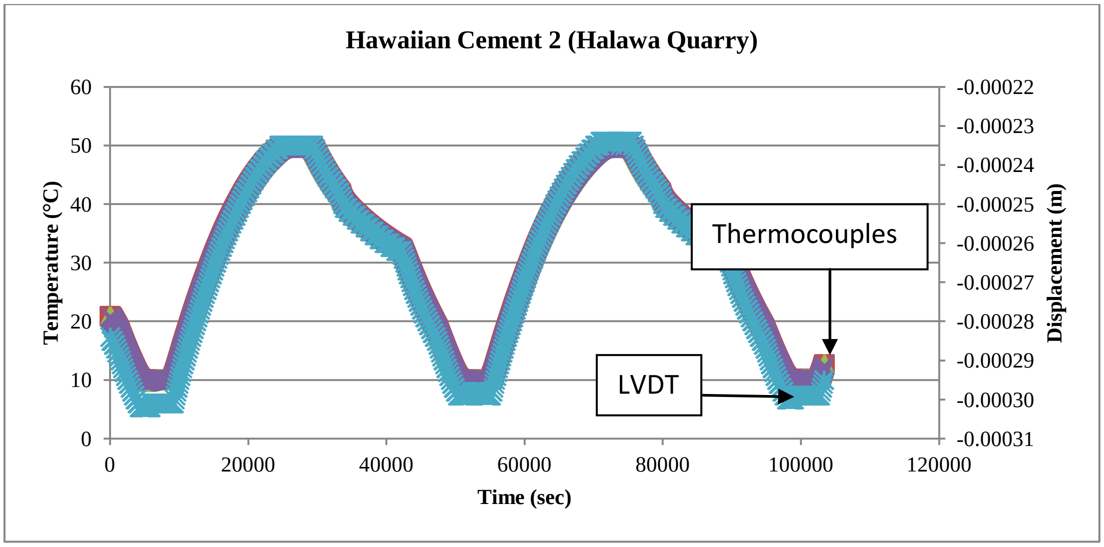

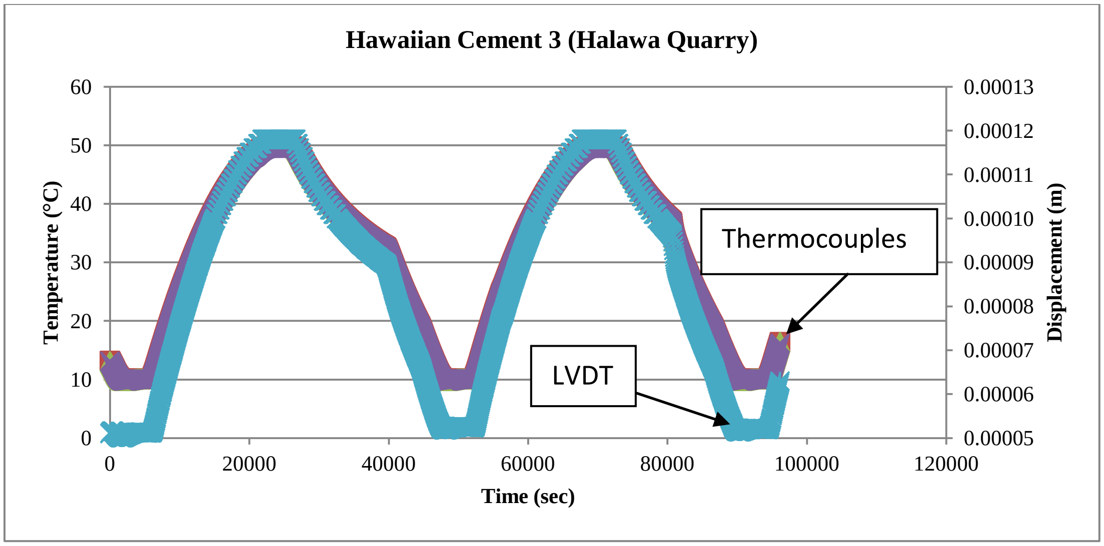
Hawaiian Cement 3 (Halawa Quarry)
Temperature (°C)
Displacement (m)
Time (sec)
Thermocouples
LVDT
0
10
20
30
40
50
60
0.00005
0.00006
0.00007
0.00008
0.00009
0.00010
0.00011
0.00012
0.00013
0
20000
40000
60000
80000
100000
120000

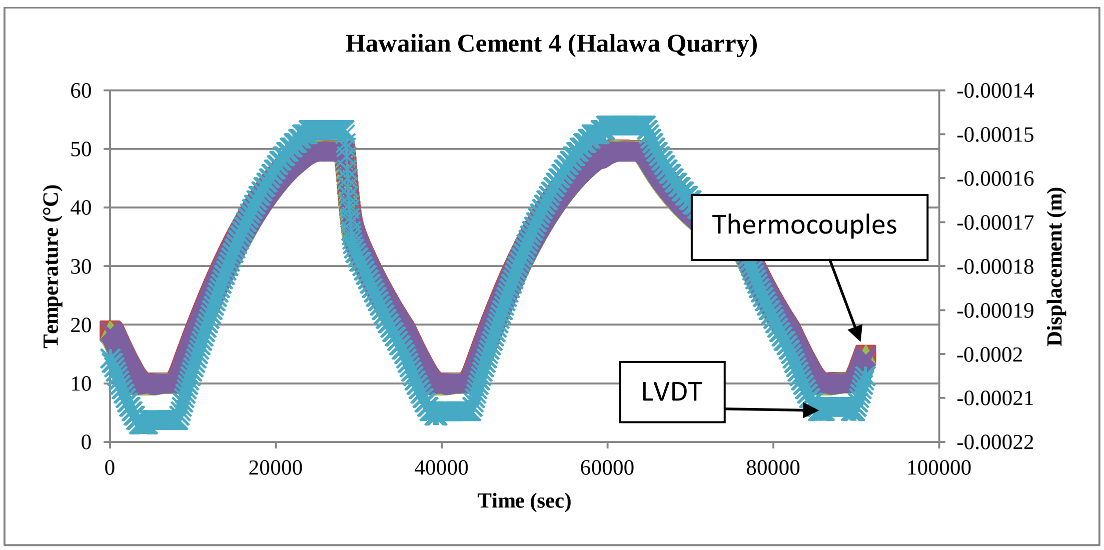
Hawaiian Cement 4 (Halawa Quarry)
Temperature (°C)
Displacement (m)
Time (sec)
Thermocouples
LVDT
0
10
20
30
40
50
60
-0.00022
-0.00021
-0.0002
-0.00019
-0.00018
-0.00017
-0.00016
-0.00015
-0.00014
0
20000
40000
60000
80000
100000

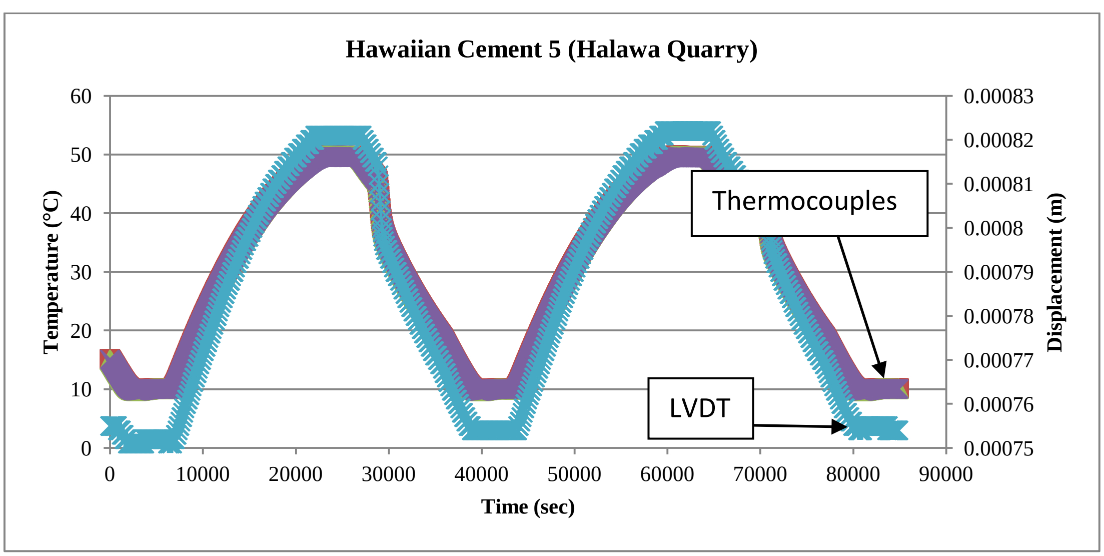
Hawaiian Cement 5 (Halawa Quarry)
Temperature (°C)
Displacement (m)
Time (sec)
Thermocouples
LVDT
0
10
20
30
40
50
60
0.00075
0.00076
0.00077
0.00078
0.00079
0.0008
0.00081
0.00082
0.00083
0
10000
20000
30000
40000
50000
60000
70000
80000
90000

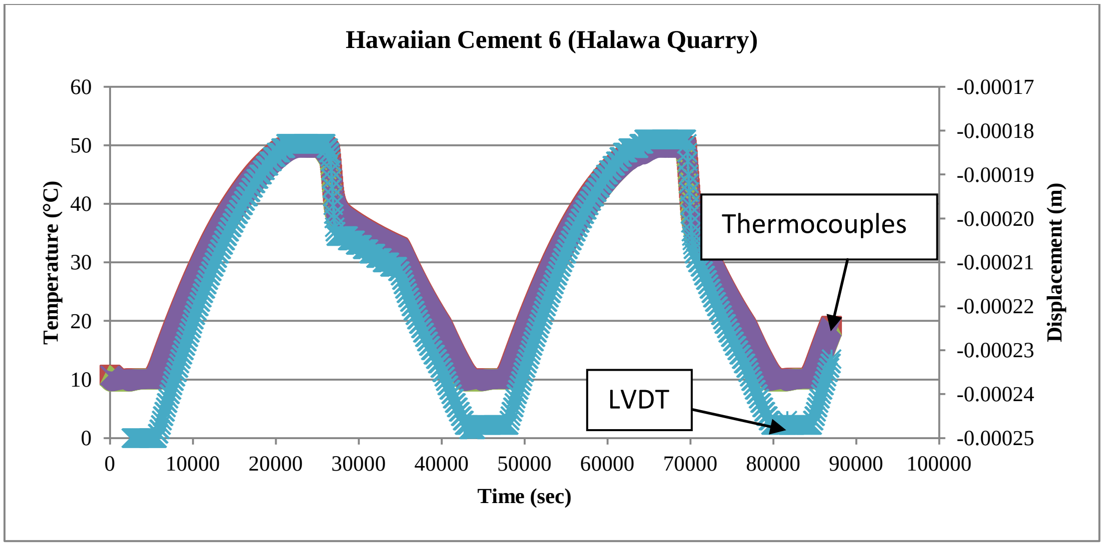
Hawaiian Cement 6 (Halawa Quarry)
Temperature (°C)
Displacement (m)
Time (sec)
Thermocouples
LVDT
0
10
20
30
40
50
60
-0.00017
-0.00018
-0.00019
-0.00020
-0.00021
-0.00022
-0.00023
-0.00024
-0.00025
0
10000
20000
30000
40000
50000
60000
70000
80000
90000
100000

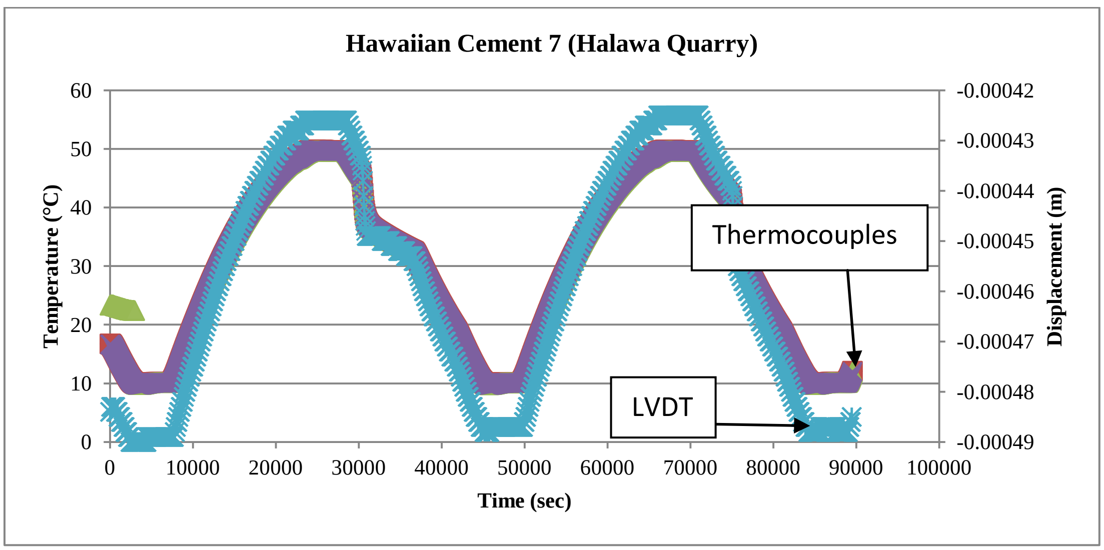
Hawaiian Cement 7 (Halawa Quarry)
Temperature (°C)
Displacement (m)
Time (sec)
Thermocouples
LVDT
0
10
20
30
40
50
60
-0.00042
-0.00043
-0.00044
-0.00045
-0.00046
-0.00047
-0.00048
-0.00049
0
10000
20000
30000
40000
50000
60000
70000
80000
90000
100000

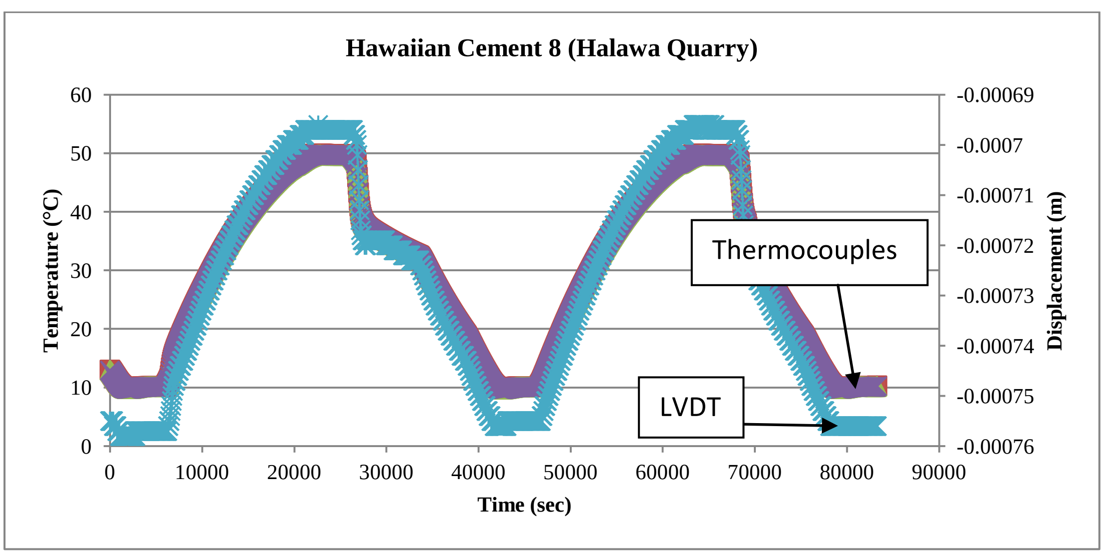
Hawaiian Cement 8 (Halawa Quarry)
Temperature (°C)
Displacement (m)
Time (sec)
Thermocouples
LVDT
0
10
20
30
40
50
60
-0.00069
-0.0007
-0.00071
-0.00072
-0.00073
-0.00074
-0.00075
-0.00076
0
10000
20000
30000
40000
50000
60000
70000
80000
90000

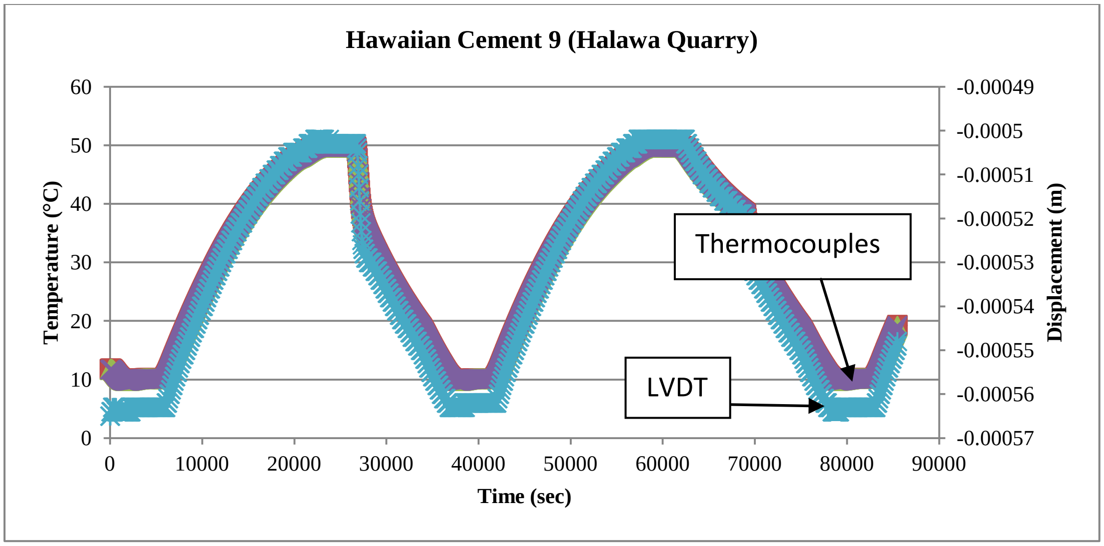
Hawaiian Cement 9 (Halawa Quarry)
Temperature (°C)
Displacement (m)
Time (sec)
Thermocouples
LVDT
0
10
20
30
40
50
60
-0.00049
-0.0005
-0.00051
-0.00052
-0.00053
-0.00054
-0.00055
-0.00056
-0.00057
0
10000
20000
30000
40000
50000
60000
70000
80000
90000

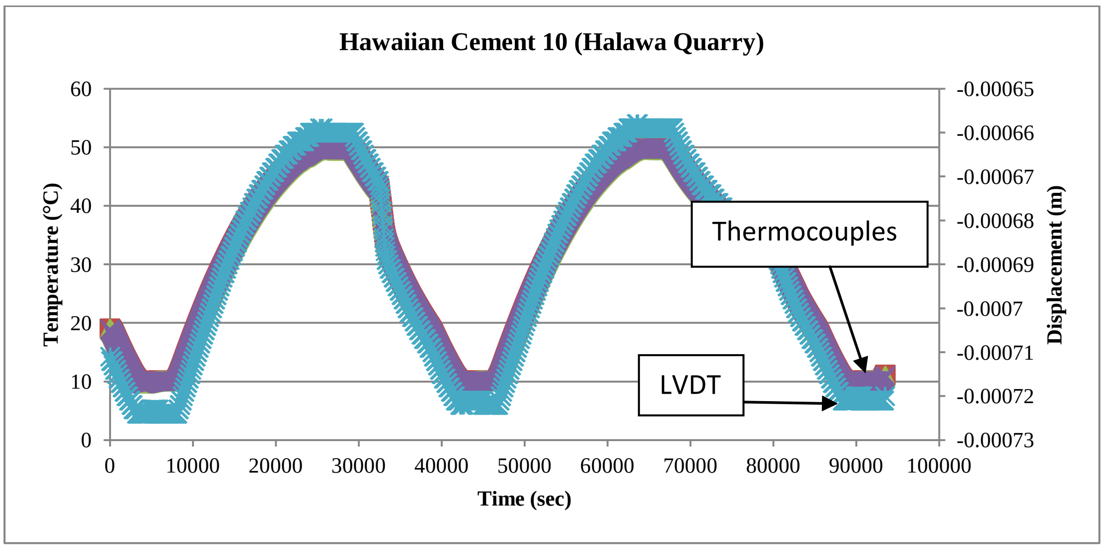
Hawaiian Cement 10 (Halawa Quarry)
Temperature (°C)
Displacement (m)
Time (sec)
Thermocouples
LVDT
0
10
20
30
40
50
60
-0.00065
-0.00066
-0.00067
-0.00068
-0.00069
-0.0007
-0.00071
-0.00072
-0.00073
0
10000
20000
30000
40000
50000
60000
70000
80000
90000
100000

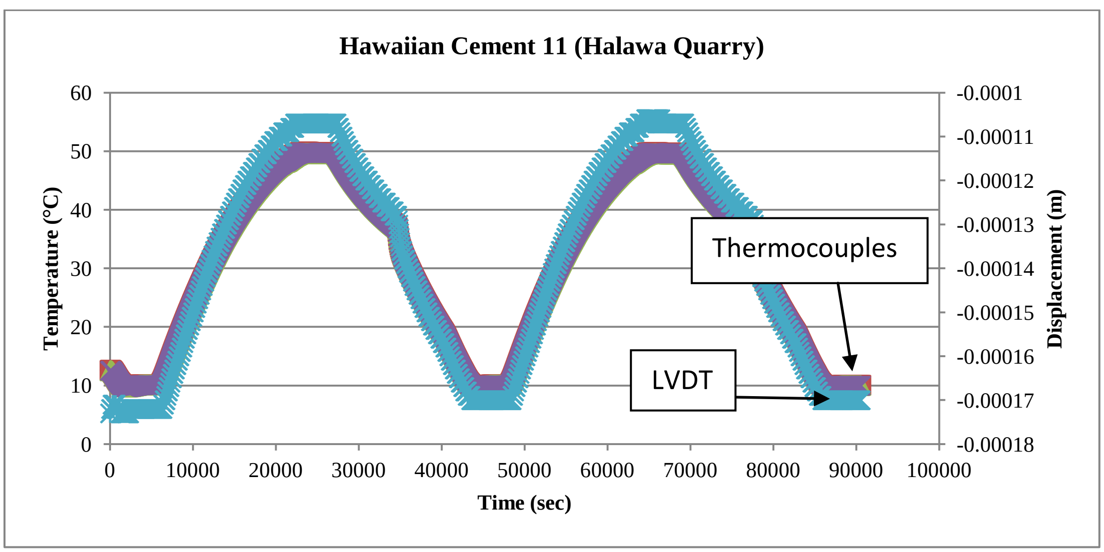
Hawaiian Cement 11 (Halawa Quarry)
Temperature (°C)
Displacement (m)
Time (sec)
Thermocouples
LVDT
0
10
20
30
40
50
60
-0.0001
-0.00011
-0.00012
-0.00013
-0.00014
-0.00015
-0.00016
-0.00017
-0.00018
0
10000
20000
30000
40000
50000
60000
70000
80000
90000
100000

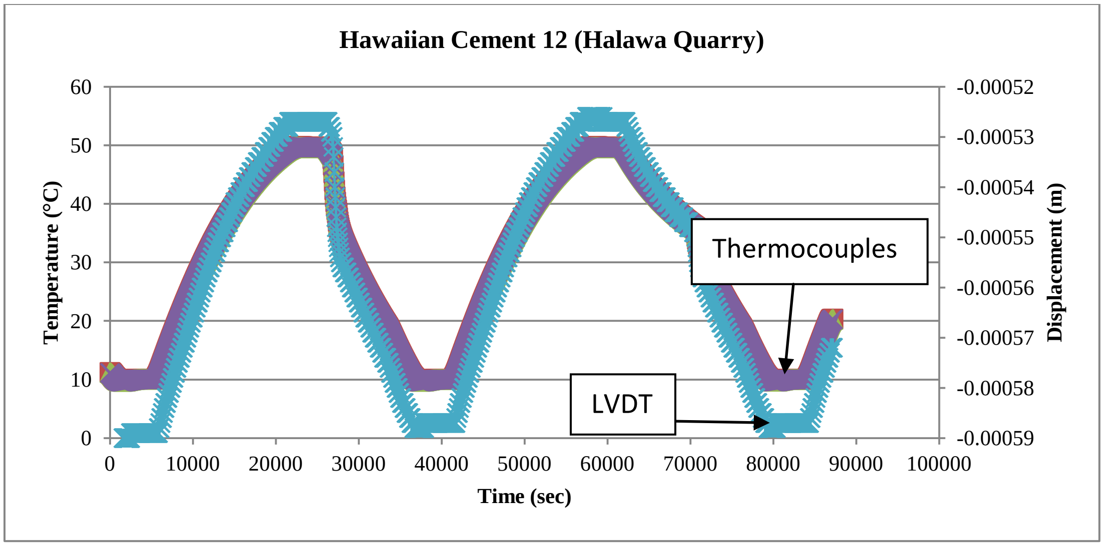
Hawaiian Cement 12 (Halawa Quarry)
Temperature (°C)
Displacement (m)
Time (sec)
Thermocouples
LVDT
0
10
20
30
40
50
60
-0.00052
-0.00053
-0.00054
-0.00055
-0.00056
-0.00057
-0.00058
-0.00059
0
10000
20000
30000
40000
50000
60000
70000
80000
90000
100000

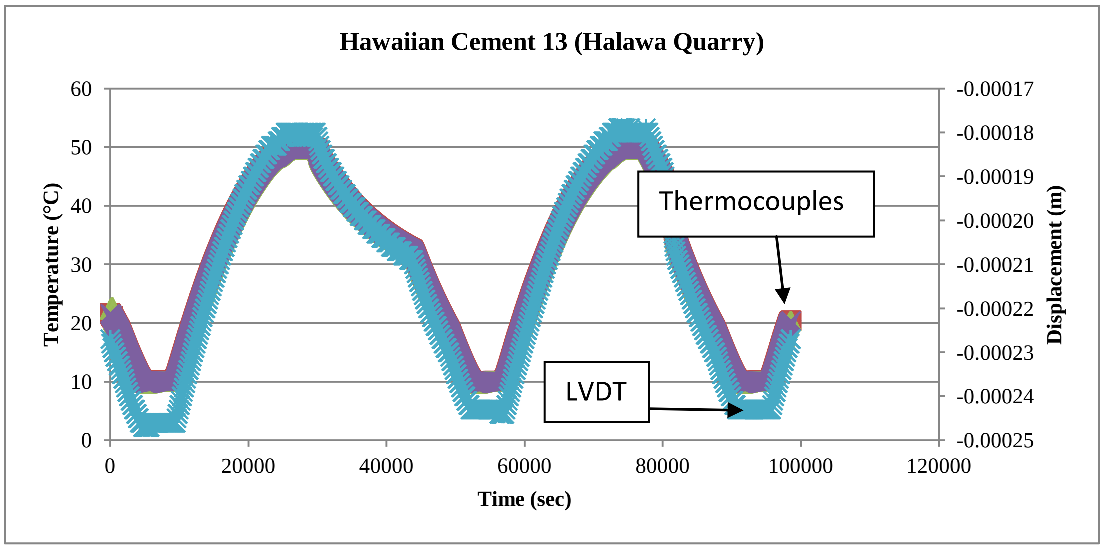
Hawaiian Cement 13 (Halawa Quarry)
Temperature (°C)
Displacement (m)
Time (sec)
Thermocouples
LVDT
0
10
20
30
40
50
60
-0.00017
-0.00018
-0.00019
-0.00020
-0.00021
-0.00022
-0.00023
-0.00024
-0.00025
0
20000
40000
60000
80000
100000
120000

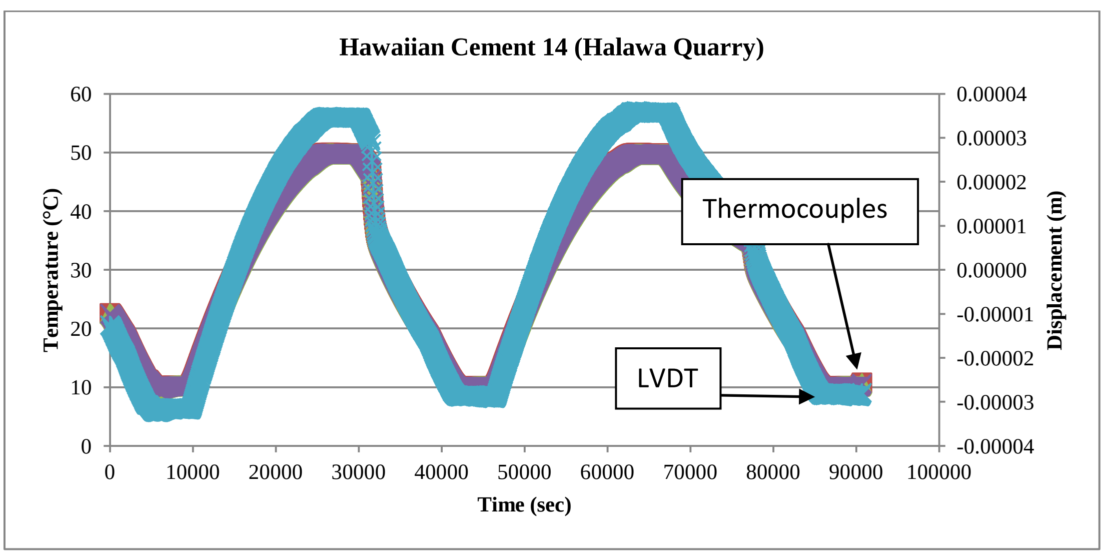
Hawaiian Cement 14 (Halawa Quarry)
Temperature (°C)
Displacement (m)
Time (sec)
Thermocouples
LVDT
0
10
20
30
40
50
60
0.00004
0.00003
0.00002
0.00001
0.00000
-0.00001
-0.00002
-0.00003
-0.00004
0
10000
20000
30000
40000
50000
60000
70000
80000
90000
100000

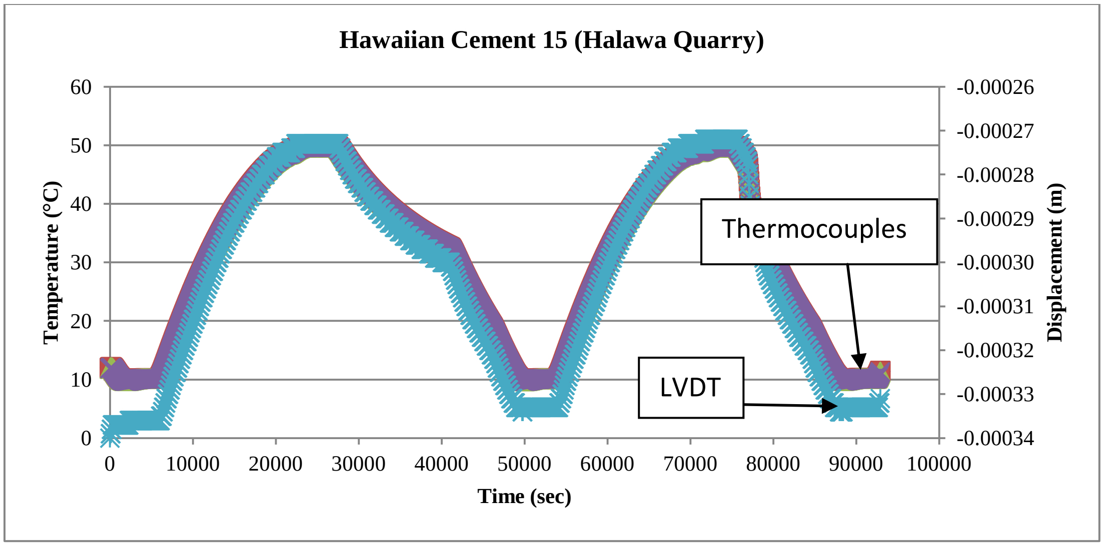

Hawaiian Cement 15 (Halawa Quarry)
Temperature (°C)
Displacement (m)
Time (sec)
Thermocouples
LVDT
0
10
20
30
40
50
60
-0.00026
-0.00027
-0.00028
-0.00029
-0.00030
-0.00031
-0.00032
-0.00033
-0.00034
0
10000
20000
30000
40000
50000
60000
70000
80000
90000
100000

	HC #1	HC #2	HC #3	HC #4	HC #5	HC #6	HC #7	HC #8	HC #9	HC #10	HC #11	HC #12	HC #13	HC #14	HC #15
	3 Day Curing			7 Day Curing			14 Day Curing			28 Day Curing			56 Day Curing		
Expansion 1															
L_0 (mm)	180.86	180.55	180.33	180.36	180.39	180.30	180.66	180.58	180.67	180.81	180.41	180.64	180.52	180.69	180.604
ΔT (°C)	40.0	39.8	39.7	39.7	39.7	39.7	39.8	39.6	39.7	39.8	39.8	39.7	39.5	39.9	39.8
ΔL_f (mm)	1.73E-02	1.72E-02	1.72E-02	1.72E-02	1.71E-02	1.71E-02	1.72E-02	1.71E-02	1.72E-02	1.72E-02	1.72E-02	1.72E-02	1.71E-02	1.72E-02	1.72E-02
ΔL_m (mm)	6.4E-02	6.7E-02	6.7E-02	6.6E-02	6.9E-02	6.7E-02	6.4E-02	6.0E-02	6.0E-02	6.3E-02	6.5E-02	6.2E-02	6.5E-02	6.7E-02	6.3E-02
ΔL_a (mm)	8.13E-02	8.42E-02	8.41E-02	8.32E-02	8.61E-02	8.41E-02	8.12E-02	7.71E-02	7.72E-02	8.02E-02	8.22E-02	7.92E-02	8.21E-02	8.38E-02	8.02E-02
CTE (microstrains/°C)	11.2E-6	11.7E-6	11.7E-6	11.6E-6	12.0E-6	11.8E-6	11.3E-6	10.8E-6	10.8E-6	11.2E-6	11.5E-6	11.0E-6	11.5E-6	11.6E-6	11.2E-6
Contraction 1															
L_0 (mm)	180.86	180.55	180.33	180.36	180.39	180.30	180.66	180.58	180.67	180.81	180.41	180.64	180.52	180.69	180.604
ΔT (°C)	-39.9	-39.9	-39.8	-39.8	-39.8	-39.7	-39.8	-39.7	-39.7	-39.7	-39.9	-39.8	-39.7	-40.0	-40.0
ΔL_f (mm)	-1.73E-02	-1.72E-02	-1.72E-02	-1.72E-02	-1.72E-02	-1.71E-02	-1.72E-02	-1.72E-02	-1.72E-02	-1.72E-02	-1.72E-02	-1.72E-02	-1.72E-02	-1.73E-02	-1.73E-02
ΔL_m (mm)	-6.1E-02	-6.4E-02	-6.6E-02	-6.4E-02	-6.7E-02	-6.4E-02	-6.1E-02	-5.8E-02	-5.9E-02	-6.1E-02	-6.3E-02	-6.0E-02	-6.2E-02	-6.3E-02	-6.0E-02
ΔL_a (mm)	-7.83E-02	-8.12E-02	-8.30E-02	-8.12E-02	-8.42E-02	-8.11E-02	-7.82E-02	-7.52E-02	-7.62E-02	-7.82E-02	-8.02E-02	-7.72E-02	-7.92E-02	-8.06E-02	-7.73E-02
CTE (microstrains/°C)	10.8E-6	11.3E-6	11.6E-6	11.3E-6	11.7E-6	11.3E-6	10.9E-6	10.5E-6	10.6E-6	10.9E-6	11.1E-6	10.7E-6	11.0E-6	11.2E-6	10.7E-6
Expansion 2															
L_0 (mm)	180.86	180.55	180.33	180.36	180.39	180.30	180.66	180.58	180.67	180.81	180.41	180.64	180.52	180.69	180.604
ΔT (°C)	39.9	39.9	39.8	39.7	39.8	39.7	39.7	39.7	39.7	39.7	39.8	39.7	40.1	39.9	39.9
ΔL_f (mm)	1.73E-02	1.72E-02	1.72E-02	1.72E-02	1.72E-02	1.71E-02	1.72E-02	1.71E-02	1.72E-02	1.72E-02	1.72E-02	1.72E-02	1.73E-02	1.72E-02	1.73E-02
ΔL_m (mm)	6.2E-02	6.5E-02	6.6E-02	6.5E-02	6.8E-02	6.5E-02	6.2E-02	5.8E-02	6.0E-02	6.2E-02	6.3E-02	6.0E-02	6.3E-02	6.4E-02	6.1E-02
ΔL_a (mm)	7.93E-02	8.22E-02	8.30E-02	8.22E-02	8.52E-02	8.21E-02	7.92E-02	7.51E-02	7.72E-02	7.92E-02	8.02E-02	7.72E-02	8.03E-02	8.17E-02	7.83E-02
CTE (microstrains/°C)	11.0E-6	11.4E-6	11.6E-6	11.5E-6	11.9E-6	11.5E-6	11.0E-6	10.5E-6	10.8E-6	11.0E-6	11.2E-6	10.8E-6	11.1E-6	11.3E-6	10.9E-6
Contraction 2															
L_0 (mm)	180.86	180.55	180.33	180.36	180.39	180.30	180.66	180.58	180.67	180.81	180.41	180.64	180.52	180.69	180.604
ΔT (°C)	-39.9	-39.7	-39.7	-39.7	-39.7	-39.7	-39.8	-39.6	-39.8	-39.7	-39.8	-39.8	-40.0	-39.9	-39.8
ΔL_f (mm)	-1.73E-02	-1.71E-02	-1.72E-02	-1.72E-02	-1.71E-02	-1.71E-02	-1.72E-02	-1.71E-02	-1.72E-02	-1.72E-02	-1.72E-02	-1.72E-02	-1.73E-02	-1.73E-02	-1.72E-02
ΔL_m (mm)	-6.2E-02	-6.5E-02	-6.6E-02	-6.4E-02	-6.7E-02	-6.5E-02	-6.2E-02	-5.9E-02	-6.1E-02	-6.1E-02	-6.3E-02	-6.0E-02	-6.3E-02	-6.4E-02	-6.1E-02
ΔL_a (mm)	-7.93E-02	-8.21E-02	-8.32E-02	-8.12E-02	-8.41E-02	-8.21E-02	-7.92E-02	-7.61E-02	-7.82E-02	-7.82E-02	-8.02E-02	-7.72E-02	-8.03E-02	-8.13E-02	-7.82E-02
CTE (microstrains/°C)	11.0E-6	11.5E-6	11.6E-6	11.3E-6	11.7E-6	11.5E-6	11.0E-6	10.6E-6	10.9E-6	10.9E-6	11.2E-6	10.7E-6	11.1E-6	11.3E-6	10.9E-6
Ave. CTE (microstrains/°C)	11.0E-6	11.4E-6	11.6E-6	11.4E-6	11.8E-6	11.5E-6	11.0E-6	10.6E-6	10.8E-6	11.0E-6	11.2E-6	10.7E-6	11.1E-6	11.3E-6	10.9E-6
Ave. CTE (per Age)(microstrains/°C)		11.3E-6			11.6E-6			10.8E-6			11.0E-6			11.1E-6	
Ave. CTE (per Age)(microstrains/°F)		6.3E-6			6.4E-6			6.0E-6			6.1E-6			6.2E-6	

West Hawaii Concrete

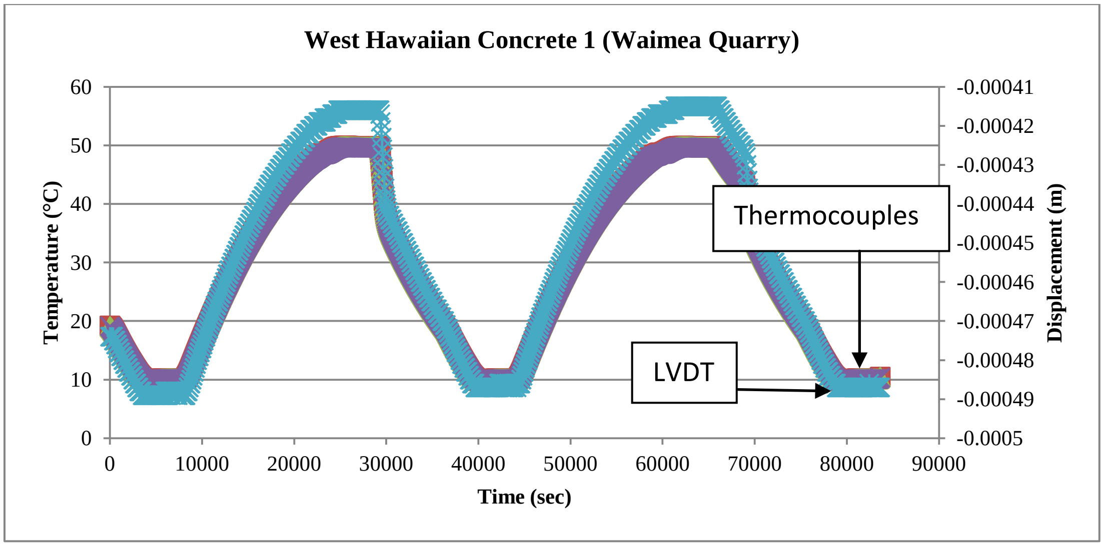

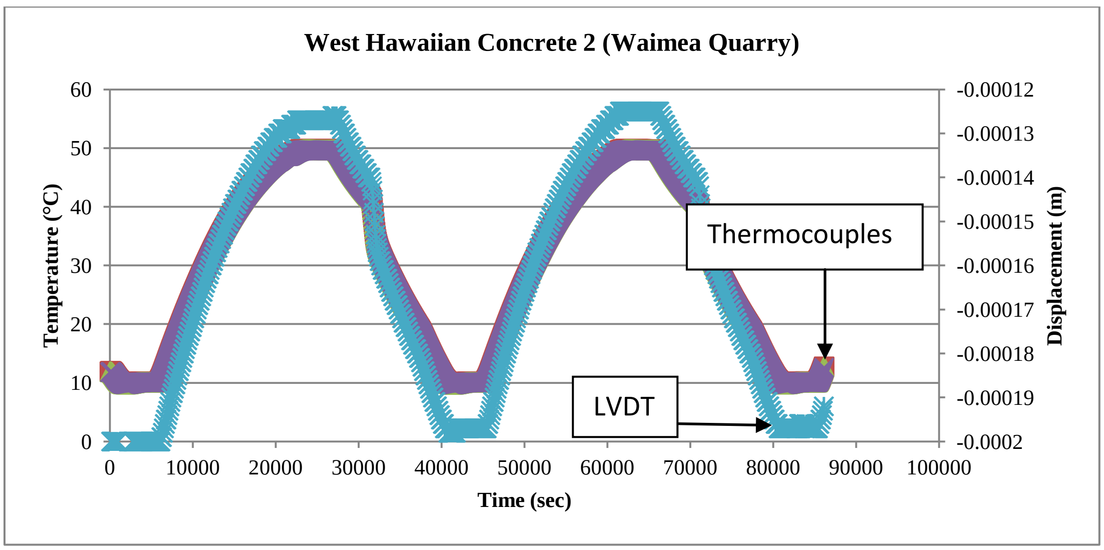

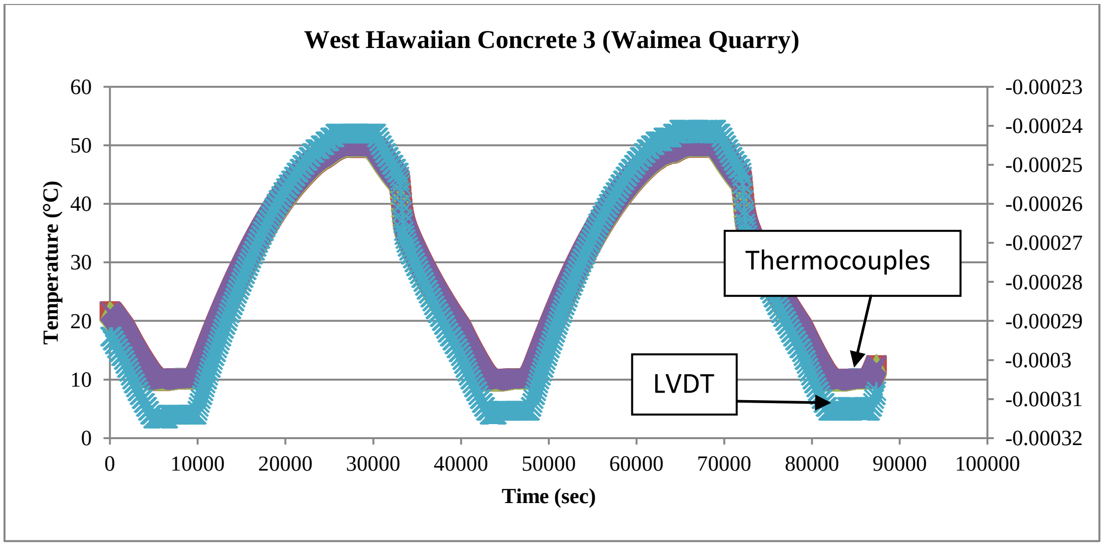
West Hawaiian Concrete 3 (Waimea Quarry)
Temperature (°C)
Time (sec)
Thermocouples
LVDT
0 10 20 30 40 50 60
0 10000 20000 30000 40000 50000 60000 70000 80000 90000 100000
-0.00023 -0.00024 -0.00025 -0.00026 -0.00027 -0.00028 -0.00029 -0.0003 -0.00031 -0.00032

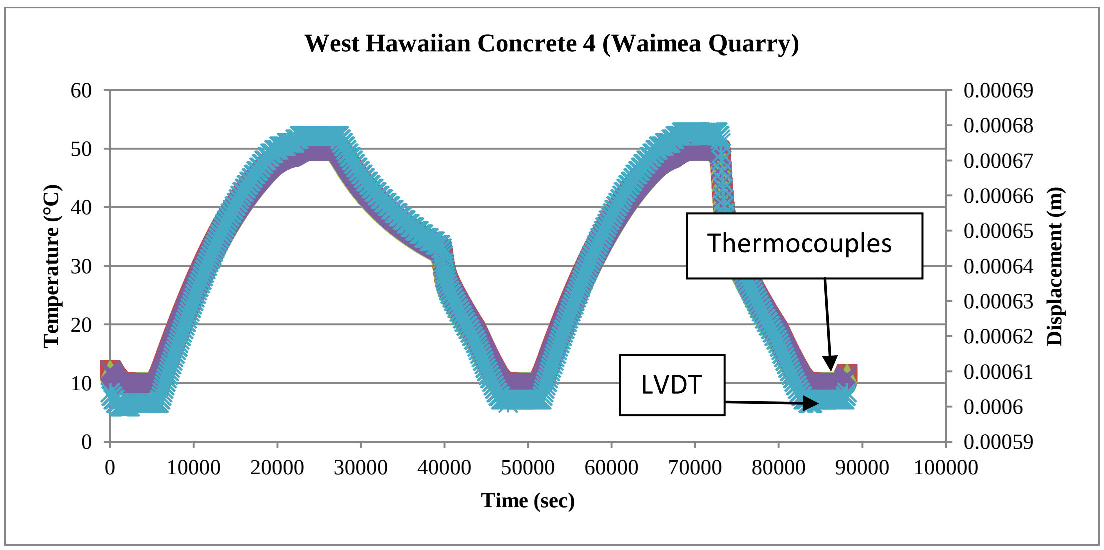
West Hawaiian Concrete 4 (Waimea Quarry)
Temperature (°C)
Displacement (m)
Time (sec)
Thermocouples
LVDT
0 10 20 30 40 50 60
0 10000 20000 30000 40000 50000 60000 70000 80000 90000 100000
0.00069 0.00068 0.00067 0.00066 0.00065 0.00064 0.00063 0.00062 0.00061 0.0006 0.00059

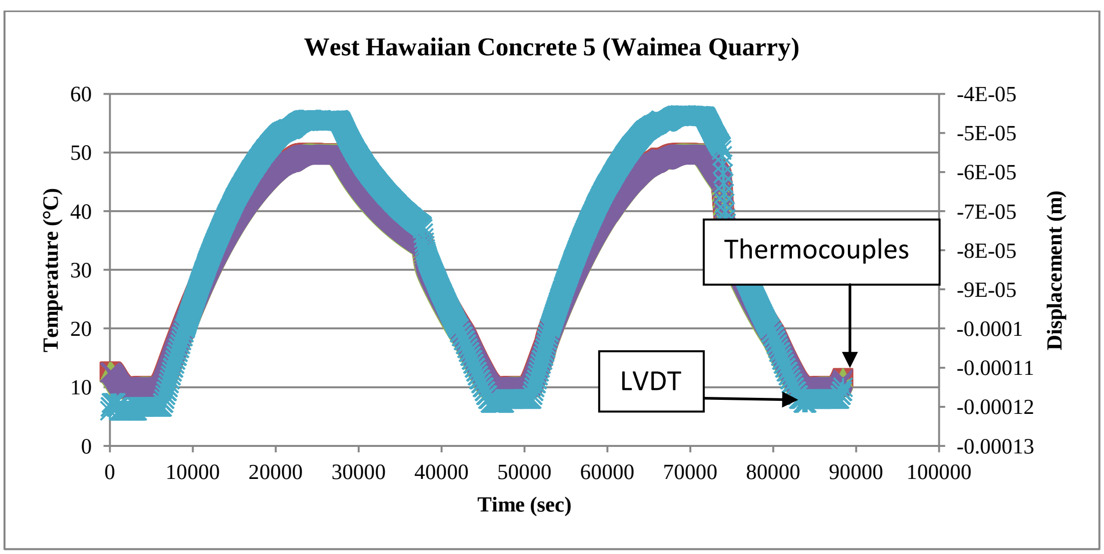
West Hawaiian Concrete 5 (Waimea Quarry)
Temperature (°C)
Displacement (m)
Time (sec)
Thermocouples
LVDT
0 10 20 30 40 50 60
0 10000 20000 30000 40000 50000 60000 70000 80000 90000 100000
-4E-05 -5E-05 -6E-05 -7E-05 -8E-05 -9E-05 -0.0001 -0.00011 -0.00012 -0.00013

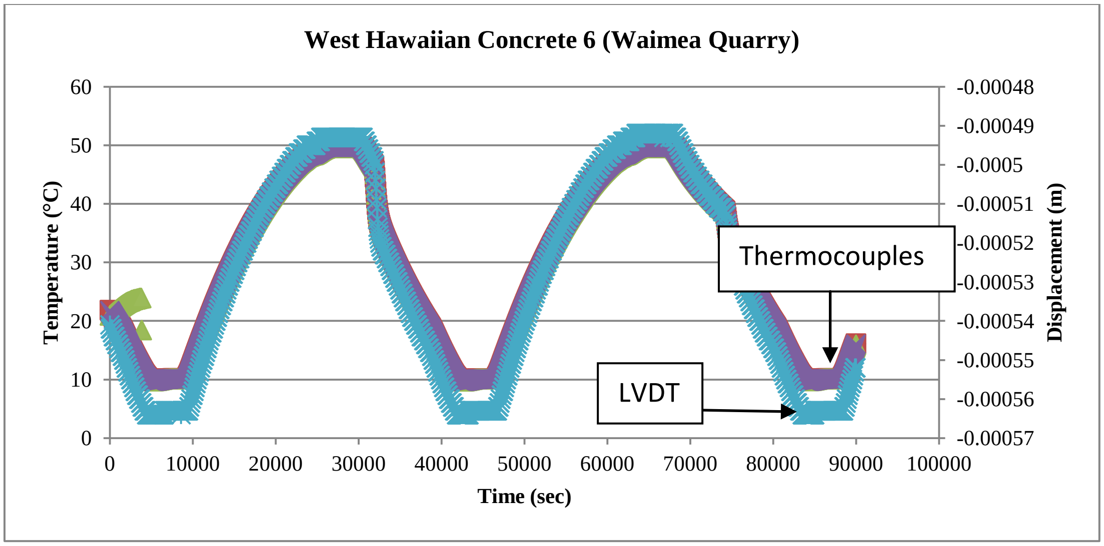
West Hawaiian Concrete 6 (Waimea Quarry)
Temperature (°C)
60
50
40
30
20
10
0
0
10000
20000
30000
40000
50000
60000
70000
80000
90000
100000
Time (sec)
-0.00048
-0.00049
-0.0005
-0.00051
-0.00052
-0.00053
-0.00054
-0.00055
-0.00056
-0.00057
Displacement (m)
Thermocouples
LVDT

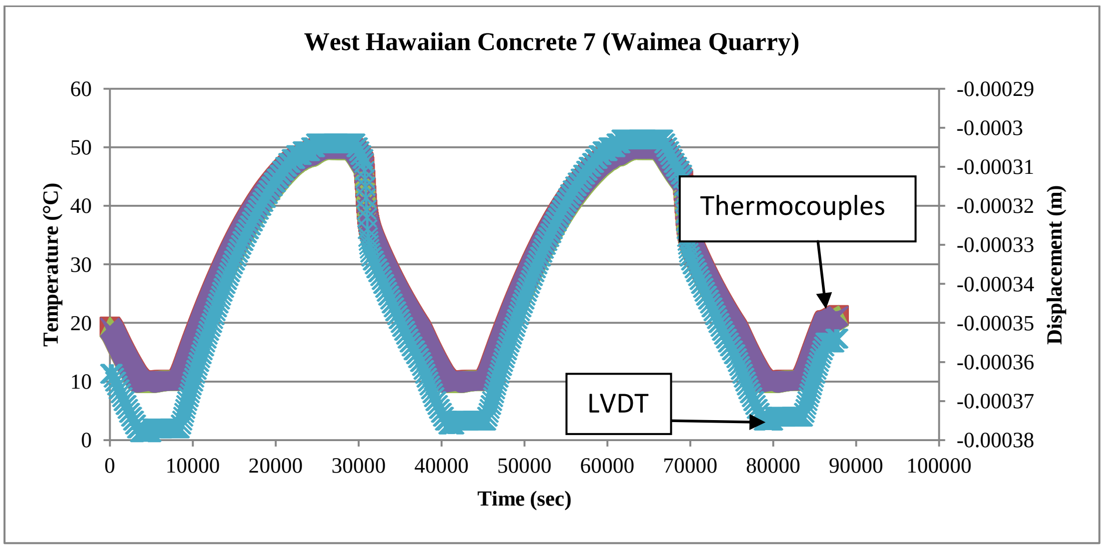
West Hawaiian Concrete 7 (Waimea Quarry)
Temperature (°C)
60
50
40
30
20
10
0
0
10000
20000
30000
40000
50000
60000
70000
80000
90000
100000
Time (sec)
-0.00029
-0.0003
-0.00031
-0.00032
-0.00033
-0.00034
-0.00035
-0.00036
-0.00037
-0.00038
Displacement (m)
Thermocouples
LVDT

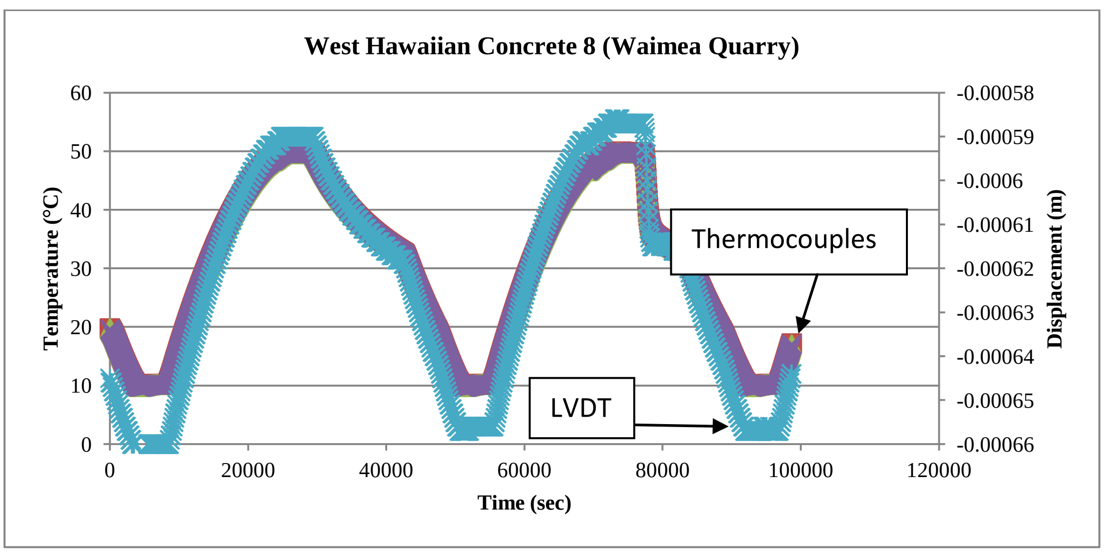
West Hawaiian Concrete 8 (Waimea Quarry)
Temperature (°C)
60
50
40
30
20
10
0
0
20000
40000
60000
80000
100000
120000
Time (sec)
-0.00058
-0.00059
-0.0006
-0.00061
-0.00062
-0.00063
-0.00064
-0.00065
-0.00066
Displacement (m)
Thermocouples
LVDT

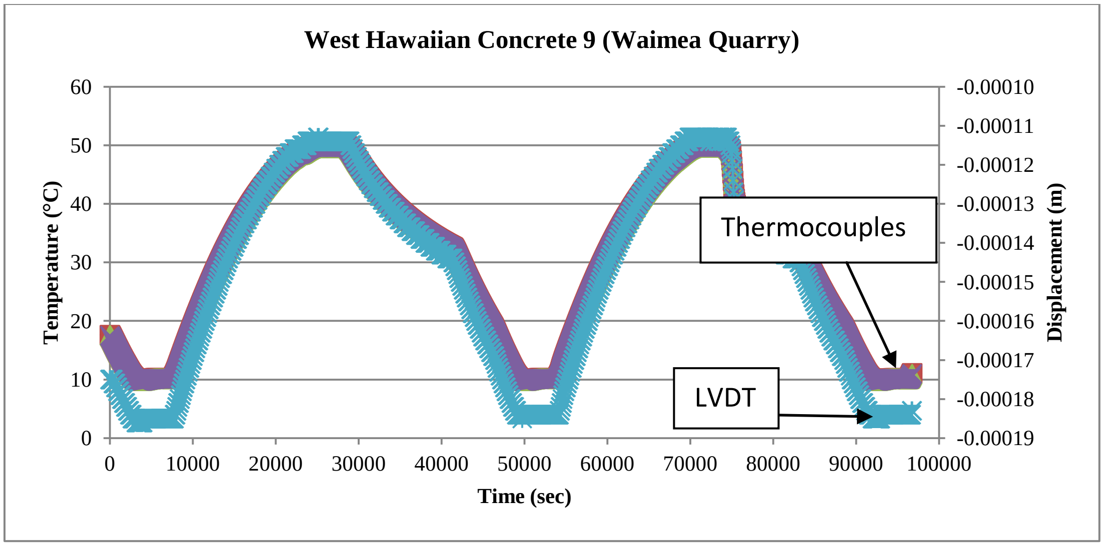
West Hawaiian Concrete 9 (Waimea Quarry)
Temperature (°C)
Displacement (m)
Time (sec)
Thermocouples
LVDT
0
10
20
30
40
50
60
-0.00010
-0.00011
-0.00012
-0.00013
-0.00014
-0.00015
-0.00016
-0.00017
-0.00018
-0.00019
0
10000
20000
30000
40000
50000
60000
70000
80000
90000
100000

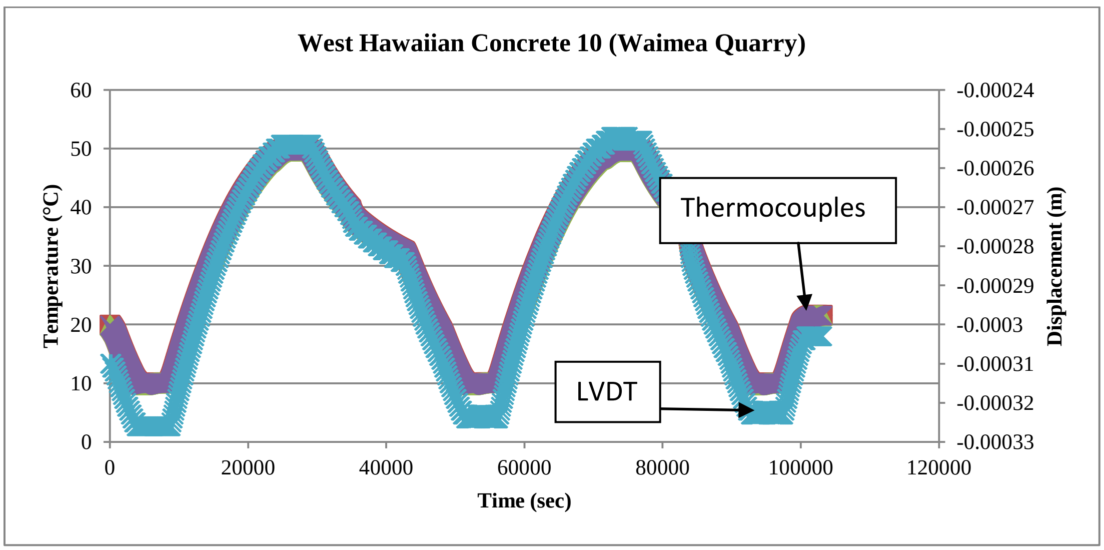
West Hawaiian Concrete 10 (Waimea Quarry)
Temperature (°C)
Displacement (m)
Time (sec)
Thermocouples
LVDT
0
10
20
30
40
50
60
-0.00024
-0.00025
-0.00026
-0.00027
-0.00028
-0.00029
-0.0003
-0.00031
-0.00032
-0.00033
0
20000
40000
60000
80000
100000
120000

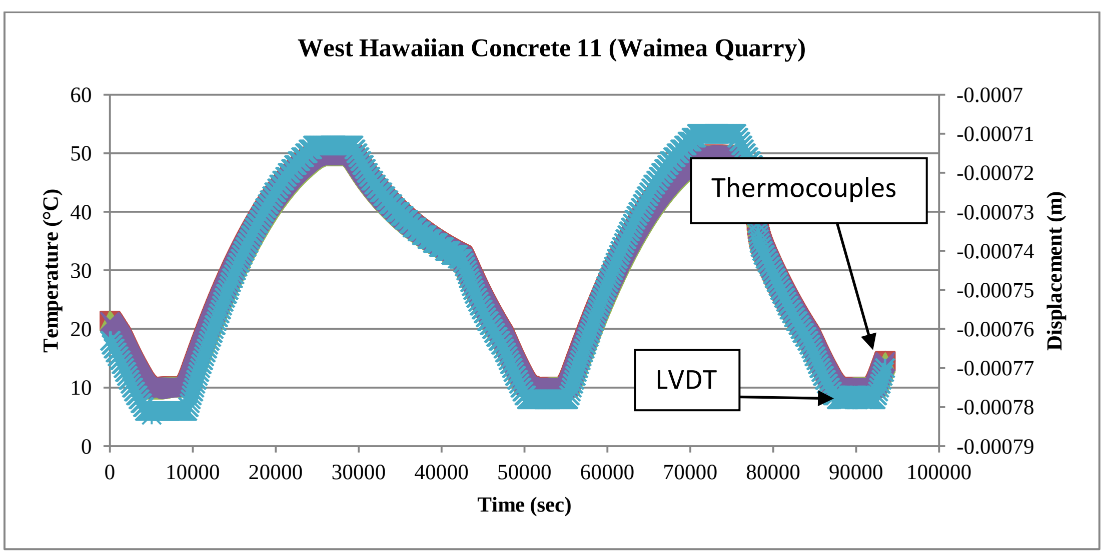
West Hawaiian Concrete 11 (Waimea Quarry)
Temperature (°C)
Displacement (m)
Time (sec)
Thermocouples
LVDT
0
10
20
30
40
50
60
-0.0007
-0.00071
-0.00072
-0.00073
-0.00074
-0.00075
-0.00076
-0.00077
-0.00078
-0.00079
0
10000
20000
30000
40000
50000
60000
70000
80000
90000
100000

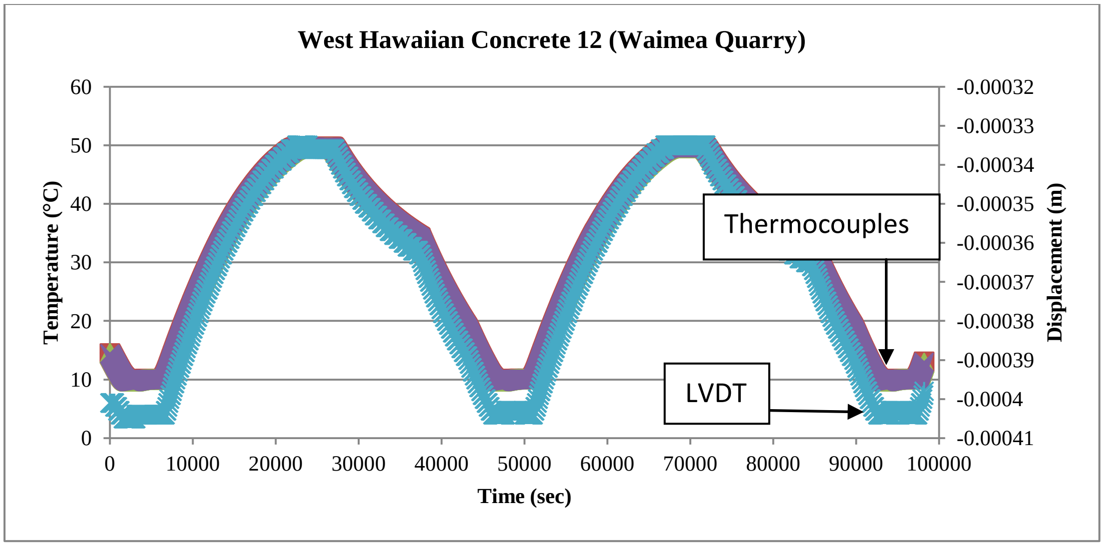
West Hawaiian Concrete 12 (Waimea Quarry)
Temperature (°C)
Displacement (m)
Time (sec)
Thermocouples
LVDT
0
10
20
30
40
50
60
-0.00032
-0.00033
-0.00034
-0.00035
-0.00036
-0.00037
-0.00038
-0.00039
-0.0004
-0.00041
0
10000
20000
30000
40000
50000
60000
70000
80000
90000
100000

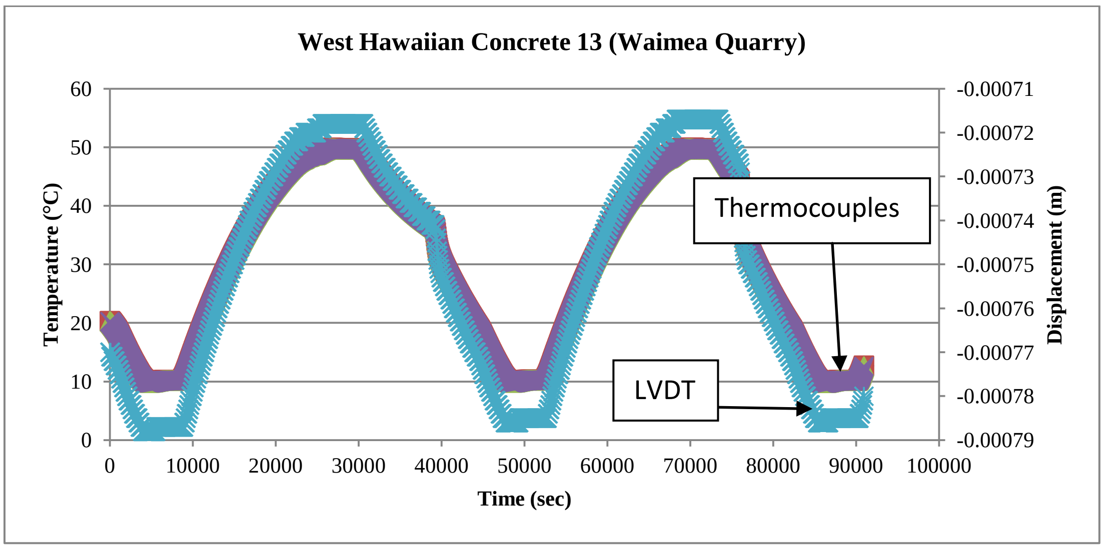
West Hawaiian Concrete 13 (Waimea Quarry)
Temperature (°C)
Displacement (m)
Time (sec)
Thermocouples
LVDT
0
10
20
30
40
50
60
-0.00071
-0.00072
-0.00073
-0.00074
-0.00075
-0.00076
-0.00077
-0.00078
-0.00079
0
10000
20000
30000
40000
50000
60000
70000
80000
90000
100000

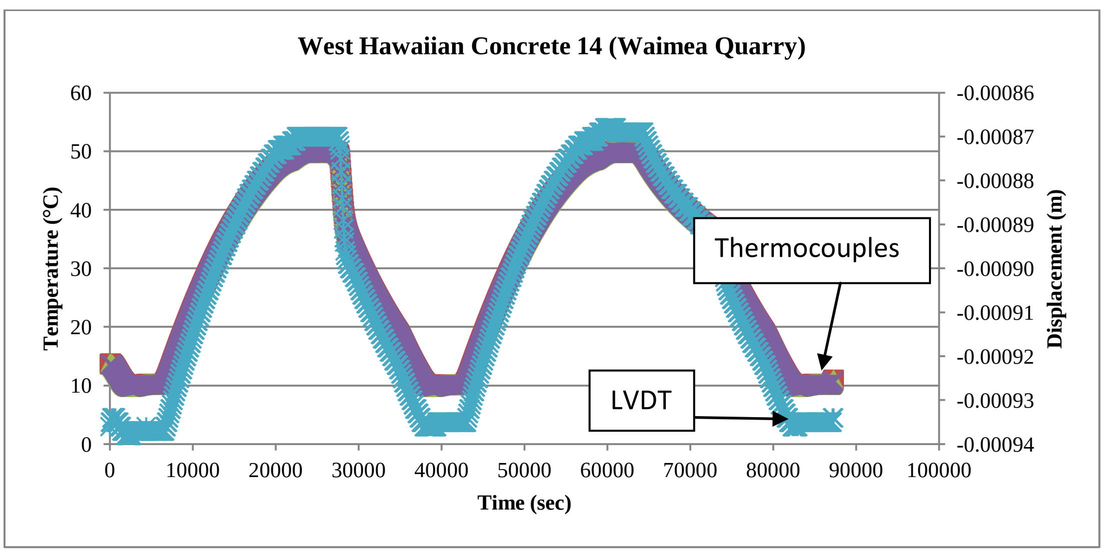
West Hawaiian Concrete 14 (Waimea Quarry)
Temperature (°C)
Displacement (m)
Time (sec)
Thermocouples
LVDT
0
10
20
30
40
50
60
-0.00086
-0.00087
-0.00088
-0.00089
-0.00090
-0.00091
-0.00092
-0.00093
-0.00094
0
10000
20000
30000
40000
50000
60000
70000
80000
90000
100000

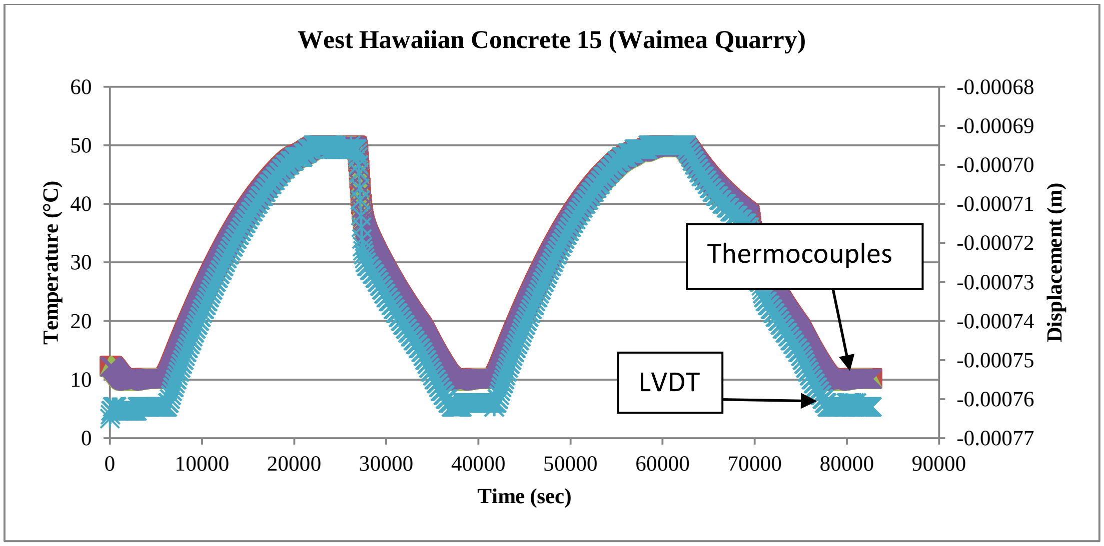
West Hawaiian Concrete 15 (Waimea Quarry)
Temperature (°C)
60
50
40
30
20
10
0
-0.00068
-0.00069
-0.00070
-0.00071
-0.00072
-0.00073
-0.00074
-0.00075
-0.00076
-0.00077
Displacement (m)
0
10000
20000
30000
40000
50000
60000
70000
80000
90000
Time (sec)
Thermocouples
LVDT

	WHC #1	WHC #2	WHC #3	WHC #4	WHC #5	WHC #6	WHC #7	WHC #8	WHC #9	WHC #10	WHC #11	WHC #12	WHC #13	WHC #14	WHC #15
		3 Day Curing			7 Day Curing			14 Day Curing			28 Day Curing			56 Day Curing	
Expansion 1															
L_0 (mm)	180.60	180.59	180.59	180.18	180.11	180.54	180.39	180.57	180.58	180.53	180.85	180.72	180.77	180.84	180.69
ΔT (°C)	39.9	39.9	39.8	39.9	39.7	39.8	39.7	39.8	39.8	39.9	39.8	39.7	39.7	39.8	39.8
ΔL_f (mm)	1.73E-02	1.73E-02	1.72E-02	1.72E-02	1.71E-02	1.72E-02	1.72E-02	1.72E-02	1.72E-02	1.72E-02	1.72E-02	1.72E-02	1.72E-02	1.72E-02	1.72E-02
ΔL_m (mm)	7.3E-02	7.4E-02	7.3E-02	7.7E-02	7.3E-02	7.1E-02	7.3E-02	7.1E-02	7.1E-02	7.2E-02	6.8E-02	6.8E-02	6.9E-02	6.7E-02	6.6E-02
ΔL_a (mm)	9.03E-02	9.13E-02	9.02E-02	9.42E-02	9.04E-02	8.82E-02	9.02E-02	8.82E-02	8.82E-02	8.92E-02	8.52E-02	8.52E-02	8.62E-02	8.42E-02	8.32E-02
CTE (microstrains/°C)	12.5E-6	12.7E-6	12.5E-6	13.1E-6	12.6E-6	12.3E-6	12.6E-6	12.3E-6	12.3E-6	12.4E-6	11.8E-6	11.9E-6	12.0E-6	11.7E-6	11.6E-6
Contraction 1															
L_0 (mm)	180.60	180.59	180.59	180.18	180.11	180.54	180.39	180.57	180.58	180.53	180.85	180.72	180.77	180.84	180.69
ΔT (°C)	-39.9	-39.9	-39.8	-39.9	-39.7	-39.8	-39.9	-39.7	-39.8	-39.7	-39.9	-39.8	-39.6	-39.9	-39.8
ΔL_f (mm)	-1.72E-02	-1.72E-02	-1.72E-02	-1.72E-02	-1.71E-02	-1.72E-02	-1.72E-02	-1.72E-02	-1.72E-02	-1.72E-02	-1.73E-02	-1.72E-02	-1.71E-02	-1.73E-02	-1.72E-02
ΔL_m (mm)	-7.1E-02	-7.0E-02	-7.1E-02	-7.5E-02	-7.1E-02	-7.0E-02	-7.1E-02	-6.6E-02	-7.0E-02	-6.9E-02	-6.5E-02	-6.7E-02	-6.7E-02	-6.5E-02	-6.5E-02
ΔL_a (mm)	-8.82E-02	-8.72E-02	-8.82E-02	-9.22E-02	-8.84E-02	-8.72E-02	-8.82E-02	-8.32E-02	-8.72E-02	-8.62E-02	-8.23E-02	-8.42E-02	-8.41E-02	-8.23E-02	-8.22E-02
CTE (microstrains/°C)	12.3E-6	12.1E-6	12.3E-6	12.8E-6	12.4E-6	12.1E-6	12.3E-6	11.6E-6	12.1E-6	12.0E-6	11.4E-6	11.7E-6	11.8E-6	11.4E-6	11.4E-6
Expansion 2															
L_0 (mm)	180.60	180.59	180.59	180.18	180.11	180.54	180.39	180.57	180.58	180.53	180.85	180.72	180.77	180.84	180.69
ΔT (°C)	39.9	39.9	39.8	40.0	39.8	39.8	39.8	39.8	39.7	39.6	39.9	39.8	39.7	39.9	39.9
ΔL_f (mm)	1.72E-02	1.72E-02	1.72E-02	1.72E-02	1.72E-02	1.72E-02	1.72E-02	1.72E-02	1.72E-02	1.71E-02	1.73E-02	1.72E-02	1.72E-02	1.73E-02	1.72E-02
ΔL_m (mm)	7.2E-02	7.2E-02	7.2E-02	7.6E-02	7.2E-02	7.1E-02	7.2E-02	7.0E-02	7.1E-02	7.1E-02	6.8E-02	6.8E-02	6.8E-02	6.6E-02	6.6E-02
ΔL_a (mm)	8.92E-02	8.92E-02	8.92E-02	9.32E-02	8.97E-02	8.82E-02	8.92E-02	8.72E-02	8.82E-02	8.81E-02	8.53E-02	8.52E-02	8.52E-02	8.33E-02	8.32E-02
CTE (microstrains/°C)	12.4E-6	12.4E-6	12.4E-6	12.9E-6	12.5E-6	12.3E-6	12.4E-6	12.1E-6	12.3E-6	12.3E-6	11.8E-6	11.8E-6	11.9E-6	11.5E-6	11.6E-6
Contraction 2															
L_0 (mm)	180.60	180.59	180.59	180.18	180.11	180.54	180.39	180.57	180.58	180.53	180.85	180.72	180.77	180.84	180.69
ΔT (°C)	-39.7	-39.8	-40.1	-39.9	-39.8	-39.7	-39.7	-39.8	-39.8	-39.7	-39.7	-39.9	-39.8	-39.9	-39.7
ΔL_f (mm)	-1.72E-02	-1.72E-02	-1.73E-02	-1.72E-02	-1.72E-02	-1.72E-02	-1.71E-02	-1.72E-02	-1.72E-02	-1.71E-02	-1.72E-02	-1.73E-02	-1.72E-02	-1.73E-02	-1.72E-02
ΔL_m (mm)	-7.2E-02	-7.2E-02	-7.2E-02	-7.6E-02	-7.2E-02	-7.1E-02	-7.1E-02	-7.1E-02	-7.1E-02	-7.0E-02	-6.7E-02	-6.9E-02	-6.8E-02	-6.6E-02	-6.7E-02
ΔL_a (mm)	-8.92E-02	-8.92E-02	-8.93E-02	-9.32E-02	-8.97E-02	-8.82E-02	-8.81E-02	-8.82E-02	-8.82E-02	-8.71E-02	-8.42E-02	-8.63E-02	-8.52E-02	-8.33E-02	-8.42E-02
CTE (microstrains/°C)	12.4E-6	12.4E-6	12.3E-6	13.0E-6	12.5E-6	12.3E-6	12.3E-6	12.3E-6	12.3E-6	12.2E-6	11.7E-6	12.0E-6	11.8E-6	11.6E-6	11.7E-6
Ave. CTE (microstrains/°C)	12.4E-6	12.4E-6	12.4E-6	13.0E-6	12.5E-6	12.3E-6	12.4E-6	12.2E-6	12.3E-6	12.2E-6	11.8E-6	11.9E-6	11.9E-6	11.5E-6	11.6E-6
Ave. CTE (per Age)(microstrains/°C)		12.4E-6			12.6E-6			12.3E-6			12.0E-6			11.7E-6	
Ave. CTE (per Age)(microstrains/°F)		6.9E-6			7.0E-6			6.8E-6			6.7E-6			6.5E-6	

APPENDIX B: MEPDG RESULTS

Typical Effect of CTE on Faulting Performance

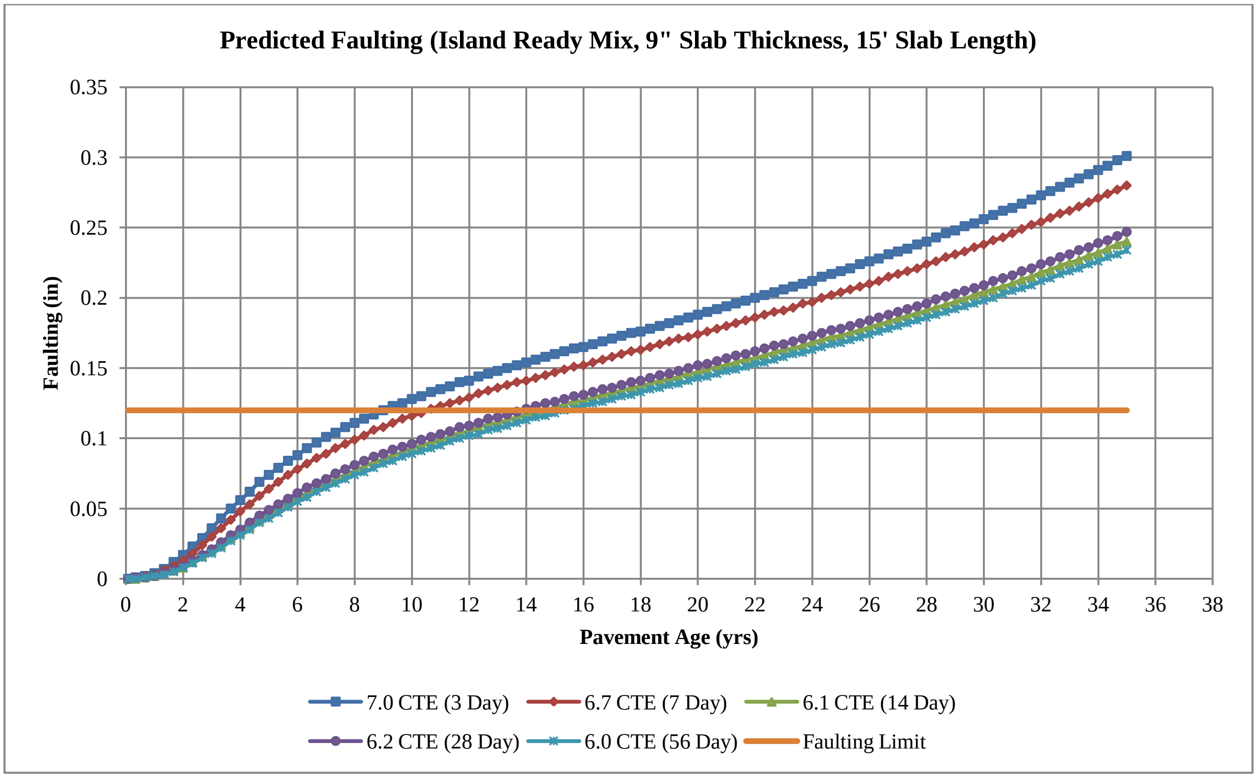

Typical Effect of Slab Length and Thickness on Faulting Performance

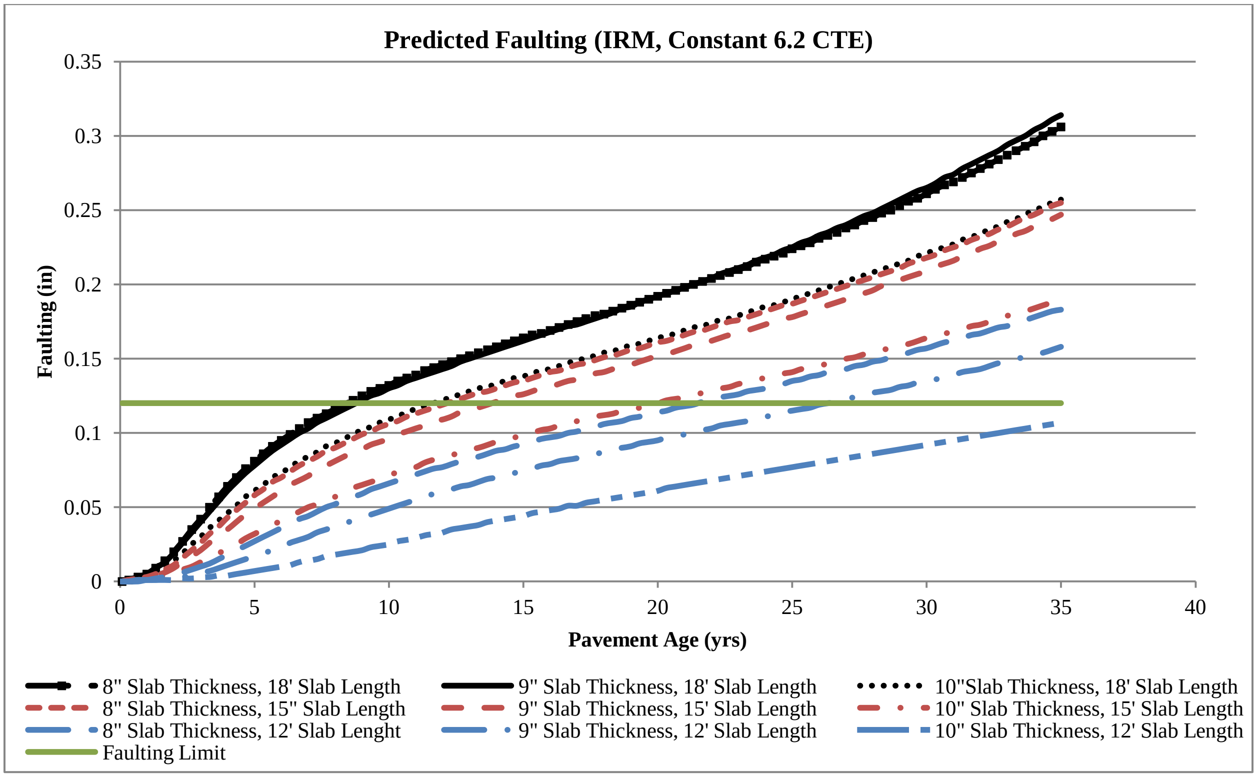

Typical Effect of CTE on Percent Slabs Cracked Performance

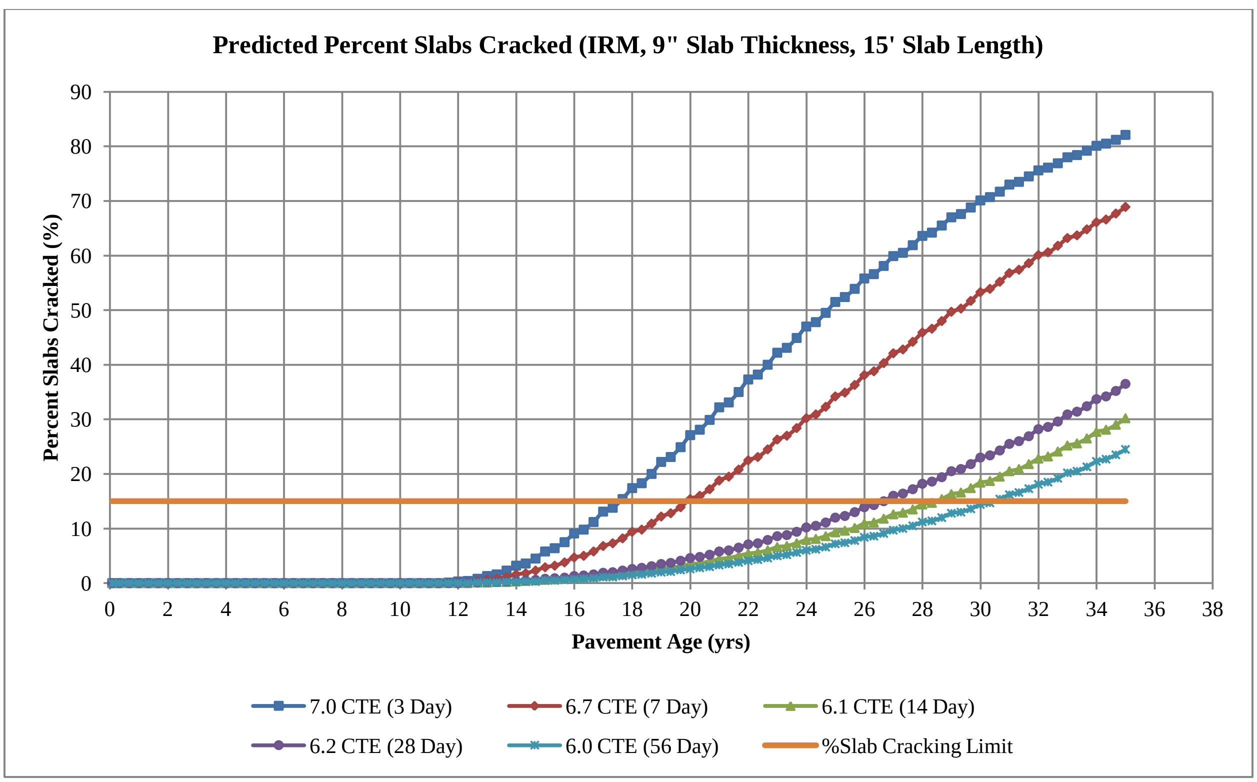

Typical Effect of Slab Length and Thickness on Percent Slabs Cracked Performance

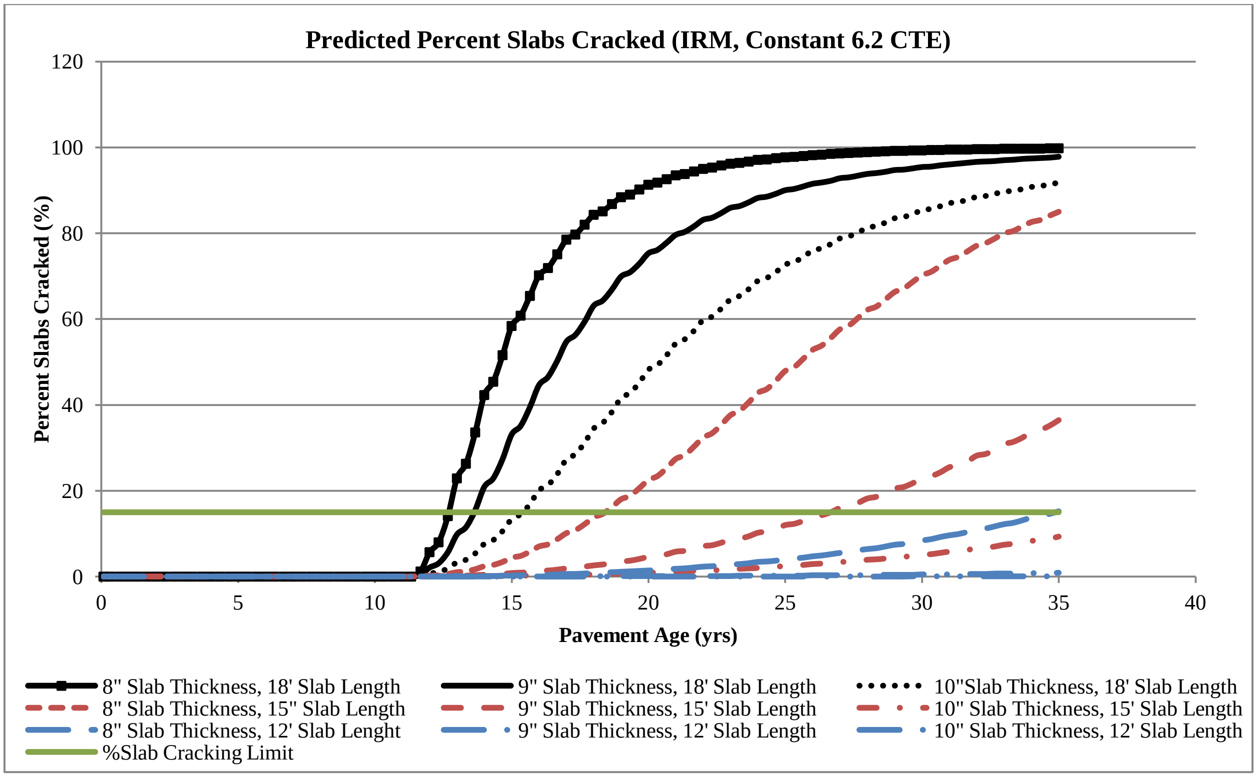

Typical Effect of CTE on International Roughness Index Performance

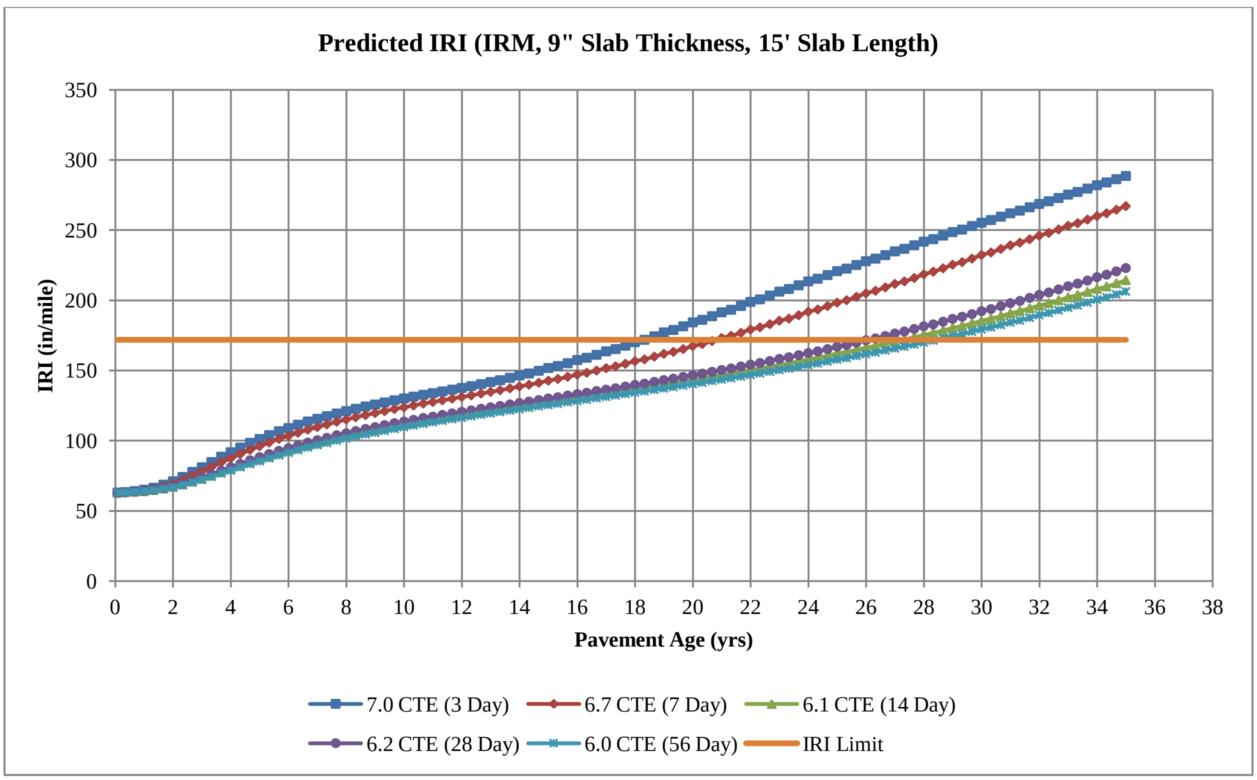

Typical Effect of Slab Length and Thickness on International Roughness Index Performance